



Laporan Akhir Projek Penyelidikan Jangka Pendek

**High wear Resistant Ceramic Cutting
Inserts With Enhanced Toughness For
High-Speed Machining**

by

Prof. Dr. Zainal Arifin Ahmad

Prof. Dr. Mani Maran Ratnam

2016



RU GRANT FINAL REPORT

RESEARCH TITLE

HIGH WEAR RESISTANT CERAMIC CUTTING INSERTS WITH ENHANCED
TOUGHNESS FOR HIGH-SPEED MACHINING

ACCOUNT NUMBER:

1001/PBAHAN/811212

NAME OF RESEARCH LEADER:

PROF. DR. HJ. ZAINAL ARIFIN HJ. AHMAD

SCHOOL OF MATERIALS & MINERAL RESOURCES ENGINEERING. ENGINEERING
CAMPUS, UNIVERSITI SAINS MALAYSIA

NAME OF CO-RESEARCHER:

PROF. DR MANI MARAN RATNAM

SCHOOL OF MECHANICAL ENGINEERING, ENGINEERING CAMPUS,
UNIVERSITI SAINS MALAYSIA

START DATE : 15TH JULY 2012

COMPLETION DATE : 14TH JANUARY 2016

Please use this checklist to self-assess your report before submitting to RCMO.
Checklist should accompany the report.

NO.	ITEM	PLEASE CHECK (✓)		
		PI	JKPTJ	RCMO
1	Completed Final Report Form	✓		✓
2	Project Financial Account Statement (e-Statement)	✓		✓
3	Asset/Inventory Return Form (Borang Penyerahan Aset/Inventori)	✓		✓
4	A copy of the publications/proceedings listed in Section D(ii) (Research Output)	✓		✓
5	Comprehensive Technical Report	✓		✓
6	Other supporting documents, if any			-
7	Project Leader's Signature	✓		✓
8	Endorsement of PTJ's Evaluation Committee			✓
9	Endorsement of Dean/ Director of PTJ's			✓



TECHNICAL REPORT

RESEARCH TITLE

**HIGH WEAR RESISTANT CERAMIC CUTTING INSERTS WITH ENHANCED
TOUGHNESS FOR HIGH-SPEED MACHINING**

ACCOUNT NUMBER:

1001/PBAHAN/8011212

NAME OF RESEARCH LEADER:

PROF. DR. HJ. ZAINAL ARIFIN HJ. AHMAD

**SCHOOL OF MATERIALS & MINERAL RESOURCES ENGINEERING. ENGINEERING
CAMPUS, UNIVERSITI SAINS MALAYSIA**

NAME OF CO-RESEARCHER:

PROF. DR MANI MARAN RATNAM

**SCHOOL OF MECHANICAL ENGINEERING, ENGINEERING CAMPUS,
UNIVERSITI SAINS MALAYSIA**

START DATE : 15TH JULY 2012

COMPLETION DATE : 14TH JANUARY 2016

Table of Content

Table of Content	i
1. Introduction	1
2. Research Objectives	2
3. Methods.....	2
4. Results and discussion	7
4.1 Part 1: Effect of CeO ₂ addition.....	7
4.2 Part 2: Effect of MgO as co-stabilizer with CeO ₂	11
4.2.1 MgO microparticles addition.....	11
4.2.2 MgO nanoparticles	14
4.3 Part 3: Wear performance	15
4.3.2 The Cutting Speed Influences on Tool Wear of ZTA	15
5. Conclusion	18
5.1 Research output.....	19
Acknowledgements	19
References	19

Part 2 is to investigate the influence of CeO₂ additions on the toughness of established ZTA0.7MgO ceramics. The ZTA0.7MgO ceramics refer to ZTA with 0.7 wt.% MgO additive which is an optimum composition from the published work by Azhar et al. (2011). However, due to the decrease of fracture toughness values with the MgO additive, the ZTA0.7MgO ceramics have been improved with different CeO₂ wt.% ranging from 0 wt.% to 10 wt.% in this work. The idea behind this works is the enhancement of toughness properties of ZTA0.7MgO ceramics. Step for samples preparation and characterization techniques are similar to Part 1.

Part 3 is to investigate the effect of MgO in nano-scale particles (abridge as MgO nanoparticles) on the toughness improvement of ZTA5CeO₂ ceramics. This part aim to optimize the properties of ZTA5CeO₂ ceramics as cutting insert using CNC high speed machining. The ZTA5CeO₂ ceramics refer to ZTA with an addition of 5 wt.% CeO₂ (as an excellent properties from Part 1). The addition of MgO nanoparticles (average particle sizes of 20 nm) ranging from 0 wt.% to 2 wt.% were added to the ZTA5CeO₂ ceramics. The sample preparations and characterization techniques are identical to Part 1. As an optimum ceramics properties compared to Part 1 and 2 the composition of this part was further prepared as cutting tool inserts and investigated for wear measurements. The cutting work is done where the captured images of inserts nose before and after machining have been analysed by Wearmon 1.0 software for nose wear area results.

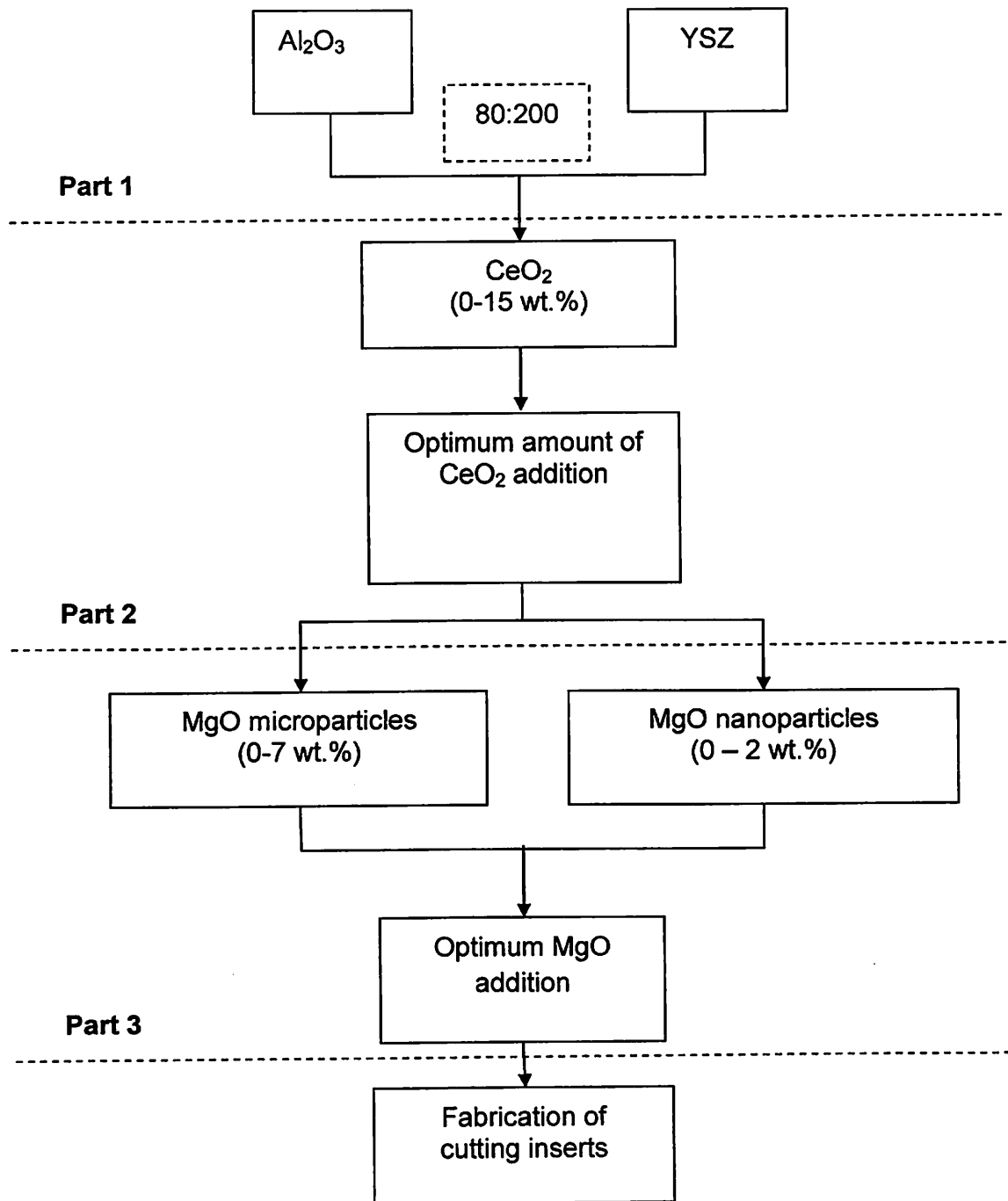


Figure 31: The scope of research.

HIGH WEAR RESISTANT CERAMIC CUTTING INSERTS WITH ENHANCED TOUGHNESS FOR HIGH-SPEED MACHINING

1. Introduction

Ceramics are often differentiated according to their application. As cutting inserts, ZTA ceramics have been found to experience premature failure due to chipping or breakage during services. This conditions occurred because of ZTA are lack of toughness and therefore, many researches have been carried out to address this problem. The main focus of these investigations is on producing higher hardness and fracture toughness ceramics. Hence, ZTA ceramics become a main object of scientific interest especially from the material properties enhancement point of view. In ZTA ceramics, Al_2O_3 as the matrix and ZrO_2 particle embedded as reinforcement agent. As the reinforcement agent, an enhancement can be made by the two states of ZrO_2 that are commonly used in ZTA ceramics, i.e., either **unstabilised** or **stabilised**. Unstabilised ZrO_2 refer to pure ZrO_2 without the presence of any stabilizer content which is not very useful as a structural materials. Stabilised ZrO_2 refer to ZrO_2 with the presence of additives which acts as phase-stabilizers such as Y_2O_3 , MgO , and CeO_2 .

These phase-stabilizers is to retain the high-temperature phase, either monoclinic, tetragonal or cubic, at room temperature, which gives ZrO_2 its required properties as an engineering ceramic [1]. The presence of stabilizer can lead the tetragonal phase to transform to monoclinic phase, related to volume expansion. These phase transformation have the ability to prevent the growth of cracks and consequently improving the fracture toughness [2]. This mechanism is known as transformation toughening, which improves the reliability and extends lifetime of ZTA ceramics. The transformation toughening mechanisms of ZTA provided a fusion of stress induced phase transformation (tetragonal to monoclinic zirconia) microcracks as well as crack deflections. In spite of utilization of stabilizer, the existence of cracks is not completely avoidable, which makes the ZTA cutting inserts are prematurely fail by chipping during high speed machining. A concern with the used of ZTA as cutting inserts material is the possibility of a spontaneous transformation from the tetragonal (t- ZrO_2) to the monoclinic (m- ZrO_2) phase [3]. The factor of spontaneous transformation are the grain size, stabilizer content and distribution, the composition of the ZrO_2 as second phase addition and residual stresses due to the thermal expansion differences between the phases [4,5]. The rate of spontaneous transformation could be increased with the presence of bigger grain size and distinction between the thermal expansions of the phases.

Therefore, the ideal ceramic would be a material that can decrease both bigger grain size and distinction between the thermal expansions of the phases. To meet these requirements, the new materials were developed by adding more than one stabilizer in ZTA ceramics which is known as co-stabilizer in literature review that prevent the abnormal grain growth, while retaining a relative high fracture toughness [6–8]. Reviews of magnesium oxide (MgO) and cerium oxide (CeO₂) has attracted this research to be carried out as relatively good and promising candidates to be added as stabilizer in ZTA ceramics. In addition, their ability as stabilizer through transformation toughening mechanisms and sintering aid of Al₂O₃ by the prevention of abnormal grain growth at the final stage of densification process which can lead to superior properties ceramics. Therefore in this research, with a detail assessments of suitability and properties effect of the combination of CeO₂ and MgO as co-stabilizer in ZTA ceramics in terms of toughening improvement will be carried out.

2. Research Objectives

The objectives of this research are as follows:

- i. To improve toughness of ZTA ceramics by CeO₂ addition.
- ii. Study the effect of particle size to ZTA mechanical properties, microstructures.
- iii. To fabricate the ceramic cutting inserts having higher wears resistant.
- iv. To optimize the fabrication parameters for an excellent properties of high speed ceramic cutting inserts.

3. Methods

Figure 1 summarize the scope of research. The research is divided into three parts. Part 1 is an evaluation on the suitability of CeO₂ as properties enhancer in ZTA ceramics. This part aim to understand the effects of microstructure on the fracture toughness (K_{Ic}). Samples with a ratio of 80:20 for Al₂O₃ and YSZ were fabricated with different CeO₂ wt.% starting from 0 wt.% to 10 wt.%. Hao et al., (2010) reported that ZTA consists yttria stabilised zirconia (YSZ) in the range of 10 wt.% - 20 wt.%, provides excellent mechanical strength and toughness as cutting tool inserts applications. The samples were pressed at 300 MPa and eventually sintered at 1600°C for 4 hours. Fracture toughness (K_{Ic}) and Vickers hardness (HV) were specified by Vickers indentation technique with a 30 kgf load. Scanning Electron Microscopy (SEM) was employed to analyses the samples microstructure. The samples were thermally etched in the same furnace used for sintering at 1400°C for 4 hours.

The wear performance of the fabricated cutting inserts was tested by machining commercially available stainless steel (316L) on an Okuma CNC LB15 lathe machine. Before the cutting process, the CNC machine cutting condition was set up to meet experimental procedures. The tool used and cutting parameters of the ZTA5CeO₂ added MgO nanoparticles cutting inserts are shown in Table 1.

Table 1 Cutting specification and properties of work piece	
Cutting Specification	
Machine Tool	Okuma LC 20 CNC Lathe
Cutting Condition	Dry
Tool Shape	Rhombic 80°
Tool Holder Model	Sandvik DTFNR 205D
	Coroturn
Depth of Cut	0.2 mm
Rotation Speed	540 rpm
Feed Rate	0.2 mm/rev
Cutting Length	40 mm
Physical and mechanical properties of the work piece	
Work Material	Stainless steel (316L)
Length	150 mm
Diameter	25 mm
Hardness	350 HV
Density	7.99 g/cm ³
Modulus of Elasticity	193 GPa

The nose wear, which is a critical mechanical property parameter in this work, was determined by the algorithms developed in previous work.[11] The nose wear area before (unworn) and after (worn) machining were captured using 2-D profile of the cutting insert tip. Figure 2 shows the layout of cutting tool nose for wear area analysis and the image of unworn tool tip captured by optical metrology measurement system (Alicona InfiniteFocus-Alicona Imaging Ltd., Austria) is presented as 2-D profile. Figure 3 shows the 2-D profile of cutting tool inserts for unworn, worn and nose wear area.

The nose wear area of cutting tool insert was measured by subtracting the 2-D profile of the unworn and worn cutting inserts to calculate the difference in the area of overlapping images. Both images were aligned automatically before subtraction. The software was able to exactly calculate the area differences between the two images (Figure 3a and 3b), and this area is indicated by the black colour. Based on nose wear area (Figure 3c), a larger black area indicates that the inserts have experienced a greater degree of wear, that is, more material loss occurred due to machining.

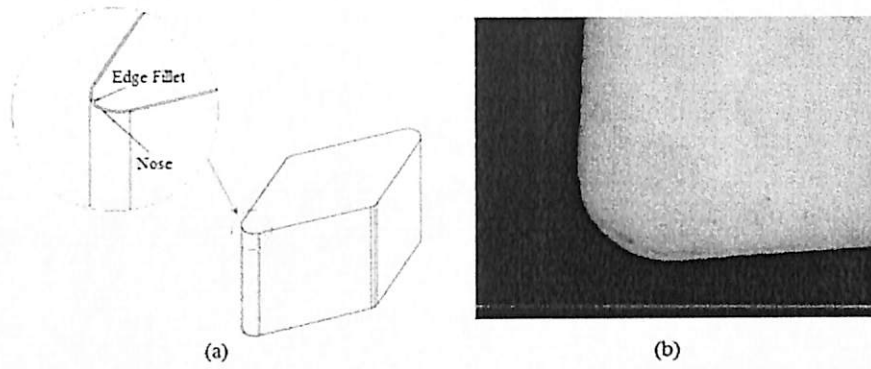


Figure 2: (a) Layout of tool insert representing the nose wear area, and (b) 2-D image of unworn tool insert captured by Alicona optical metrology system.

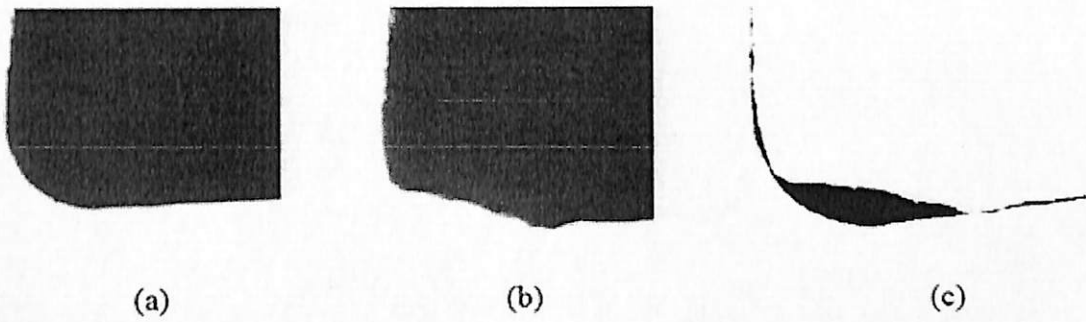


Figure 3: Images of cutting tool tips: (a) Unworn cutting tool tip, (b) worn cutting tool tip after machining, and (c) wear area obtained by subtraction.

4. Results and discussion

The results and discussion of experimental works are divided into 3 parts. Part 1 is to investigate the effect of CeO₂ addition on ZTA ceramics. The output of this part is the determination of CeO₂ suitability as ZTA toughness enhancer. Part 2 is investigated the effect of CeO₂ as co-stabilizer on ZTA0.7MgO ceramics. The objective is to improve the toughness for ZTA0.7MgO ceramics using CeO₂ as a co-stabilizer. Part 3 is the analysis for the effect of MgO nanoparticles on ZTA5CeO₂ ceramics. Part 3 highlighted the toughness improvement contributed by MgO nanoparticles. Composition with an optimum properties in term of toughness will be further studied for its wear performance.

4.1 Part 1: Effect of CeO₂ addition

The suitability of CeO₂ additives as ZrO₂ stabilizer managed to improve the fracture toughness and Vickers hardness of ZTA. Figure 4 shows the addition of 5 wt.% CeO₂ recorded the optimum values of 8.38 MPa. \sqrt{m} and 1678 HV, respectively. This results indicate that CeO₂ is suitable for enhance the fracture toughness which is improved the values up to 30 % compared to pure ZTA (5.87 MPa. \sqrt{m}). Table 4.2 summarize an overall result in Part 1. These result suggested that the presence of an abnormal grain growth such as platelet grains among ZrO₂ grains when 10 wt.% and 15 wt.% CeO₂ additions which correspond to the formation of Ce₂Zr₃O₁₀ phase, as detected by EDX results (Figure 5). Structural analyses showed the presence of the Ce₂Zr₃O₁₀ phase refer to the overstabilised due to CeO₂ addition in ZTA ceramics (Figure 6).

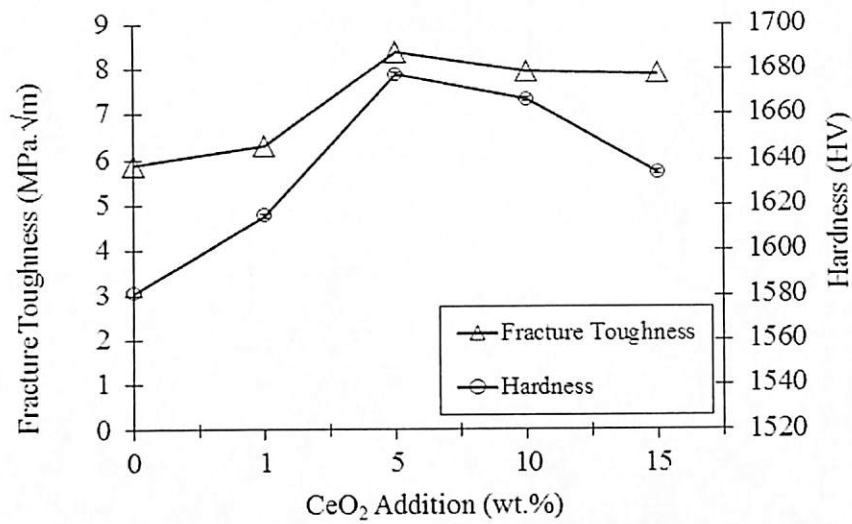


Figure 4: Results of fracture toughness and Vickers hardness for varied CeO₂ addition in ZTA ceramics.

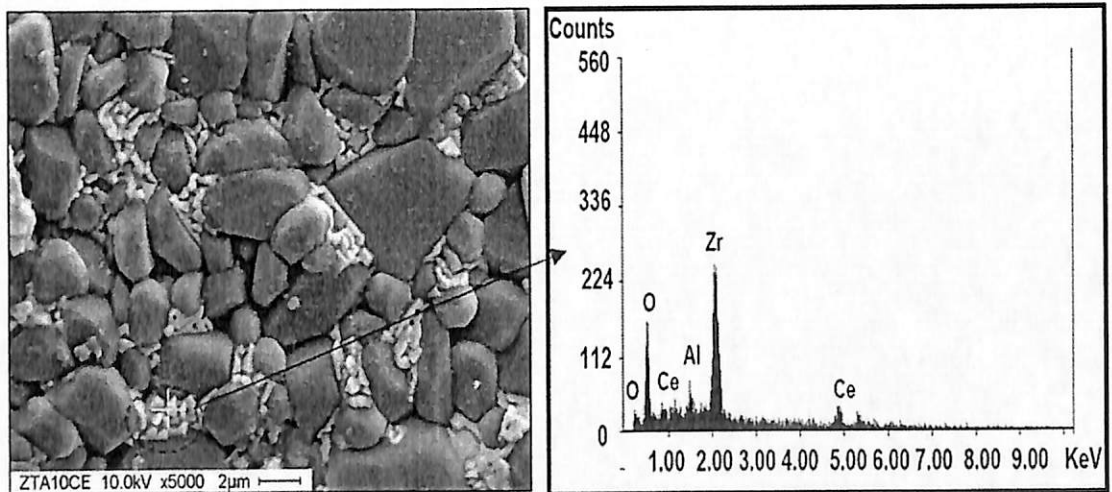


Figure 5: Microstructure and EDX results for ZTA with 15 wt.% CeO₂ ceramics. Platelet grains in white colour refer to Ce₂Zr₃O₁₀ compound.

A : Al₂O₃

ZY : (Zr_{0.935}Y_{0.065})O_{1.968}

CZ : Ce₂Zr₂O₁₀

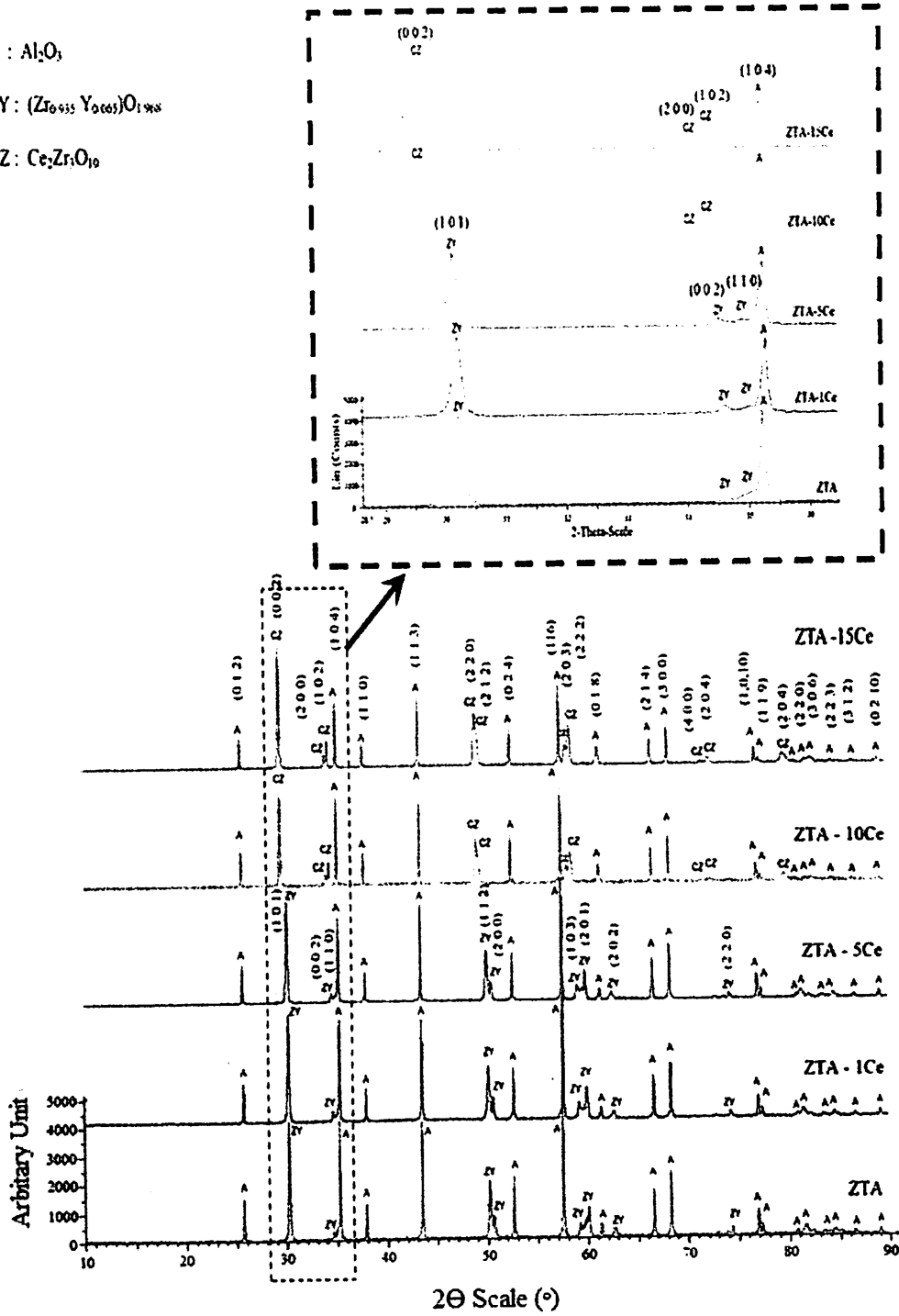


Figure 6: XRD results of CeO₂ addition in ZTA ceramics.

Figure 8 shows the formation of $\text{CeAl}_{11}\text{O}_{18}$ influence the Vickers hardness and fracture toughness values. Based on the presence of crack propagation, $\text{CeAl}_{11}\text{O}_{18}$ grains would likely to experience transgranular crack rather than intergranular crack. Intergranular crack are known to absorb more energy from the propagated crack, while transgranular crack will absorbed less energy.

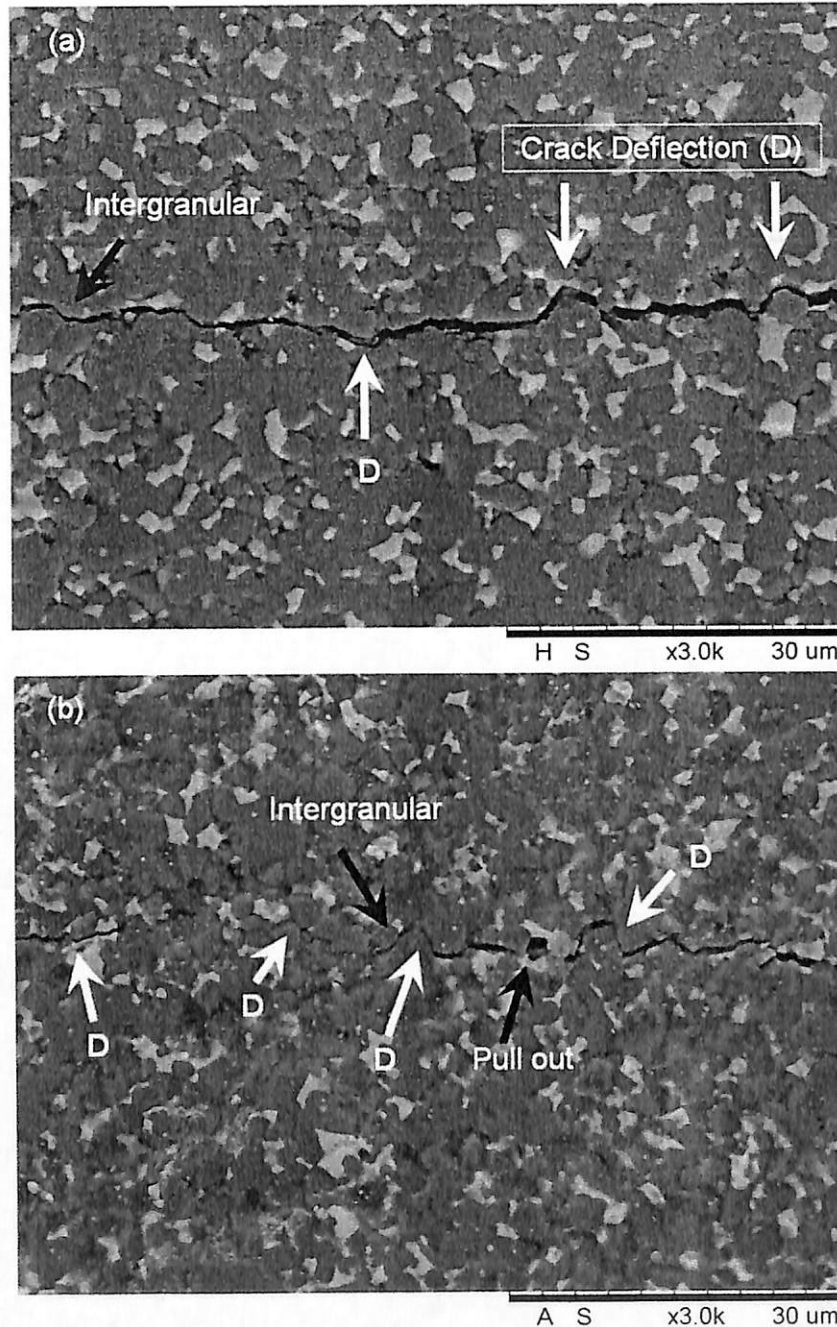


Figure 8: Crack path in the (a) ZTA0.7MgO without CeO_2 and (b) ZTA0.7MgO-1.0 wt.% CeO_2 induced by Vickers indentation. Crack propagation from right to left. Arrows indicates that major toughening mechanisms are crack deflection.

4.3 Part 3: Wear performance

The continuation from Part 1 and 2, three types of additives were fabricated as cutting inserts rhombic and wear performance is investigated. There are MgO with average of 500 micro particle size (Alfa Aesar) from now on is denoted as ZMM, nano particle MgO in average particle sizes of 20 nm (Strem Chemicals), is ZMN and CeO₂ (Sigma-Aldrich Corporation, 99.0%) represent as ZMC was added to the Al₂O₃/YSZ. Figure 9 shows SEM micrographs of the flank and notch wear of ZTA ceramic cutting tool.

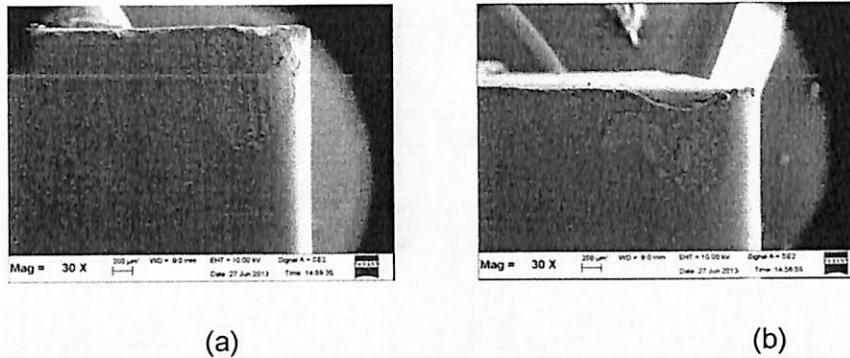


Figure 9: SEM micrographs of the (a) flank wear and (b) notch wear of ZTA ceramic cutting tool.

4.3.2 The Cutting Speed Influences on Tool Wear of ZTA

The result of the nose and crater tool wear plotted in Figure 10 and 11 shows that by rising the cutting speed, both nose wear and crater wear showing increment of tool wear for all types of cutting tool used. By rising the cutting speed, abrasion between the cutting tip and the cutting surface will be increased and therefore resulting higher wear [12]. There are two ways of abrasion wear may happen while machining using ceramic insert. It is due to hard wear debris of micro chipped ceramic tool and work materials debris [13] that are sandwiched between the machine surface and the tool at the cutting interface. These debris plough in the tool and causing wear increment. Another way that abrasion wear may occur at high cutting temperature as plastic flow of the tool material occur. The lamina (thin layer) of chip flow may abrade the plasticized tool layer [13]. Therefore, as the cutting speed is raised, the cutting temperature also will rise and increased the abrasion on the cutting tip thus causing greater tool wear.

However, reversal result observed in surface roughness where by increasing the cutting speed, the value of roughness average (Ra) decreased although the tool wear keep increasing. The result is shows in Figure 12. This condition occurs in high

COMPLETED FINAL REPORT FORM

 	<h2 style="margin: 0;">RU GRANT FINAL REPORT FORM</h2>
---	--

Please email a softcopy of this report to rcmo@usm.my

A	PROJECT DETAILS
i	Title of Research: HIGH WEAR RESISTANT CERAMIC CUTTING INSERTS WITH ENHANCED TOUGHNESS FOR HIGH-SPEED MACHINING
ii	Account Number: 1001/PBAHAN/811212
iii	Name of Research Leader: PROF. DR. HJ. ZAINAL ARIFIN HJ. AHMAD
iv	Name of Co-Researcher: PROF. DR MANI MARAN RATNAM
v	Duration of this research: <ul style="list-style-type: none"> a) Start Date : 15th JULY 2012 b) Completion Date : 14th JULY 2015 c) Duration : 42 MONTHS d) Revised Date (if any) : 14th JANUARY 2016
B	ABSTRACT OF RESEARCH
	<p>There are three parts in this research. Part 1 implicates the effect of CeO₂ addition into ZTA which indicates the addition of 5 wt.% of CeO₂ (ZMC) produces the optimum fracture toughness of 8.38 MPa.√m with Vickers hardness value is 1678 HV. The reduction of fracture toughness and Vickers hardness values is due to the appearance of Ce₂Zr₃O₁₀ phase which is related to the over-stabilised. Part 2 is focused on the effect of CeO₂ into ZTA with the addition of 0.7 wt.% MgO (ZMM) ceramics. This part showed the relation between crack and fracture toughness which indicates that the value is increase from 6.19 ± 0.26 MPa.√m to 6.59 ± 0.23 MPa.√m with the presence of crack deflection. However, the formation of CeAl₁₁O₁₈ phase was observed; this consequently decreases the hardness and fracture toughness of the ZMM ceramics. Part 3 is focused on the effect of MgO nanoparticles on ZMN ceramics. The addition of 0.5 wt. % nano-MgO showed the highest fracture toughness value of 9.14 MPa.√m with Vickers hardness value is 1591 HV. This optimum result is due to the appearance of minority phases, i.e., MgAl₁₁CeO₁₉ and MgAl₂O₄ as detected by XRD which started to present at 0.5 wt. % nano-MgO. Both phases hinder the grain growth known as pinning effect. Wear measurement has been carried out by fabricate all the ZMN with MgO nanoparticles additions as rhombic 80° cutting inserts and further for machining process. The result shows that the additions of 0 to 0.5 wt.% decreased the nose wear areas from 0.0578 to 0.0528 mm² which is refer to good wear resistance. Therefore, various toughness and hardness values of ZTA ceramics can be produced through the manipulation of ZrO₂ co-stabilizers.</p>

Abstrak

Terdapat tiga bahagian dalam kajian ini. Bahagian pertama membabitkan kesan penambahan CeO₂ ke atas ZTA yang menunjukkan penambahan 5 wt.% CeO₂ (ZMC) menghasilkan ketiatan optimum (8.38 MPa.√m) dengan nilai kekerasan Vickers adalah 1678 HV. Penurunan nilai ketiatan dan kekerasan Vickers ini disebabkan oleh kemunculan fasa Ce₂Zr₃O₁₀ yang berkaitan dengan lebih penstabil (overstabilise). Bahagian kedua difokuskan pada kesan CeO₂ ke atas ZTA dengan penambahan 0.7 wt.% MgO (ZMM). Bahagian ini menunjukkan hubungan antara pesongan retak dan ketiatan yang menunjukkan bahawa peningkatan dari 6.19 ± 0.26 MPa.√m kepada 6.59 ± 0.23 MPa.√m dengan kehadiran retak penyambung dan retak pesongan. Walau bagaimanapun, pembentukan fasa CeAl₁₁O₁₈ telah dikesan. Ini menurunkan nilai kekerasan dan ketiatan seramik ZMM. Bahagian ketiga memberi tumpuan kepada kesan nanopartikel MgO ke atas seramik ZMN. Kemunculan fasa minoriti, iaitu MgAl₁₁CeO₁₉ pada penambahan 0.3 % berat dan 0.5 % berat seperti yang dikesan oleh XRD dan butiran memanjang yang diperhatikan melalui mikrograf SEM, memainkan peranan penting terhadap penambahbaikan sifat-sifat mekanikal seramik ZMN. Penambahan 0.5 % berat MgO nanopartikel menunjukkan nilai ketiatan patah (9.14 MPa.√m) yang paling tinggi dengan nilai kekerasan Vickers (1591 HV). Hasil optimum ini dipercayai kerana kemunculan fasa minoriti, iaitu MgAl₁₁CeO₁₉ dan MgAl₂O₄ yang mula hadir pada 0.5 wt. % MgO nanopartikel seperti yang dikesan oleh XRD. Kedua-dua fasa ini menghalang pertumbuhan butir yang dikenali sebagai kesan penyematan. Pengukuran kehausan telah dijalankan dengan menggunakan seramik ZMN dengan penambahan MgO nanopartikel sebagai mata alat pemotong berbentuk rombuk 80° untuk proses pemesinan. Keputusan menunjukkan kehausan mata alat pemotong menurun dari 0.0578 -0.0528 mm² dengan penambahan 0 – 0.5 % berat MgO nanopartikel dan ini merujuk kepada rintangan haus yang baik. Oleh itu, melalui kajian ini, kepelbagaian terhadap kekuatan seramik ZTA boleh dihasilkan dengan memanipulasikan bahan penstabil bersama ZrO₂.

C BUDGET & EXPENDITURE

i Total Approved Budget : RM 208 500.00

Yearly Budget Distributed

Year 1 : RM 108 500.00

Year 2 : RM 47 500.00

Year 3 : RM 52 500.00

Total Expenditure : RM 192 179.36

Balance : RM 16 320.64

Percentage of Amount Spent (%) : 92.17%

Please attach final account statement (eStatement) to indicate the project expenditure

ii Equipment Purchased Under Vot 35000

No.	Name of Equipment	Amount (RM)	Location	Status
1.	High temperature Chamber Furnace	33230.00	School of Materials & Mineral Resources Engineering, Engineering Campus, Universiti Sains Malaysia, Seri Ampangan, 14300 Nibong Tebal, Penang, Malaysia.	Active
2.	Hand Press	16830.00	School of Materials & Mineral Resources Engineering, Engineering Campus, Universiti Sains Malaysia, Seri Ampangan, 14300 Nibong Tebal, Penang, Malaysia.	Active

Please attach the Asset/Inventory Return Form (Borang Penyerahan Aset/Inventori) – Appendix 1

D	RESEARCH ACHIEVEMENTS																			
i	Project Objectives (as stated/approved in the project proposal)																			
	<table border="1"> <thead> <tr> <th>No.</th> <th>Project Objectives</th> <th>Achievement</th> </tr> </thead> <tbody> <tr> <td>1</td> <td>Improve toughness of ZTA ceramics by CeO₂ addition</td> <td>100%</td> </tr> <tr> <td>2</td> <td>Study the effect of particle size of MgO to ZTA-CeO₂ ceramics microstructures and mechanical properties.</td> <td>100%</td> </tr> <tr> <td>3</td> <td>To fabricate the ceramic cutting inserts having higher wears resistant.</td> <td>100%</td> </tr> <tr> <td>4</td> <td>To optimize the fabrication parameters for an excellent properties of high speed ceramic cutting inserts</td> <td>100%</td> </tr> <tr> <td>5</td> <td>Final Report</td> <td>100%</td> </tr> </tbody> </table>	No.	Project Objectives	Achievement	1	Improve toughness of ZTA ceramics by CeO ₂ addition	100%	2	Study the effect of particle size of MgO to ZTA-CeO ₂ ceramics microstructures and mechanical properties.	100%	3	To fabricate the ceramic cutting inserts having higher wears resistant.	100%	4	To optimize the fabrication parameters for an excellent properties of high speed ceramic cutting inserts	100%	5	Final Report	100%	
No.	Project Objectives	Achievement																		
1	Improve toughness of ZTA ceramics by CeO ₂ addition	100%																		
2	Study the effect of particle size of MgO to ZTA-CeO ₂ ceramics microstructures and mechanical properties.	100%																		
3	To fabricate the ceramic cutting inserts having higher wears resistant.	100%																		
4	To optimize the fabrication parameters for an excellent properties of high speed ceramic cutting inserts	100%																		
5	Final Report	100%																		

ii	Research Output																						
	<p>a) Publications in ISI Web of Science/Scopus</p> <p>b)</p>																						
	<table border="1"> <thead> <tr> <th>No.</th> <th>Publication (authors,title,journal,year,volume,pages,etc.)</th> <th>Status of Publication (published/accepted/ under review)</th> </tr> </thead> <tbody> <tr> <td>1</td> <td>N.A. Rejab, A.Z.A. Azhar, M.M. Ratnam, Z.A. Ahmad, Role of MgO nanoparticles on zirconia-toughened alumina-5 wt-% CeO₂ ceramics mechanical properties, Mater. Sci. Technol. (2016) 1–8. doi:10.1080/02699931.2011.628301 (ISI Web of Science)</td> <td>Published</td> </tr> <tr> <td>2</td> <td>N.A. Rejab, A.Z.A. Azhar, K.S. Kian, M.M. Ratnam, Z.A. Ahmad, Effects of MgO addition on the phase, mechanical properties, and microstructure of zirconia-toughened alumina added with CeO₂ (ZTA–CeO₂) ceramic composite, Mater. Sci. Eng. A. 595 (2014) 18–24. doi:10.1016/j.msea.2013.11.091. (ISI Web of Science)</td> <td>Published</td> </tr> <tr> <td>3</td> <td>N.A. Rejab, A.Z.A. Azhar, M.M. Ratnam, Z.A. Ahmad, The relationship between microstructure and fracture toughness of zirconia toughened alumina (ZTA) added with MgO and CeO₂, Int. J. Refract. Met. Hard Mater. 41 (2013) 522–530. doi:10.1016/j.ijrmhm.2013.07.002. (ISI Web of Science)</td> <td>Published</td> </tr> <tr> <td>4</td> <td>N.A. Rejab, A.Z.A. Azhar, M.M. Ratnam, Z.A. Ahmad, The effects of CeO₂ addition on the physical, microstructural and mechanical properties of yttria stabilized zirconia toughened alumina (ZTA), Int. J. Refract. Met. Hard Mater. 36 (2013) 162–166. doi:10.1016/j.ijrmhm.2012.08.010. (ISI Web of Science)</td> <td>Published</td> </tr> <tr> <td>5</td> <td>N.A. Rejab, A.Z.A. Azhar, M.M. Ratnam, Z.A. Ahmad, Structural and Microstructure Relationship with Fracture Toughness of CeO₂ Addition into Zirconia Toughened Alumina (ZTA) Ceramic Composites, Adv. Mater. Res. 620 (2012) 252–256. doi:10.4028/www.scientific.net/AMR.620.252. (Scopus)</td> <td>Published</td> </tr> <tr> <td>6</td> <td>N.A. Rejab, D.I.S. Zhwan, M.A. Afifah, A. Zainal Arifin, Role of Ce₂Zr₃O₁₀ phase on the Microstructure and Fracture Toughness of ZTA Composites, 840 (2016) 57–60. doi:10.4028/www.scientific.net/MSF.840.57. (Scopus)</td> <td>Published</td> </tr> </tbody> </table>	No.	Publication (authors,title,journal,year,volume,pages,etc.)	Status of Publication (published/accepted/ under review)	1	N.A. Rejab, A.Z.A. Azhar, M.M. Ratnam, Z.A. Ahmad, Role of MgO nanoparticles on zirconia-toughened alumina-5 wt-% CeO ₂ ceramics mechanical properties, Mater. Sci. Technol. (2016) 1–8. doi:10.1080/02699931.2011.628301 (ISI Web of Science)	Published	2	N.A. Rejab, A.Z.A. Azhar, K.S. Kian, M.M. Ratnam, Z.A. Ahmad, Effects of MgO addition on the phase, mechanical properties, and microstructure of zirconia-toughened alumina added with CeO ₂ (ZTA–CeO ₂) ceramic composite, Mater. Sci. Eng. A. 595 (2014) 18–24. doi:10.1016/j.msea.2013.11.091. (ISI Web of Science)	Published	3	N.A. Rejab, A.Z.A. Azhar, M.M. Ratnam, Z.A. Ahmad, The relationship between microstructure and fracture toughness of zirconia toughened alumina (ZTA) added with MgO and CeO ₂ , Int. J. Refract. Met. Hard Mater. 41 (2013) 522–530. doi:10.1016/j.ijrmhm.2013.07.002. (ISI Web of Science)	Published	4	N.A. Rejab, A.Z.A. Azhar, M.M. Ratnam, Z.A. Ahmad, The effects of CeO ₂ addition on the physical, microstructural and mechanical properties of yttria stabilized zirconia toughened alumina (ZTA), Int. J. Refract. Met. Hard Mater. 36 (2013) 162–166. doi:10.1016/j.ijrmhm.2012.08.010. (ISI Web of Science)	Published	5	N.A. Rejab, A.Z.A. Azhar, M.M. Ratnam, Z.A. Ahmad, Structural and Microstructure Relationship with Fracture Toughness of CeO ₂ Addition into Zirconia Toughened Alumina (ZTA) Ceramic Composites, Adv. Mater. Res. 620 (2012) 252–256. doi:10.4028/www.scientific.net/AMR.620.252. (Scopus)	Published	6	N.A. Rejab, D.I.S. Zhwan, M.A. Afifah, A. Zainal Arifin, Role of Ce ₂ Zr ₃ O ₁₀ phase on the Microstructure and Fracture Toughness of ZTA Composites, 840 (2016) 57–60. doi:10.4028/www.scientific.net/MSF.840.57. (Scopus)	Published	
No.	Publication (authors,title,journal,year,volume,pages,etc.)	Status of Publication (published/accepted/ under review)																					
1	N.A. Rejab, A.Z.A. Azhar, M.M. Ratnam, Z.A. Ahmad, Role of MgO nanoparticles on zirconia-toughened alumina-5 wt-% CeO ₂ ceramics mechanical properties, Mater. Sci. Technol. (2016) 1–8. doi:10.1080/02699931.2011.628301 (ISI Web of Science)	Published																					
2	N.A. Rejab, A.Z.A. Azhar, K.S. Kian, M.M. Ratnam, Z.A. Ahmad, Effects of MgO addition on the phase, mechanical properties, and microstructure of zirconia-toughened alumina added with CeO ₂ (ZTA–CeO ₂) ceramic composite, Mater. Sci. Eng. A. 595 (2014) 18–24. doi:10.1016/j.msea.2013.11.091. (ISI Web of Science)	Published																					
3	N.A. Rejab, A.Z.A. Azhar, M.M. Ratnam, Z.A. Ahmad, The relationship between microstructure and fracture toughness of zirconia toughened alumina (ZTA) added with MgO and CeO ₂ , Int. J. Refract. Met. Hard Mater. 41 (2013) 522–530. doi:10.1016/j.ijrmhm.2013.07.002. (ISI Web of Science)	Published																					
4	N.A. Rejab, A.Z.A. Azhar, M.M. Ratnam, Z.A. Ahmad, The effects of CeO ₂ addition on the physical, microstructural and mechanical properties of yttria stabilized zirconia toughened alumina (ZTA), Int. J. Refract. Met. Hard Mater. 36 (2013) 162–166. doi:10.1016/j.ijrmhm.2012.08.010. (ISI Web of Science)	Published																					
5	N.A. Rejab, A.Z.A. Azhar, M.M. Ratnam, Z.A. Ahmad, Structural and Microstructure Relationship with Fracture Toughness of CeO ₂ Addition into Zirconia Toughened Alumina (ZTA) Ceramic Composites, Adv. Mater. Res. 620 (2012) 252–256. doi:10.4028/www.scientific.net/AMR.620.252. (Scopus)	Published																					
6	N.A. Rejab, D.I.S. Zhwan, M.A. Afifah, A. Zainal Arifin, Role of Ce ₂ Zr ₃ O ₁₀ phase on the Microstructure and Fracture Toughness of ZTA Composites, 840 (2016) 57–60. doi:10.4028/www.scientific.net/MSF.840.57. (Scopus)	Published																					

7	A.Z.A. Azhar, N.A. Rejab, M. Hasmaliza, M.M. Ratnam, A.A. Zainal, The Effects of Cr ₂ O ₃ Addition on Fracture Toughness and Phases of ZTA Ceramic Composite, Adv. Mater. Res. 620 (2012) 35–39. doi:10.4028/www.scientific.net/AMR.620.35. (Scopus)	Published
8	Z.D.I. Sktani, A.Z.A. Azhar, M.M. Ratnam, Z.A. Ahmad, The influence of in-situ formation of hibonite on the properties of zirconia toughened alumina (ZTA) composites, Ceram. Int. 40 (2014) 6211–6217. doi:10.1016/j.ceramint.2013.11.076. (ISI Web of Science)	Published
9	Z. Dilshad, I. Sktani, M.M. Ratnam, Z.A. Ahmad, Influence of Combined CaO and CaCO ₃ Additions on the Microstructure and Properties of ZTA, J. Aust. Ceram. Soc. 52 (2016) 167–176. (ISI Web of Science)	Published
10	A. Arab, Z. Ahmad, R. Ahmad, Effects of yttria stabilized zirconia (3Y-TZP) percentages on the ZTA dynamic mechanical properties, Int. J. Refract. Met. Hard Mater. 50 (2015) 157–162. (ISI Web of Science)	Published
11	Ali Arab, Roslan Ahmad, Zainal Arifin Ahmad, Effect of SrCO ₃ additive on the dynamic compressive strength of ZTA, International Journal of Minerals, Metallurgy and Materials, Accepted for publication on Mon 11/16/2015 6:07 PM, IJM-09-2015-0766.R1. (ISI, Q3, Impact Factors = 0.791) (ISI Web of Science)	Accepted
12	A.M. Ali, A. Zahirani, A. Azhar, M.M. Ratnam, Z.A. Ahmad, Wear Analysis of ZTA-MgO Ceramic Cutting Inserts On Stainless Steel 316L Machining, Adv. Mater. Res. 1087 (2015) 101–105. doi:10.4028/www.scientific.net/AMR.1087.101. (Scopus)	Published
13	A.M. Ali, N.S. Abdullah, M. Ratnam, Z.A. Ahmad, The Cutting Speed Influences on Tool Wear of ZTA Ceramic Cutting Tools and Surface Roughness of Work Material Stainless Steel 316L During High Speed Machining, Mater. Sci. Forum. 840 (2016) 315–320. doi:10.4028/www.scientific.net/MSF.840.315. (Scopus)	Published
14	H. Manshor, S. Md Aris, A.Z.A. Azhar, E.C. Abdullah, Z.A. Ahmad, Effect of titania (TiO ₂) addition to zirconia toughened alumina (ZTA) phases, hardness and microstructure, Advanced Materials Research vol. 1087 (2015) 293-298. Doi:10.4028/www.scientific.net/AMR.1087.293 (Scopus)	Published

c) Publications in Other Journals

No.	Publication (authors, title, journal, year, volume, pages, etc.)	Status of Publication (published/accepted/ under review)

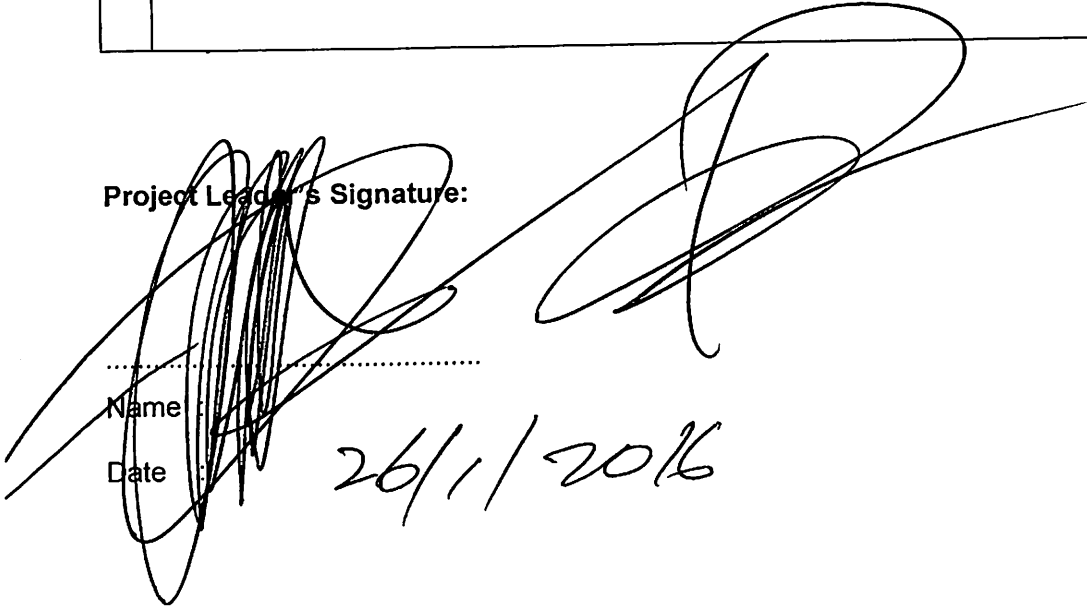
d) Other Publications

(book, chapters in book, monograph, magazine, etc.)

No.	Publication (authors, title, journal, year, volume, pages, etc.)	Status of Publication (published/accepted/ under review)

G	PROBLEMS/CONSTRAINTS/CHALLENGES IF ANY
	<i>(Please provide issues arising from the project and how they were resolved)</i>
H	RECOMMENDATION
	<i>(Please provide recommendations that can be used to improve the delivery of information, grant management, guidelines and policy, etc.)</i>

Project Leader's Signature:



.....
Name :

Date :

26/1/2016

I

COMMENTS, IF ANY/ENDORSEMENT BY PTJ'S RESEARCH COMMITTEE

The output of this project is excellent. The researchers have published 8 ISI papers and 6 Scopus listed journals.

Signature and Stamp of Chairperson of PTJ's Evaluation Committee

Name :
Date : 1/2/16

PROFESOR MADYA DR. KHAIRUNISAK ABDUL RAZAK
Timbalan Dekan
Penyelidikan, Siswazah dan Jaringan
Pusat Peng. Kej. Bahan & Sumber Mineral
Kampus Kejuruteraan
Universiti Sains Malaysia

Signature and Stamp of Dean/ Director of PTJ

Name :
Date : 1/2/2016.

PROFESOR DR. ZUHAILAWATI HUSSAIN
Dekan
P. Peng. Kej. Bahan & Sumber Mineral
Kampus Kejuruteraan
Universiti Sains Malaysia

**PROJECT FINANCIAL ACCOUNT
STATEMENT (E-STATEMENT)**

Maklumat Asas

Kod : U0902
No. Rujukan : 2012/0390
Jenis : RUI (Individual)
Tajuk : High Wear Resistant Ceramic Cutting Inserts With Enhanced Toughness For High-Speed Machining
Pusat Tanggungjawab : PUSAT PENGAJIAN KEJURUTERAAN BAHAN DAN SUMBER MINERAL

Peralatan yang Diluluskan :

Bil	Peralatan	Harga (RM)
1	High Temperature Chamber Furnance	50,000.00
2	Hand Press	12,000.00

Kelas RU : Individual
Status : AKTIF
Tarikh Mula : 15 July 2012
Tarikh Hingga - Asal : 14 July 2015
Tarikh Hingga - Lanjutan Pertama : 14 January 2016
Tarikh Tamat : 14 January 2016

Peringatan laporan Kemajuan :

Bil	Tarikh Peringatan / Tarikh Luput	Tarikh Terima
1	31 January 2013	Tiada Maklumat

Dokumen Berkaitan :

Bil	Dokumen
1	U0902.pdf

Maklumat Penyelidik

Ketua Penyelidik : PROFESOR DR. ZAINAL ARIFIN BIN AHMAD (AKTIF)

Penyelidik Bersama :

Bil	Nama	Institusi/PTJ	Status
1	PROFESOR DR. MANI MARAN A/L RATNAM	PUSAT PENGAJIAN KEJURUTERAAN MEKANIK	AKTIF

Maklumat Kewangan

No. Akaun : 1001 / PBAHAN / 811212

Penaja : USM (RU)
Kategori Penaja : USM
Peruntukan Diluluskan : RM 208,500.00

Pecahan Peruntukan Diluluskan Mengikut Tahun

Tahun 2012 : RM 108,500.00
 Tahun 2013 : RM 47,500.00
 Tahun 2014 : RM 52,500.00

Peruntukan yang Telah Diterima : RM 208,500.00

Pecahan Peruntukan yang Telah Diterima Mengikut Tahun

Tahun 2012 : RM 108,500.00
 Tahun 2013 : RM 47,500.00
 Tahun 2014 : RM 52,500.00

Pecahan Vot

Vot	Butiran Vot	Asal (RM)	Tambahan (RM)	Jumlah (RM)
2012				
11000	Gaji Dan Upahan	24,000.00	0.00	24,000.00
21000	Perbelanjaan Perjalanan Dan Sara Hidup	1,000.00	0.00	1,000.00
23000	Perhubungan Utiliti	500.00	0.00	500.00
27000	Bekalan Dan Bahan-bahan Lain	15,000.00	0.00	15,000.00
28000	Penyelenggaraan Dan Pembaikan Kecil Yang Dibeli	2,000.00	0.00	2,000.00
29000	Perkhidmatan Iktisas Dan Perkhidmatan Lain Yang Dibeli Dan Hospitaliti	4,000.00	0.00	4,000.00
35000	Harta Modal - Harta Modal Lain	62,000.00	0.00	62,000.00
Jumlah Peruntukan Tahun 2012 (RM)		108,500.00	0.00	108,500.00
2013				
11000	Gaji Dan Upahan	24,000.00	0.00	24,000.00
21000	Perbelanjaan Perjalanan Dan Sara Hidup	1,000.00	0.00	1,000.00
23000	Perhubungan Utiliti	500.00	0.00	500.00

27000	Bekalan Dan Bahan-bahan Lain	15,000.00	0.00	15,000.00
28000	Penyelenggaraan Dan Pembaikan Kecil Yang Dibeli	3,000.00	0.00	3,000.00
29000	Perkhidmatan Iktisas Dan Perkhidmatan Lain Yang Dibeli Dan Hospitaliti	4,000.00	0.00	4,000.00
Jumlah Peruntukan Tahun 2013 (RM)		47,500.00	0.00	47,500.00
2014				
11000	Gaji Dan Upahan	24,000.00	0.00	24,000.00
21000	Perbelanjaan Perjalanan Dan Sara Hidup	8,000.00	0.00	8,000.00
23000	Perhubungan Utiliti	500.00	0.00	500.00
27000	Bekalan Dan Bahan-bahan Lain	8,000.00	0.00	8,000.00
28000	Penyelenggaraan Dan Pembaikan Kecil Yang Dibeli	3,000.00	0.00	3,000.00
29000	Perkhidmatan Iktisas Dan Perkhidmatan Lain Yang Dibeli Dan Hospitaliti	9,000.00	0.00	9,000.00
Jumlah Peruntukan Tahun 2014 (RM)		52,500.00	0.00	52,500.00
Jumlah Keseluruhan (RM)		208,500.00	0.00	208,500.00

Maklumat Staf Projek

Bil	Nama	Jawatan	Tarikh Mula	Tarikh Tamat	Catatan
1	ABDUL RASHID BIN JAMALUDIN	Pegawai Penyelidik - Sarjana (N41)	17 Ogos 2015	16 November 2015	
2	ABDUL RASHID BIN JAMALUDIN	Pegawai Penyelidik - Sarjana (N41)	17 November 2015	14 Januari 2016	Pelanjutan Perkhidmatan dan Pertukaran Gred Gaji Dari Harian ke Bulanan
3	AHMAD ZAHIRANI BIN AHMAD AZHAR	Pegawai Penyelidik - Sarjana (N41)	3 September 2012	2 November 2012	Pelantikan Baru
4	AHMAD ZAHIRANI BIN AHMAD AZHAR	Pegawai Penyelidik - Sarjana (N41)	1 November 2012	31 Disember 2012	Pelantikan Baru
5	AHMAD ZAHIRANI BIN AHMAD AZHAR	Pegawai Penyelidik - Sarjana (N41)	2 Januari 2013	31 Mac 2013	Pelantikan Baru
6	AHMAD ZAHIRANI BIN AHMAD AZHAR	Pegawai Penyelidik - Sarjana (N41)	1 April 2013	31 Mei 2013	Pelantikan Baru
7	ERNY RAUDHOH BT MOHD SHAFIE	Pegawai Penyelidik - Ijazah (N41)	2 November 2015	31 Disember 2015	
8	MOHAMAD SHAUFI BIN ISHAK	Pembantu Penyelidik - SPM (N17)	1 Julai 2013	15 Ogos 2013	Pelantikan Baru
9	NIK AKMAR BIN REJAB	Pegawai Penyelidik -	1 Disember	31 Mei 2015	Pelantikan Baru

		Sarjana (N41)	2014		
10	NIK AKMAR BIN REJAB	Pegawai Penyelidik - Sarjana (N41)	1 Jun 2015	31 Ogos 2015	Pelanjutan Perkhidmatan
11	NIK AKMAR BIN REJAB	Pegawai Penyelidik - Sarjana (N41)	1 Jun 2015	31 Ogos 2015	Penamatan Perkhidmatan
12	WAN FAHMIN FAIZ BIN WAN ALI	Pegawai Penyelidik - Sarjana (N41)	1 April 2015	14 Julai 2015	
13	WAN FAHMIN FAIZ BIN WAN ALI	Pegawai Penyelidik - Sarjana (N41)	15 Julai 2015	14 Oktober 2015	
14	WAN FAHMIN FAIZ BIN WAN ALI	Pegawai Penyelidik - Doktor Falsafah (N41)	16 Oktober 2015	31 Disember 2015	Pelanjutan Perkhidmatan dan Pertukaran Gred Jawatan Dari Pegawai Penyelidik (Sarjana) ke Pegawai Penyelidik (PhD)

ima Projek

nyelidik

<u>Bil</u>	<u>Kod Dok</u>	<u>No Dok.</u>	<u>Tarikh Dokumen</u>	<u>Kod Akaun</u>	<u>Amaun</u>	<u>Keterangan</u>
DT	111					
1	WR	3295	10/9/2012	1001.111.PBAHAN.811212.	\$2,393.15	GAJI HARIAN BLN 10/2012 (ii)
2	WR	3338	11/7/2012	1001.111.PBAHAN.811212.	\$2,646.85	GAJI HARIAN BLN 11/2012
3	WR	3394	12/5/2012	1001.111.PBAHAN.811212.	\$2,142.25	GAJI HARIAN BLN 12/2012
4	WR	3446	1/14/2013	1001.111.PBAHAN.811212.	\$2,517.65	GAJI HARIAN BLN 01/2013 (ii)
5	WR	3488	2/5/2013	1001.111.PBAHAN.811212.	\$2,393.15	GAJI HARIAN BLN 02/2013
6	WR	3552	3/12/2013	1001.111.PBAHAN.811212.	\$2,014.85	GAJI HARIAN BLN 03/2013 (ii)
7	WR	3609	4/10/2013	1001.111.PBAHAN.811212.	\$2,393.15	GAJI HARIAN 04/2013 II
8	WR	3649	5/13/2013	1001.111.PBAHAN.811212.	\$2,517.65	GAJI HARIAN 05/2013 II
9	WR	3682	6/13/2013	1001.111.PBAHAN.811212.	\$2,014.85	GAJI HARIAN 06/2013 IV
10	WR	3758	8/15/2013	1001.111.PBAHAN.811212.	\$1,192.17	GAJI HARIAN BLN 08/2013 (i)
11	WR	4565	12/23/2014	1001.111.PBAHAN.811212.	\$3,149.68	GAJI PROJEK BULAN 12/2014-1
12	WR	4604	1/26/2015	1001.111.PBAHAN.811212.	\$3,149.68	GAJI PROJEK BULAN 1/2015-1
13	WR	4636	2/24/2015	1001.111.PBAHAN.811212.	\$3,149.68	GAJI PROJEK BULAN 2/2015-1
14	WR	4684	3/24/2015	1001.111.PBAHAN.811212.	\$3,149.68	GAJI PROJEK BULAN 3/2015-1
15	WR	4720	4/23/2015	1001.111.PBAHAN.811212.	\$3,149.68	GAJI PROJEK BULAN 4/2015-1
16	WR	4735	5/5/2015	1001.111.PBAHAN.811212.	\$3,149.68	BAYARAN GAJI TAMBAHAN A05/2015-1
17	WR	4757	5/25/2015	1001.111.PBAHAN.811212.	\$6,299.36	GAJI PROJEK 05/2015-1
18	WR	4798	6/25/2015	1001.111.PBAHAN.811212.	\$6,299.36	GAJI PROJEK 06/2015-1
19	WR	4845	7/24/2015	1001.111.PBAHAN.811212.	\$3,149.68	GAJI PROJEK 07/2015-1
20	WR	4854	8/4/2015	1001.111.PBAHAN.811212.	\$1,422.38	BAYARAN GAJI TAMBAHAN 2015/A08-1
21	WR	4878	8/24/2015	1001.111.PBAHAN.811212.	\$3,149.68	GAJI PROJEK 08/2015-1
22	WR	4888	9/3/2015	1001.111.PBAHAN.811212.	\$1,729.15	BAYARAN GAJI TAMBAHAN 2015/A09-1
23	WR	4918	9/21/2015	1001.111.PBAHAN.811212.	\$3,149.68	GAJI PROJEK 09/2015-1
24	WR	4969	11/2/2015	1001.111.PBAHAN.811212.	\$1,422.38	BAYARAN GAJI TAMBAHAN 2015/A11-1
25	WR	4975	11/12/2015	1001.111.PBAHAN.811212.	\$1,785.61	BAYARAN GAJI TAMBAHAN 2015/D11-1
26	WR	4977	11/12/2015	1001.111.PBAHAN.811212.	\$6,422.85	BAYARAN GAJI HARIAN 2015/E11-1
27	WR	4994	11/20/2015	1001.111.PBAHAN.811212.	\$3,458.53	GAJI PROJEK 11/2015-1

na Projek

nyelidik

<u>Sl</u>	<u>Kod Dok</u>	<u>No Dok.</u>	<u>Tarikh Dokumen</u>	<u>Kod Akaun</u>	<u>Amaun</u>	<u>Keterangan</u>
28	WR	5005	12/3/2015	1001.111.PBAHAN.811212.	\$2,742.04	BAYARAN GAJI TAMBAHAN 2015/A12-2
29	WR	5009	12/3/2015	1001.111.PBAHAN.811212.	\$1,468.79	BAYARAN GAJI TAMBAHAN 2015/D12-1
30	WR	5029	12/10/2015	1001.111.PBAHAN.811212.	\$1,387.55	BAYARAN GAJI HARIAN 2015/E12-1
31	WR	5040	12/22/2015	1001.111.PBAHAN.811212.	\$6,608.21	GAJI PROJEK 12/2015-1
32	WR	5041	12/22/2015	1001.111.PBAHAN.811212.	\$2,837.03	GAJI PROJEK 12/2015-2
					\$94,456.08	

<u>Sl</u>	<u>Kod Dok</u>	<u>No Dok.</u>	<u>Tarikh Dokumen</u>	<u>Kod Akaun</u>	<u>Amaun</u>	<u>Keterangan</u>
IT 221						
33	BV	43312	1/30/2013	1001.221.PBAHAN.811212.	\$198.00	PENDAHULUAN DIRI/TUNTUTAN PERJALANAN
34	BV	43312	1/30/2013	1001.221.PBAHAN.811212.	\$540.00	PENDAHULUAN DIRI/TUNTUTAN PERJALANAN
35	BV	43312	1/30/2013	1001.221.PBAHAN.811212.	\$838.00	PENDAHULUAN DIRI/TUNTUTAN PERJALANAN
36	BV	52335	8/1/2013	1001.221.PBAHAN.811212.	\$296.00	Bayaran:PFPBAHAN30000 00002656
37	BV	69402	7/2/2014	1001.221.PBAHAN.811212.	\$1,600.00	Bayaran:PHPBAHAN30000 00000192
38	BV	90826	10/2/2015	1001.221.PBAHAN.811212.	\$539.64	Bayaran:PHPBAHAN30000 00000252
39	BV	95533	12/2/2015	1001.221.PBAHAN.811212.	\$24.00	Bayaran:PFPBAHAN30000 00004943
40	BV	95533	12/2/2015	1001.221.PBAHAN.811212.	\$103.40	Bayaran:PFPBAHAN30000 00004943
41	BV	95533	12/2/2015	1001.221.PBAHAN.811212.	\$338.20	Bayaran:PFPBAHAN30000 00004943
42	BV	95533	12/2/2015	1001.221.PBAHAN.811212.	\$402.15	Bayaran:PFPBAHAN30000 00004943
43	BV	95533	12/2/2015	1001.221.PBAHAN.811212.	(\$1.35)	Bayaran:PFPBAHAN30000 00004943
44	JP	9464	12/21/2015	1001.221.PBAHAN.811212.	(\$402.15)	PELARASAN BV95533
45	JP	9464	12/21/2015	1001.221.PBAHAN.811212.	(\$338.20)	PELARASAN BV95533
46	JP	9464	12/21/2015	1001.221.PBAHAN.811212.	(\$103.40)	PELARASAN BV95533
47	JP	9464	12/21/2015	1001.221.PBAHAN.811212.	(\$24.00)	PELARASAN BV95533
					\$4,010.29	

<u>Sl</u>	<u>Kod Dok</u>	<u>No Dok.</u>	<u>Tarikh Dokumen</u>	<u>Kod Akaun</u>	<u>Amaun</u>	<u>Keterangan</u>
OT 226						
48	BV	84102	5/8/2015	1001.226.PBAHAN.811212.	\$470.00	Bayaran:PSPBAHAN30000 00005087
49	JR	28926	8/20/2015	1001.226.PBAHAN.811212.	\$85.00	Bayaran:PDPBAHAN30000 00001484

ma Projek

nyelidik

<u>Bil</u>	<u>Kod Dok</u>	<u>No Dok.</u>	<u>Tarikh Dokumen</u>	<u>Kod Akaun</u>	<u>Amount</u>	<u>Keterangan</u>
50	BV	91971	10/20/2015	1001.226.PBAHAN.811212.	\$806.00	Bayaran:PSPBAHAN30000 00005513
51	BV	92964	10/29/2015	1001.226.PBAHAN.811212.	\$2,700.00	Bayaran:PSPBAHAN30000 00005517
52	BV	94864	12/3/2015	1001.226.PBAHAN.811212.	\$2,120.00	Bayaran:PSPBAHAN30000 00005730
53	BV	95592	12/14/2015	1001.226.PBAHAN.811212.	\$2,700.00	Bayaran:PSPBAHAN30000 00005745
54	BV	95593	12/14/2015	1001.226.PBAHAN.811212.	\$806.00	Bayaran:PSPBAHAN30000 00005747
					\$9,687.00	
BT	227					
55	BV	44156	3/4/2013	1001.227.PBAHAN.811212.	\$164.19	Bayaran:PSPBAHAN30000 00002486
56	BV	44157	3/4/2013	1001.227.PBAHAN.811212.	\$4,200.00	Bayaran:PSPBAHAN30000 00002498
57	BV	48853	5/23/2013	1001.227.PBAHAN.811212.	\$1,254.65	Bayaran:PSPBAHAN30000 00002712
58	BV	52335	8/1/2013	1001.227.PBAHAN.811212.	\$8.00	Bayaran:PFBAHAN30000 00002656
59	BV	54230	9/12/2013	1001.227.PBAHAN.811212.	\$177.64	Bayaran:PSPBAHAN30000 00003048
60	BV	55733	10/9/2013	1001.227.PBAHAN.811212.	\$2,720.00	Bayaran:PSPBAHAN30000 00003049
61	BV	60438	12/27/2013	1001.227.PBAHAN.811212.	\$638.35	Bayaran:PSPBAHAN30000 00003485
62	BV	60440	12/27/2013	1001.227.PBAHAN.811212.	\$973.75	Bayaran:PSPBAHAN30000 00003510
63	BV	61332	1/21/2014	1001.227.PBAHAN.811212.	\$151.00	Bayaran:PSPBAHAN30000 00003598
64	BV	61728	2/4/2014	1001.227.PBAHAN.811212.	\$100.00	Bayaran:PSPBAHAN30000 00003709
65	BV	61891	2/12/2014	1001.227.PBAHAN.811212.	\$1,169.90	Bayaran:PSPBAHAN30000 00003633
66	BV	61892	2/12/2014	1001.227.PBAHAN.811212.	\$1,798.30	Bayaran:PSPBAHAN30000 00003632
67	BV	62786	3/3/2014	1001.227.PBAHAN.811212.	\$500.00	Bayaran:PSPBAHAN30000 00003109
68	BV	62933	3/7/2014	1001.227.PBAHAN.811212.	\$3,000.00	Bayaran:PSPBAHAN30000 00003838
69	BV	66105	5/5/2014	1001.227.PBAHAN.811212.	\$124.00	Bayaran:PSPBAHAN30000 00003811
70	BV	66465	5/14/2014	1001.227.PBAHAN.811212.	\$120.00	Bayaran:PSPBAHAN30000 00004074
71	BV	69431	7/2/2014	1001.227.PBAHAN.811212.	\$148.00	Bayaran:PSPBAHAN30000 00004218
72	BV	79871	2/5/2015	1001.227.PBAHAN.811212.	\$318.00	Bayaran:PSPBAHAN30000 00004680
73	BV	80151	2/10/2015	1001.227.PBAHAN.811212.	\$556.00	Bayaran:PSPBAHAN30000 00004761
74	BV	81158	3/11/2015	1001.227.PBAHAN.811212.	\$1,950.00	Bayaran:PSPBAHAN30000 00004858

na Projek

nyelidik

<u>Bil</u>	<u>Kod Dok</u>	<u>No Dok.</u>	<u>Tarikh Dokumen</u>	<u>Kod Akaun</u>	<u>Amaun</u>	<u>Keterangan</u>
75	BV	82291	3/26/2015	1001.227.PBAHAN.811212.	\$153.00	Bayaran:PSPBAHAN30000 00004878
76	BV	84099	5/8/2015	1001.227.PBAHAN.811212.	\$2,610.00	Bayaran:PSPBAHAN30000 00004768
77	BV	95517	12/14/2015	1001.227.PBAHAN.811212.	\$1,620.00	Bayaran:PSPBAHAN30000 00005694
78	BV	95568	12/14/2015	1001.227.PBAHAN.811212.	\$195.00	Bayaran:PSPBAHAN30000 00005749
79	BV	95569	12/14/2015	1001.227.PBAHAN.811212.	\$1,214.00	Bayaran:PSPBAHAN30000 00005830
80	BV	95570	12/14/2015	1001.227.PBAHAN.811212.	\$1,182.00	Bayaran:PSPBAHAN30000 00005831
81	BV	96170	12/16/2015	1001.227.PBAHAN.811212.	\$237.92	Bayaran:PFPBAHAN30000 00004985
					<u>\$27,283.70</u>	
BT 228						
82	BV	60445	12/27/2013	1001.228.PBAHAN.811212.	\$630.00	Bayaran:PSPBAHAN30000 00003656
					<u>\$630.00</u>	
BT 229						
83	BV	52335	8/1/2013	1001.229.PBAHAN.811212.	\$1,000.00	Bayaran:PFPBAHAN30000 00002656
84	BV	54135	9/13/2013	1001.229.PBAHAN.811212.	\$75.00	Bayaran:PFPBAHAN30000 00002723
85	BV	69139	6/24/2014	1001.229.PBAHAN.811212.	\$500.00	Bayaran:PFPBAHAN30000 00003478
86	JR	28896	8/20/2015	1001.229.PBAHAN.811212.	\$3,400.00	Bayaran:PDPBAHAN30000 00001511
87	JR	29903	12/16/2015	1001.229.PBAHAN.811212.	\$600.00	Bayaran:PDPBAHAN30000 00001345
					<u>\$5,575.00</u>	
BT 335						
88	BFA	2725	3/4/2013	1001.335.PBAHAN.811212.	\$33,230.00	Bayaran:PAPBAHAN30000 00000139
89	BFA	2811	5/22/2013	1001.335.PBAHAN.811212.	\$16,830.00	Bayaran:PAPBAHAN30000 00000145
					<u>\$50,060.00</u>	
BT 552						
90	BV	95517	12/14/2015	1001.552.PBAHAN.811212.	\$97.20	Bayaran:PSPBAHAN30000 00005694
91	BV	95568	12/14/2015	1001.552.PBAHAN.811212.	\$11.70	Bayaran:PSPBAHAN30000 00005749
92	BV	95569	12/14/2015	1001.552.PBAHAN.811212.	\$72.84	Bayaran:PSPBAHAN30000 00005830
93	BV	95570	12/14/2015	1001.552.PBAHAN.811212.	\$70.92	Bayaran:PSPBAHAN30000 00005831

ma Projek

nyelidik

<u>Bil</u>	<u>Kod Dok</u>	<u>No Dok.</u>	<u>Tarikh</u> <u>Dokumen</u>	<u>Kod Akaun</u>	<u>Amaun</u>	<u>Keterangan</u>
94	BV	95592	12/14/2015	1001.552.PBAHAN.811212.	\$162.00	Bayaran:PSPBAHAN30000 00005745
95	BV	95593	12/14/2015	1001.552.PBAHAN.811212.	\$48.36	Bayaran:PSPBAHAN30000 00005747
96	BV	96170	12/16/2015	1001.552.PBAHAN.811212.	\$14.27	Bayaran:PFPBAHAN30000 00004985
					<u>\$477.29</u>	
				Jumlah	<u>\$192,179.36</u>	

ASSET/INVENTORY RETURN FORM
(BORANG PENYERAHAN
ASET/INVENTORI)

BORANG PENYERAHAN ASET / INVENTORI
A. BUTIR PENYELIDIK

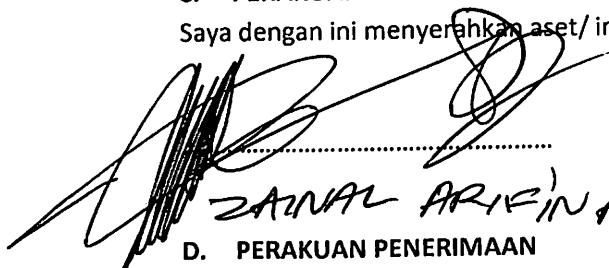
1. NAMA PENYELIDIK : PROF. ZAINAL ARIFIN B. AHMAD
2. NO STAF : AE 50019
3. PTJ :
4. KOD PROJEK : 2012/0390
5. TARIKH TAMAT PENYELIDIKAN : 14 JANUARY 2016

B. MAKLUMAT ASET / INVENTORI

BIL	KETERANGAN ASET	NO HARTA	NO. SIRI	HARGA (RM)
1	High Temperature Chamber Furnace	AK00007059 PBAHAN 2013	HT-127-12- 1700X	33230.00
2	Hand Press	AK00007114 PBAHAN 2013	01096SC	16830.00

C. PERAKUAN PENYERAHAN

Saya dengan ini menyerahkan aset/ inventori seperti butiran B di atas kepada pihak Universiti:



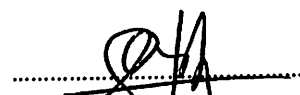
ZAINAL ARIFIN AHMAD Tarikh: 26/1/2016

D. PERAKUAN PENERIMAAN

Saya telah memeriksa dan menyemak setiap alatan dan didapati :

- Lengkap
- Rosak
- Hilang : Nyatakan.....
- Lain-lain : Nyatakan

Diperakukan Oleh :



 Pandatangan Nama : MOHD SAYUTI AZEMAN
 Pegawai Aset PTJ Tarikh : 26/1/2016

*Nota : Sesalinan borang yang telah lengkap perlulah dikemukakan kepada Unit Pengurusan Harta, Jabatan Bendahari dan Pejabat RCMO untuk tujuan rekod.

speed machining as the temperature increased when the cutting speed is increased making it easier for chip formation [14]. At high cutting speed, the heat generated in shear zone cannot be distributed during short time of machining [15] and therefore soften the metal, thus the chip flow easier and resulting better surface roughness. Other than that, it also due to the transformation toughening mechanism that occurs on the cutting tip [12]. As the cutting speed increased, the temperature around the tool tips increased allowing the toughening mechanism which observed in Sornakumar et al., works [16], reducing the surface roughness. Nevertheless, the negative effect on the Ra value will be seen when the cutting speed is increased to certain point where the tool failure take place.

Conversely, among these three type of tools, ZMN shows the best performance where the tool wear and surface roughness are low compared to other tools as shown in Figure 10-12.

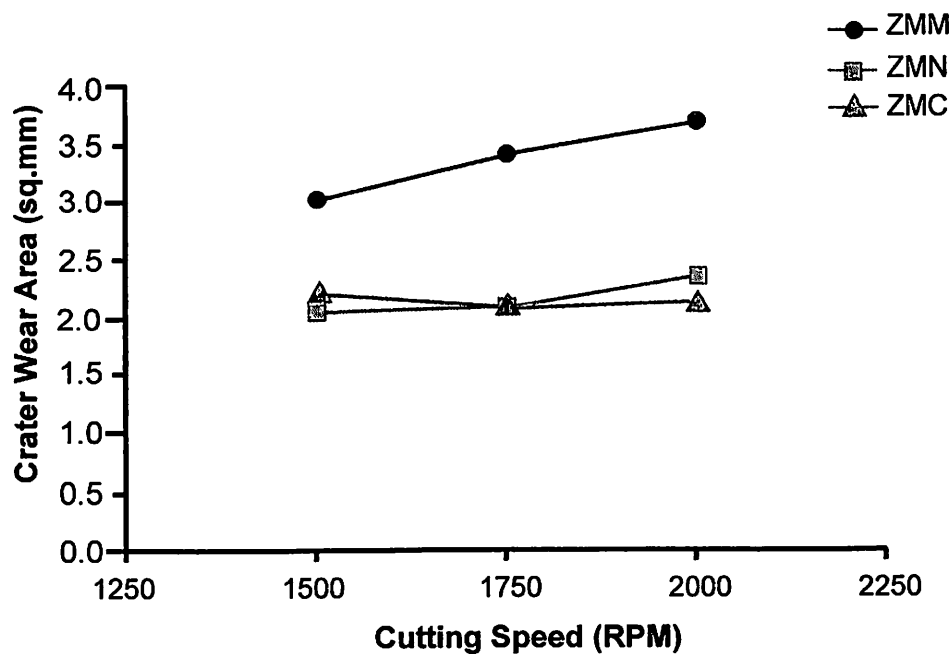


Figure 10: The effect of cutting speed on crater wear on cutting tool of machined surface

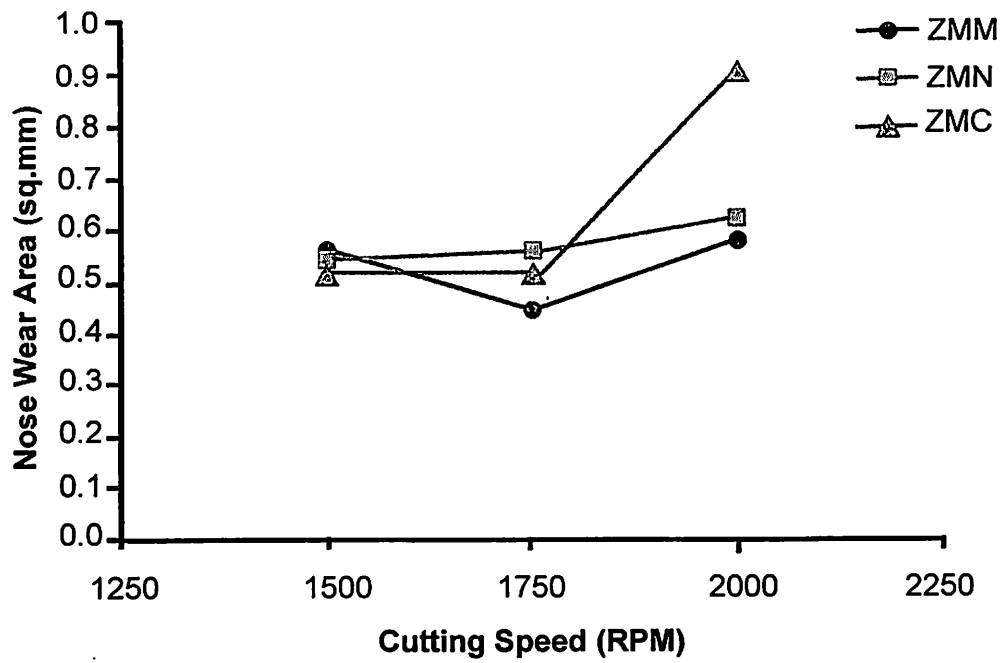


Figure 11: The effect of cutting speed on cutting tool nose wear of machined surface

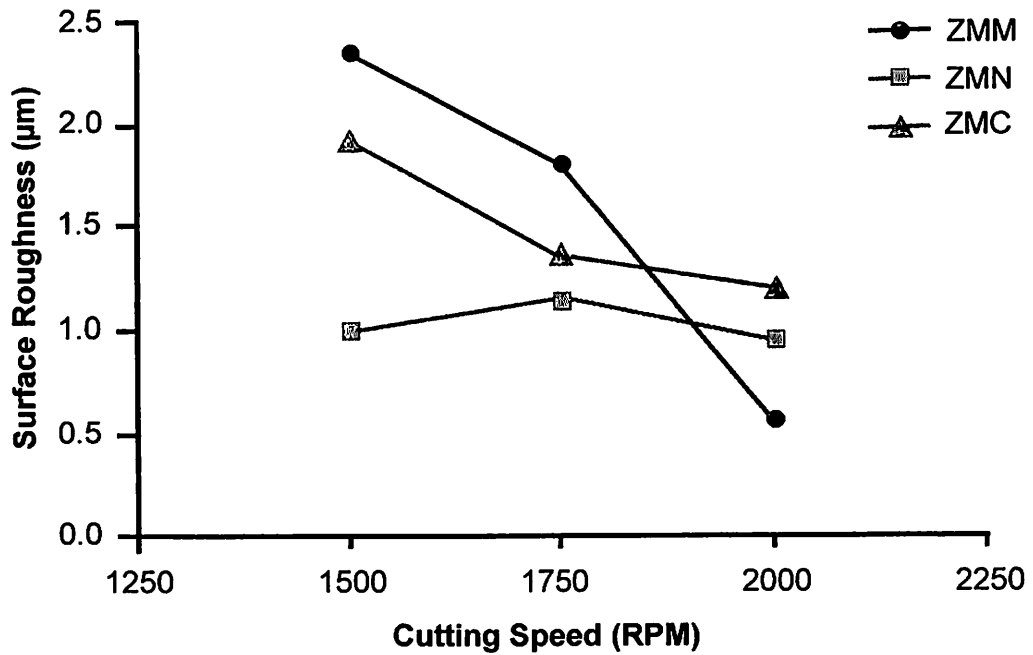


Figure 12: The effect of cutting speed on surface roughness of machined surface

5.1 Research output

No.	Category	2012	2013	2014	2015	2016	Total
1.	Research Publications	1	2 (2 ISI)	2 (2 ISI)	4 (2 ISI)	4 (2 ISI)	14 (8 ISI)
2.	PhD & MSc	-	2	4	-	-	6
3.	Potential Applications	-	-	-	1	-	1
4	Possible External Research Grants to be Acquired	-	-	-	1	-	1

Acknowledgements

This research received support from the grant 1001/PBAHAN/811212, awarded to the School of Materials & Mineral Resources Engineering by the Universiti Sains Malaysia (USM), Malaysia.

References

- [1] A.H. De Aza, J. Chevalier, G. Fantozzi, M. Schehl, R. Torrecillas, Crack growth resistance of alumina, zirconia and zirconia toughened alumina ceramics for joint prostheses., *Biomaterials*. 23 (2002) 937–45. <http://www.ncbi.nlm.nih.gov/pubmed/11774853>.
- [2] P.M. Kelly, L.R.F. Rose, The martensitic transformation in ceramics - Its role in transformation toughening, *Prog. Mater. Sci.* 47 (2002) 463–557.
- [3] S.G. Huang, J. Vleugels, L. Li, O. Van der Biest, P.L. Wang, Composition design and mechanical properties of mixed (Ce,Y)-TZP ceramics obtained from coated starting powders, *J. Eur. Ceram. Soc.* 25 (2005) 3109–3115. doi:10.1016/j.jeurceramsoc.2004.07.003.
- [4] J. Vleugels, Z.X. Yuan, O. Van Der Biest, Mechanical properties of Y₂O₃/Al₂O₃-coated Y-TZP ceramics, *J. Eur. Ceram. Soc.* 22 (2002) 873–881.
- [5] S.G. Huang, K. Vanmeensel, O. Van der Biest, J. Vleugels, Development of ZrO₂-WC composites by pulsed electric current sintering, *J. Eur. Ceram. Soc.* 27 (2007) 3269–3275. doi:10.1016/j.jeurceramsoc.2006.11.079.
- [6] A. Rittidech, R. Somrit, T. Tunkasiri, Effect of adding Y₂O₃ on structural and mechanical properties of Al₂O₃-ZrO₂ ceramics, *Ceram. Int.* 39 (2013) S433–S436. doi:10.1016/j.ceramint.2012.10.108.

- [36] A. Arab, Z.A. Ahmad, and R. Ahmad, Effects of yttria stabilized zirconia (3Y-TZP) percentages on the ZTA dynamic mechanical properties, *Int. J. Refract. Met. Hard Mater.*, 50(2015), p. 157.
- [37] S. Huang, J. Binnerl, B. Vaidhyanathan, P. Brownz, C. Hampson, and C. Spacie, Development of nano zirconia toughened alumina for ceramic armor applications, *Adv. Ceram. Armor VII: Ceram. Eng. Sci. Proc.*, 32(2011), p. 103.
- [38] K. Niihara, R. Morena, and D.P.H. Hasselman, Evaluation of K_{Ic} of brittle solids by the indentation method with low crack-to-indent ratios, *J. Mater. Sci. Lett.*, 1(1982), No. 1, p. 13.
- [39] S. Sarva and S. Nemat-Nasser, Dynamic compressive strength of silicon carbide under uniaxial compression. *Mater. Sci. Eng. A*, 317(2001), No. 1-2, p. 140.
- [40] D.J. Frew, M.J. Forrestal, and W. Chen, Pulse shaping techniques for testing brittle materials with a split Hopkinson pressure bar, *Exp. Mech.*, 42(2002), No. 1, p. 93.
- [41] J.M. Lifshitz and H. Leber, Data processing in the split Hopkinson pressure bar tests, *Int. J. Impact Eng.*, 15(1994), No. 6, p. 723.
- [42] V.K. Singh and K.K. Sharma, Low-temperature synthesis of calcium hexa-aluminate, *J. Am. Ceram. Soc.*, 85(2002), No. 4, p. 769.
- [43] K. Vishista, and F.D. Gnanam, Effect of strontia on the densification and mechanical properties of sol-gel alumina, *Ceram. Int.*, 32(2006), No. 8, p. 917.
- [44] K. Vishista, F.D. Gnanam, and H. Awaji, Sol-gel synthesis and characterization of alumina-calcium hexaaluminate composites, *J. Am. Ceram. Soc.*, 88(2005), No. 5, p. 1175.
- [45] C.Y. Huang, G. Subhash, and S.J. Vitton, A dynamic damage growth model for uniaxial compressive response of rock aggregates, *Mech. Mater.*, 34(2002), No. 5, p. 267.
- [46] B. Paliwal, K.T. Ramesh, and J.W. McCauley, Direct observation of the dynamic compressive failure of a transparent polycrystalline ceramic (AlON), *J. Am. Ceram. Soc.*, 89(2006), No. 7, p. 2128.
- [47] X.D. Chen, S.X. Wu, and J.K. Zhou, Influence of porosity on compressive and tensile strength of cement mortar, *Construct. Build. Mater.*, 40(2013), p. 869.

Questions:

1. Page 1: does "SA6" represent $SrAl_{12}O_{19}$?
2. Page 2: is "TZP" the abbreviation of tetragonal zirconia polycrystal?; does 99% represent purity? is "YSZ" the abbreviation of yttria-stabilized zirconia?
3. Page 3: is "SHPB" the abbreviation of split Hopkinson pressure bar? what does "SUJ2" represent?
4. Page 6: in Fig. 3(g), the label for red circle is unclear, and scale bar is also unclear; in addition, under Fig. 3(g), Table is unclear and there is not table tile; what do "SA2" and "SA" represent, respectively?
5. Page 9: the scale bar in Fig.7 is unclear.
6. Page 11: what does " dD/dt " represent? Furthermore, what do "D" and "t" represent?
7. Page 13: in Fig. 9, what "z" does represent? What does "arrows" acted on the upper surface and lower surface represent?

Please answer the above questions and give the corresponding revisions.



USM

UNIVERSITI SAINS MALAYSIA

APEX

THIS IS TO CERTIFY THAT

NIK AKMAR REJAB

from the School of Material & Mineral Resources Engineering

HAS BEEN RECOGNIZED WINNER OF

SANGGAR SANJUNG AWARDS

FOR EXCELLENT ACHIEVEMENT IN CATEGORY OF

Journal Publications
FOR THE YEAR 2013

PROFESSOR DATO' DR. OMAR OSMAN
VICE CHANCELLOR
UNIVERSITI SAINS MALAYSIA

beautiful minds
Inspire
others

MAJLIS PERSADA KENCANA '15

COMPREHENSIVE TECHNICAL REPORT

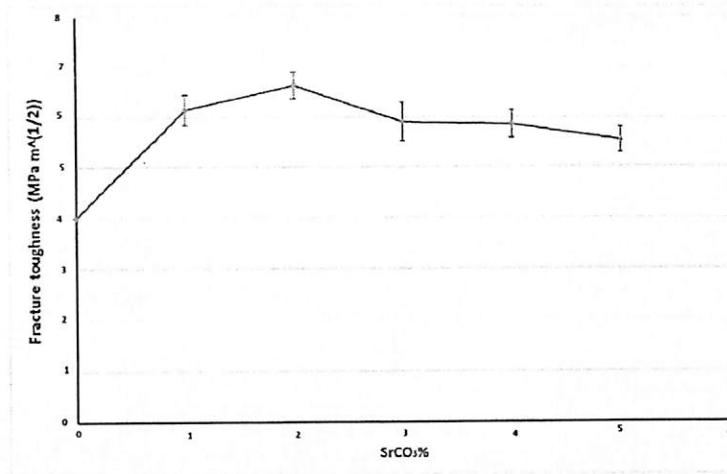


Fig . 6. Fracture toughness of ZTA as function of SrCO₃,

Fig. 6. Fracture toughness of ZTA as function of SrCO₃.

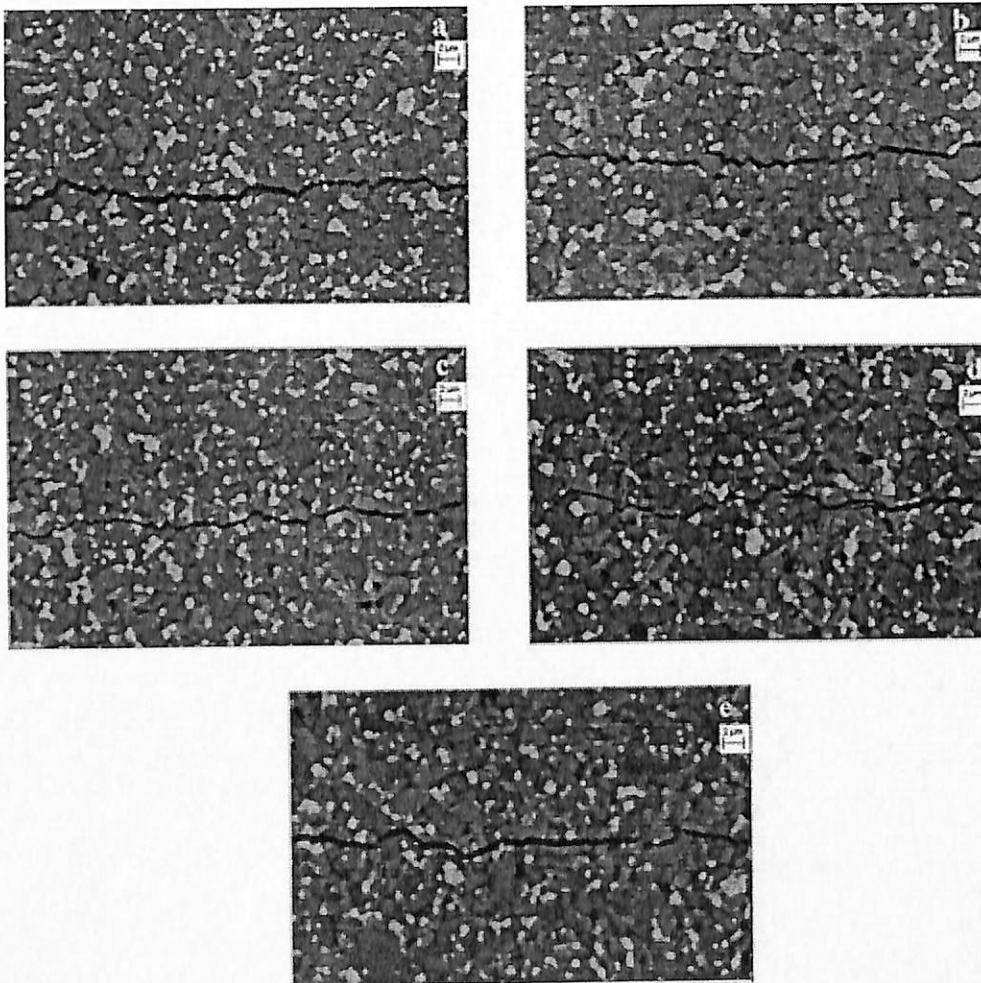


Fig.7 .Fracture mechanism in the ZTA with different percentage of SrCO₃ a)1% SrCO₃, b) 2% SrCO₃, c) 3% SrCO₃, d) 4% SrCO₃, and e) 5% SrCO₃

rm@ustb.edu.cn

Gmail

Move to Inbox

COMPOSE

IJM-09-2015-0766-questions

Inbox x

Inbox (10,457)

Starred

Important

Sent Mail

Drafts (8)

All Mail

Spam

More



zainalarifin

Rare Metals rm@ustb.edu.cn via staffusm.onmicrosoft.com to Zainal

Dear Author,

We are pleased to inform you that your paper is nearing publication. The letters in the text and listed at the end of manuscript, and please careful sections that you made should be shown by coloured letters or highlight. facilitate rapid publication by returning the corrected paper to rm@ustb.edu.cn

Thank you for your cooperation

With Kind regards,

Jia Xian
The Editor
International Journal of Minerals, Metallurgy and Materials
T: 010-62333436-802
E: rm@ustb.edu.cn
journals.ustb.edu.cn
www.springer.com/materials/special+types/journal/12613
[2016-01-18](http://www.springer.com/materials/special+types/journal/12613)

No Hangouts Contacts
[Find someone](#)

Effect of SiO₂ addition on the dynamic compressive strength of ZTA
Jia Xian* and Zainal Arifin
*Institute of Mechanical Engineering, Liaoning University of Engineering, 111000 Wafangdian,
Fenxi, Liaoning
Institute of Materials Science and Engineering, Liaoning University of Engineering, Liaoning
University of Engineering, 111000 Wafangdian, Fenxi, Liaoning
Corresponding author: zainalarifin@ustb.edu.cn Email: zainalarifin@ustb.edu.cn
(Received: 20 September 2015; revised: 10 November 2015; accepted: 17 November 2015)

W MaterialScience-I..

Effect of SrCO₃ addition on the dynamic compressive strength of ZTA

Ali Arab^{1,2)}, Roslan Ahmad¹⁾, and Zainal Arifin Ahmad²⁾

1) School of Mechanical Engineering, Universiti Sains Malaysia, Engineering Campus, 14300 Nibong Tebal, Penang, Malaysia

2) Structural Materials Niche Area, School of Materials and Mineral Resources Engineering, Universiti Sains Malaysia, Engineering Campus, 14300 Nibong Tebal, Penang, Malaysia

Corresponding author: Zainal Arifin Ahmad E-mail: srzainal@usm.my

(Received: 29 September 2015; revised: 16 November 2015; accepted: 17 November 2015)

Abstract: Ceramic parts usually experience dynamic load in armor applications. Therefore, studying the dynamic behaviors of ceramics is important. Limited data are available on the dynamic behaviors of ceramics; thus, it is helpful to predict the dynamic strength of ceramics on the basis of their mechanical properties. In this paper, the addition of SrCO₃ into zirconia-toughened alumina (ZTA) was demonstrated to improve the fracture toughness of ZTA due to the formation of the SrAl₁₂O₁₉ (SA6) phase. The porosity of ZTA was found to be increased by the addition of SrCO₃. These newly formed pores served as the nucleation sites of cracks under dynamic load; these cracks eventually coalesced to form damaged zones in the samples. Although the K_{IC} values of the samples were improved, the dynamic strength was not enhanced because of the increase in porosity; in fact, the dynamic strength of ZTA ceramic decreased with the addition of SrCO₃.

Keywords: fracture toughness; ZTA; Split-Hopkinson pressure bar, dynamic compressive strength; SrCO₃

1. Introduction

Armor is one of the most interesting applications for ceramic materials. Zirconia-toughened alumina (ZTA) is suitable for armor applications because of its high hardness and fracture toughness [1–7]. The high fracture toughness of ZTA diminishes and localizes the shattering and failure areas to the region near the impacted zone [7–13]. According to Ravichandran and Subhash [14], improving the fracture toughness simultaneously increases the compressive strength of the ceramic, thereby making it suitable for multi-hit armor applications. However, the increase in fracture toughness may negatively influence other mechanical properties of the ceramic. Consequently, the ballistic performance of the ceramic-based armor may be directly affected [15].

A good understanding of a ceramic's ballistic performance is important for armor applications. The constitutive model of ceramics has been extensively studied [16–22]. In all these studies, fracture toughness was

the key factor used to evaluate the damage, fragmentation, and strength of the ceramic products. Ravichandran and Subhash [14] demonstrated that higher fracture toughness leads to a higher compressive strength. Kimberly *et al.* [21] found that the compressive strength is related to the fracture toughness and crack length; a similar finding was reported by other researchers [23–27]. Ceramic failure occurs because of wing cracks that begin with flaws in the ceramic. To develop advanced ceramics that can withstand dynamic loading, it is essential to investigate the influence of fracture toughness on dynamic strength. For this purpose, ZTA has been selected because of its good fracture toughness.

Many studies have been conducted to improve the mechanical properties of ZTA. The addition of a third phase to ZTA matrix can improve the mechanical properties of ZTA [4,28–30]. One such additive is SrO, which has been added to tetragonal zirconia polycrystal (TZP) as a sintering aid [31]. Culter *et al.* [32] studied the effect of the addition of SrZrO₃ into Ce-TZP/Al₂O₃ and found that SrZrO₃ reacted with Al₂O₃ to form a new phase SrAl₁₂O₁₉ (SA6) that improved the material's fracture toughness by 75%. Other researchers have reported that hexaluminate phases such as CaAl₁₂O₁₉ and LaAl₁₂O₁₉ can also improve the strength of the alumina matrix [33–34]. Oungkulsolmongkol *et al.* [35] observed SA6 when SrCO₃ was added into the matrix of ZTA. He found that the SA6 phase improved the fracture toughness but reduced the hardness. Therefore, it is prudent to investigate the effects of SrO on the fracture toughness and dynamic strength of ZTA.

Many studies have investigated the ballistic properties of ZTA ceramic armor [8,10,12]. However, few reports on the dynamic properties of ZTA are available in the literature [36–37]. In the present study, we investigated the mechanical properties of ZTA–SrCO₃ with a focus on improving the fracture toughness and the dynamic compressive strength of ZTA.

2. Experimental details

2.1. Sample fabrication

The raw materials used were Al₂O₃ powder (Martinswerck, 99% purity, average particle size of 0.5 μm), yttria-stabilized zirconia (YSZ) powder (Goodfellow (ZR616010), 5.4wt% Y₂O₃ as stabilizer, average particle size 1.5 μm), and SrCO₃. In all samples, the ratio between Al₂O₃ and YSZ was fixed at 80/20 with the addition of SrCO₃ (0–5wt%). The raw materials were wet-mixed with an ABB mixer using ZrO₂ balls for 8 h. The mixture was then dried in the oven at 100°C for 24 h. The prepared powder was uniaxially pressed at 300 MPa for 2 min. Cylindrical samples with two different sizes were prepared; the dimensions of the sample for hardness and fracture toughness testing were 10 mm (diameter) × 4 mm, while those of the sample for dynamic

testing were 4.5 mm (diameter) × 6 mm. The pressed specimens were sintered in air at 1600°C for 4 h with a heating and cooling rate of 5°C/min.

2.2. Tests

The hardness, fracture toughness, and dynamic compressive strength of the samples were measured. A Shimadzu Vickers hardness tester HSV-20 (Japan) was used to measure Vickers hardness at a load of 30 kN using the point-indentation technique. The indenter indented the surface of the highly polished sample perpendicularly. Using these indentation measurements, the fracture toughness of the sample was calculated using Eq. (1), as proposed by Niihara *et al.* [38]:

$$3K_{IC(HV30)} = 0.035(Ha^{1/2}) \left(\frac{3E}{H} \right)^{0.4} \left(\frac{d}{a} \right)^{-0.5} \quad (1)$$

where H is the Vickers hardness, a is the half-distance of the indent diagonal, E is Young's modulus, and d is the crack length.

Archimedes principle was used to measure the bulk density and porosity of the sintering samples. First, dry samples were weighed (W_a), submerged in water, and kept under the vacuum for 1 h to ensure that all open pores were filled by water. Following this, the samples were weighed in the water (W_b). After their surfaces were wiped dry with tissue, the samples were then weighed again (W_c). The density (ρ_b) and porosity (P_A) of the sample were calculated as follows:

$$\rho_b = \frac{W_a}{W_c - W_b} \times \rho_{\text{water}} \quad (2)$$

$$P_A = \frac{W_c - W_a}{W_c - W_b} \times \rho_{\text{water}} \quad (3)$$

The modified split Hopkinson pressure bar (SHPB) was employed to assess and measure the dynamic compressive strength of the fabricated samples [27,39]. SHPB (Fig. 1) is traditionally designed for testing metals under plastic conditions and requires modification for use with brittle materials. A copper pulse shaper (length of 2 mm and diameter of 10 mm) [40] was placed between the striker and incident bars to change the rectangular-shaped pulse to a ramp-shaped pulse, which was suitable for ceramic materials. The ceramic sample was harder than the material of the incident and transmitted bar. To prevent contact with the ceramic sample, tungsten carbide platens were placed between the samples and the bars. These platens had the same impedance as the bars. Both the incident and transmission bars were made of SUJ2 with diameters of 12 mm and lengths of

150 cm. The specimens' stress, strain, and strain rates were calculated using Eqs. (4), (5), and (6), respectively [41]:

$$\sigma_s(t) = -E_b \frac{A_b}{A_s} \varepsilon_t(t) \quad (4)$$

$$\varepsilon_s = 2 \frac{C_0}{L_s} \int_0^t \varepsilon_r(t) dt \quad (5)$$

$$\dot{\varepsilon}_s = 2 \frac{C_0}{L_s} \dot{\varepsilon}_r(t) \quad (6)$$

where the subscripts *b* and *s* refer to the bar and sample, respectively, *A* is the cross-sectional area, and *L* is the length. C_0 is $\sqrt{E/\rho}$, where *E* and ρ are the Young's modulus and density of the bar, respectively, ε_t is the transmitted signal strain, and ε_r is the reflected strain signal.

The different phases in the samples were identified and analyzed by X-ray diffraction (XRD; Bruker model D8 with copper anode). Bruker EVA software was used to identify the XRD peaks and match them to XRD data files (International Center for Diffraction Data (ICDD)). A high-speed camera (Olympus i-speed 2) was used to observe the failure mechanisms of the samples. The schematic arrangement of the light source and camera is shown in Fig. 1. The sample surfaces were ground, polished, and thermally etched at 1400°C for 1 h prior to the examination under FESEM (Zeiss Supra 35VP) to observe the relationship between the three measured properties and their microstructures.

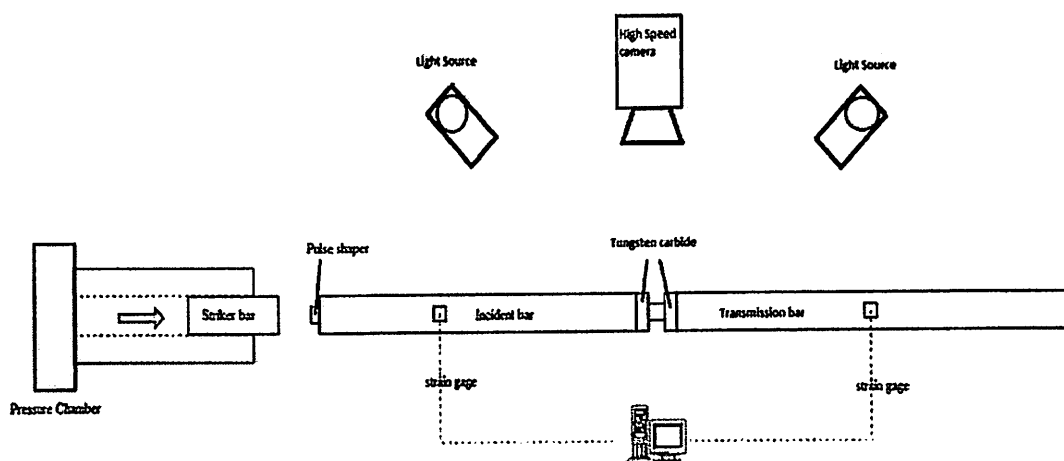


Fig. 1. Schematic diagram of the modified SHPB set up for testing ceramic materials

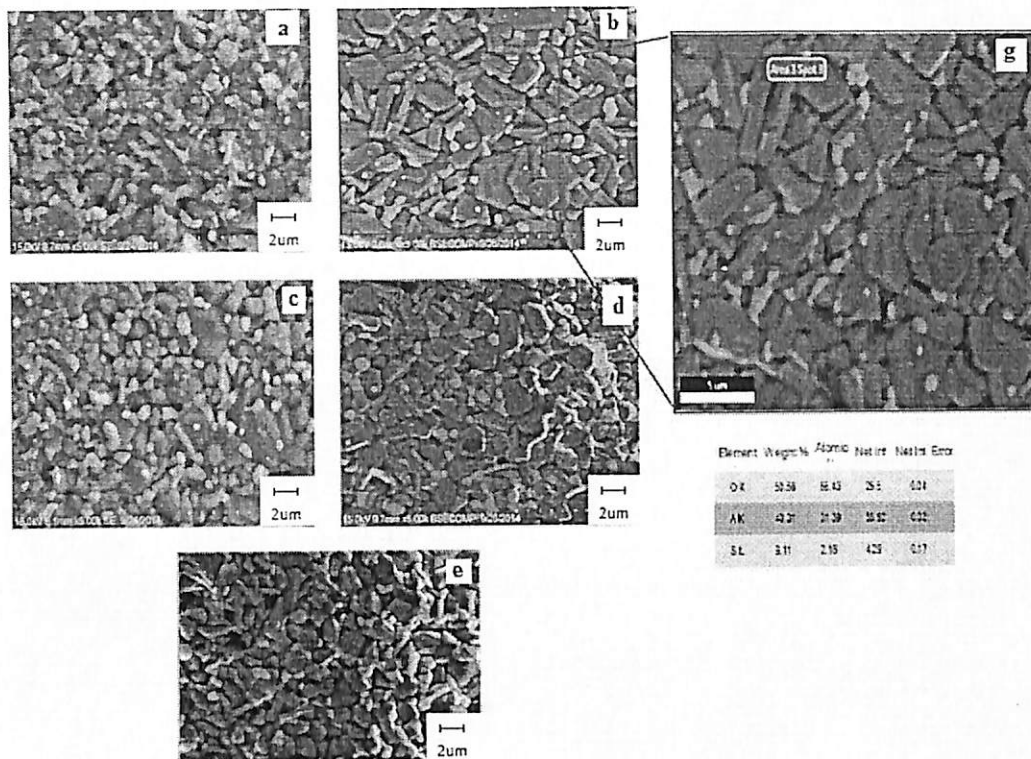
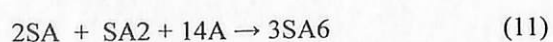
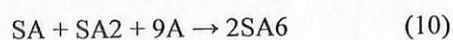
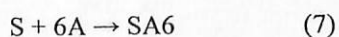


Fig. 3 .Microstructure of ZTA samples added with various amount of SrCO₃. a) 1wt.% SrCO₃, b) 2 wt.% SrCO₃, c) 3 wt.% SrCO₃, d) 4 wt.% SrCO₃, e) 5 wt.% SrCO₃, and g) SrAl₁₂O₁₉ grain shape

Fig. 3. Microstructures of ZTA samples containing different amounts of SrCO₃: (a) 1wt%; (b) 2wt%; (c) 3wt%; (d) 4wt%; and (e) 5wt% SrCO₃; (g) SA6 grain shape.

SrAl₁₂O₁₉ (SA6) is formed by one of the following routes, as proposed by Vishista & Gnanam [31]: (i) the reaction between Al₂O₃ (A) and SrO (S) obtained from the low-temperature dissolution of strontia and gamma alumina; (ii) the reaction between S and A; (iii) the reaction between SA2 and A; or (iv) the reaction among SA, SA2, and A.

SA and SA2 are reaction intermediates. The contents of SA and SA2 are minimized with the formation of SA6. The different routes to SA6 formation are represented by the following reactions [31]:



The same mechanisms are observed for the formation of calcium aluminates [6].

The intensities of the SA6 XRD peaks of the ZTA composite increase with the amount of added SrCO₃. The amount of SA6 was determined by XRD quantitative analysis (Bruker EVA software), as shown in Table 1. The amount of SA6 increased from 12.6wt% for the addition of 1wt% SrCO₃ to 27.2wt% for the addition of 5wt% SrCO₃, which is in accordance with one mole of Sr²⁺ reacting with 12 moles of Al³⁺. This explains why the amount of Al₂O₃ significantly decreased as the amount of added SrCO₃ increased.

Table 1. Quantitative XRD analysis of ZTA samples containing different amounts of SrCO₃

Sample	Al ₂ O ₃ / wt%	YSZ / wt%	SA6 / wt%
ZTA + 1wt% SrCO ₃	68.4	19.0	12.6
ZTA + 2wt% SrCO ₃	62.0	19.3	18.7
ZTA + 3wt% SrCO ₃	62.4	18.4	19.2
ZTA + 4wt% SrCO ₃	58.9	19.6	21.6
ZTA + 5wt% SrCO ₃	53.5	19.3	27.2

3.2. Mechanical properties

Fig. 4 shows the effects of SrCO₃ on the ZTA matrix, density, and porosity. Pore formation is related to the decomposition of SrCO₃, SrO, and CO₂. In addition, during the formation of SA6, the elongated grains of SA6 were possibly interlocked, creating pores. This observation is similar to the result reported by Sktani *et al.* [6] and Vishista *et al.* [44] for the addition of CaCO₃ to ZTA.

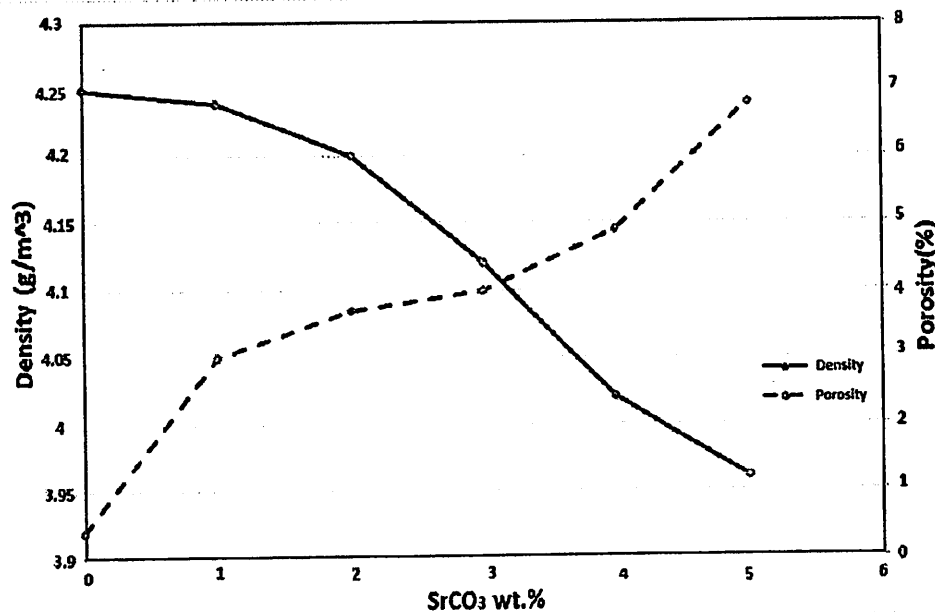


Fig.4 . Bulk density and percentage of porosity for ZTA samples as a function of SrCO₃

Fig. 4. Bulk density and porosity of ZTA samples as a function of SrCO₃ content.

Fig. 3 shows the FESEM micrographs of the samples; the dark grains represent either alumina or SA6. The well-distributed brighter grains were identified as YSZ, which was embedded within alumina and/or SA6 grains with minor agglomeration. The sample hardness decreased from 1603.4 to 1153.0 HV when the amount of added SrCO₃ was increased (Fig. 5). This reduction in hardness is basically related to the increase in porosity. This also reduced the hardness of SA6 rather than that of pure alumina [43].

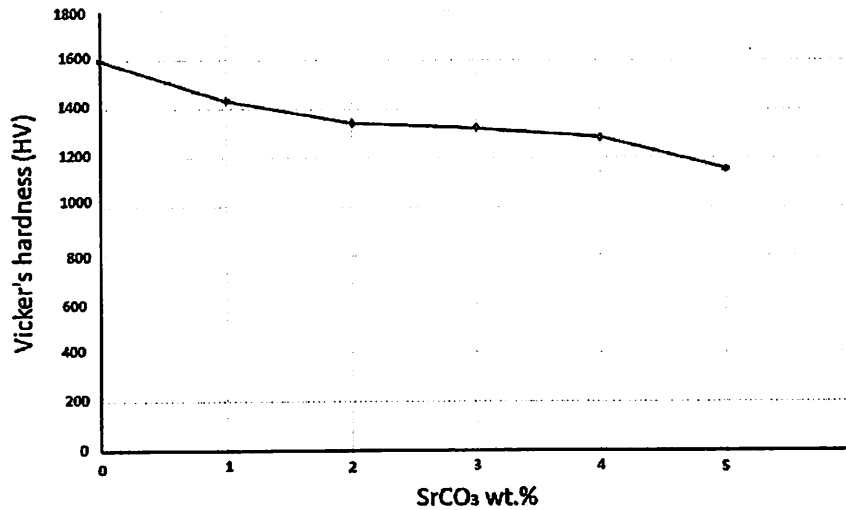


Fig . 5 . The hardness of ZTA-SrO as function of SrCO₃

Fig. 5. Hardness of ZTA-SrO as function of SrCO₃.

The effect of SrCO₃ on fracture toughness is shown in Fig. 6. Fracture toughness rapidly increased to 6.64 MPa·m^{1/2} as the amount of added SrCO₃ increased to 2wt%. However, upon further increases in the amount of SrCO₃, fracture toughness gradually decreased. The improvement in fracture toughness with the initial increases in added SrCO₃ can be attributed to the crack deflection mechanism due to the presence of SA6. More crack deflections were observed when the percentage of SA6 increased (arrows in Fig. 7). However, at SrCO₃ contents above 2wt%, fracture toughness decreased because of the higher amount of pores in the samples (Fig. 3). Both intergranular and transgranular fracture modes were observed in all the samples. Moreover, with increasing SrCO₃ content, more transgranular fractures were observed, particularly in the samples containing 4wt% and 5wt% SrCO₃. Transgranular fractures require more energy to form than intergranular fractures [6]. However, the increasing porosity is overcome as the fracture toughness decreases.

Summary

The experiments of ZTA-ceramic cutting tool are satisfactory with the conclusion that can be made as:

1. The tool wear increased with the increment of cutting speed due to the high abrasion on the cutting tips.
2. The surface roughness decreased with the increment of cutting speed as the temperature rises allowing better chip formation and due to the transformation toughening mechanism that occur on the tool tips.
3. ZMN shown the best performance compared to ZMM and ZMC.

Acknowledgement

This work was funded by Universiti Sains Malaysia (USM) under grant 1001/PBAHAN/811212. The authors are grateful to Mr. Shahril, Mr. Wan Fahmin Faiz and Mr. Nik Akmar for their technical support.

References

- [1] S.J. George, *Cutting Tools Application*, ASM International, 2002.
- [2] Z. Liu, X. Ai, H. Zhang, Z. Wang, Y. Wan, Wear patterns and mechanisms of cutting tools in high-speed face milling, *J. Mater. Process. Technol.* 129 (2002) 222–226.
- [3] K. Aslantas, İ. Uçun, a. Çicek, Tool life and wear mechanism of coated and uncoated Al₂O₃/TiCN mixed ceramic tools in turning hardened alloy steel, *Wear.* 274-275 (2012) 442–451.
- [4] N.A. Rejab, A.Z.A. Azhar, M.M. Ratnam, Z.A. Ahmad, The effects of CeO₂ addition on the physical, microstructural and mechanical properties of yttria stabilized zirconia toughened alumina (ZTA), *Int. J. Refract. Met. Hard Mater.* 36 (2013) 162–166.
- [5] A.Z.A. Azhar, H. Mohamad, M.M. Ratnam, Z.A. Ahmad, Effect of MgO particle size on the microstructure, mechanical properties and wear performance of ZTA–MgO ceramic cutting inserts, *Int. J. Refract. Met. Hard Mater.* 29 (2011) 456–461.
- [6] A. Senthil Kumar, a. Raja Durai, T. Sornakumar, Development of yttria and ceria toughened alumina composite for cutting tool application, *Int. J. Refract. Met. Hard Mater.* 25 (2007) 214–219.
- [7] a. Senthil Kumar, a. Raja Durai, T. Sornakumar, Development of alumina–ceria ceramic composite cutting tool, *Int. J. Refract. Met. Hard Mater.* 22 (2004) 17–20.
- [8] N.A. Rejab, A.Z.A. Azhar, K.S. Kian, M.M. Ratnam, Z.A. Ahmad, Effects of MgO addition on the phase, mechanical properties, and microstructure of zirconia-toughened alumina added with CeO₂ (ZTA-CeO₂) ceramic composite, *Mater. Sci. Eng. A.* 595 (2014) 18–24.
- [9] C. Xu, X. Ai, C. Huang, Fabrication and performance of an advanced ceramic tool material, *Wear.* 249 (2001) 503–508.
- [10] D. Wang, N.F. Ismail, N.A. Badarulzaman, Effect of MgO Additive on Microstructure of Al₂O₃, *Adv. Mater. Res.* 488-489 (2012) 335–339.
- [11] A.Z.A. Azhar, H. Mohamad, M.M. Ratnam, Z.A. Ahmad, The effects of MgO addition on microstructure, mechanical properties and wear performance of zirconia-toughened alumina cutting inserts, *J. Alloys Compd.* 497 (2010) 316–320.
- [12] A.Z.A. Azhar, F.T. Kong, H. Mohamad, M.M. Ratnam, Z.A. Ahmad, Effect of Particle Sizes of Magnesium Oxide on Zirconia Toughened Alumina Vickers Hardness, *Adv. Mater. Res.* 173 (2010) 29–34.

- [13] N. Mandal, B. Doloi, B. Mondal, Development of flank wear prediction model of Zirconia Toughened Alumina (ZTA) cutting tool using response surface methodology, *Int. J. Refract. Met. Hard Mater.* 29 (2011) 273–280.
- [14] A Senthil Kumar, a Raja Durai, T. Sornakumar, Machinability of hardened steel using alumina based ceramic cutting tools, *Int. J. Refract. Met. Hard Mater.* 21 (2003) 109–117.
- [15] E.O. Ezugwu, J. Bonney, R.B. Da Silva, a. R. Machado, Evaluation of the performance of different nano-ceramic tool grades when machining nickel-base, inconel 718, alloy, *J. Brazilian Soc. Mech. Sci. Eng.* 26 (2004) 12–16.
- [16] A. Kaçal, F. Yıldırım, High Speed Hard Turning of AISI S1 (60WCrV8) Cold Work Tool Steel, 10 (2013) 169–186.
- [17] R. Arunachalam, M.. Mannan, a. . Spowage, Residual stress and surface roughness when facing age hardened Inconel 718 with CBN and ceramic cutting tools, *Int. J. Mach. Tools Manuf.* 44 (2004) 879–887
- [18] T. Sornakumar, R. Krishnamurthy, C.V. Gokularathnam, Machining performance of phase transformation toughened alumina and partially stabilised zirconia composite cutting tools, *J. Eur. Ceram. Soc.* 12 (1993) 455–460

The Cutting Speed Influences on Tool Wear of ZTA Ceramic Cutting Tools and Surface Roughness of Work Material Stainless Steel 316L during High Speed Machining
10.4028/www.scientific.net/MSF.840.315

DOI References

- [1] S.J. George, Cutting Tools Application, ASM International, (2002).
10.1109/icosp.2002.1180016
- [2] Z. Liu, X. Ai, H. Zhang, Z. Wang, Y. Wan, Wear patterns and mechanisms of cutting tools in high-speed face milling, *J. Mater. Process. Technol.* 129 (2002) 222-226.
10.1016/s0924-0136(02)00605-2
- [3] K. Aslantas, İ. Uçun, a. Çicek, Tool life and wear mechanism of coated and uncoated Al₂O₃/TiCN mixed ceramic tools in turning hardened alloy steel, *Wear.* 274-275 (2012) 442-451.
10.1016/j.wear.2011.11.010
- [4] N.A. Rejab, A.Z.A. Azhar, M.M. Ratnam, Z.A. Ahmad, The effects of CeO₂ addition on the physical, microstructural and mechanical properties of yttria stabilized zirconia toughened alumina (ZTA), *Int. J. Refract. Met. Hard Mater.* 36 (2013) 162-166.
10.1016/j.ijrmhm.2012.08.010
- [5] A.Z.A. Azhar, H. Mohamad, M.M. Ratnam, Z.A. Ahmad, Effect of MgO particle size on the microstructure, mechanical properties and wear performance of ZTA-MgO ceramic cutting inserts, *Int. J. Refract. Met. Hard Mater.* 29 (2011) 456-461.
10.1016/j.ijrmhm.2011.02.002
- [6] A. Senthil Kumar, a. Raja Durai, T. Sornakumar, Development of yttria and ceria toughened alumina composite for cutting tool application, *Int. J. Refract. Met. Hard Mater.* 25 (2007) 214-219.
10.1016/j.ijrmhm.2006.05.002
- [7] a. Senthil Kumar, a. Raja Durai, T. Sornakumar, Development of alumina-ceria ceramic composite cutting tool, *Int. J. Refract. Met. Hard Mater.* 22 (2004) 17-20.
10.1016/j.ijrmhm.2003.10.005
- [8] N.A. Rejab, A.Z.A. Azhar, K.S. Kian, M.M. Ratnam, Z.A. Ahmad, Effects of MgO addition on the phase, mechanical properties, and microstructure of zirconia-toughened alumina added with CeO₂ (ZTA-CeO₂) ceramic composite, *Mater. Sci. Eng. A.* 595 (2014).
10.1016/j.msea.2013.11.091
- [9] C. Xu, X. Ai, C. Huang, Fabrication and performance of an advanced ceramic tool material, *Wear.* 249 (2001) 503-508.
10.1016/s0043-1648(01)00581-6
- [10] D. Wang, N.F. Ismail, N.A. Badarulzaman, Effect of MgO Additive on Microstructure of Al₂O₃, *Adv. Mater. Res.* 488-489 (2012) 335-339.
10.4028/www.scientific.net/amr.488-489.335
- [11] A.Z.A. Azhar, H. Mohamad, M.M. Ratnam, Z.A. Ahmad, The effects of MgO addition on microstructure, mechanical properties and wear performance of zirconia-toughened alumina cutting inserts, *J. Alloys Compd.* 497 (2010) 316-320.
10.1016/j.jallcom.2010.03.054
- [12] A.Z.A. Azhar, F.T. Kong, H. Mohamad, M.M. Ratnam, Z.A. Ahmad, Effect of Particle Sizes of

- Magnesium Oxide on Zirconia Toughened Alumina Vickers Hardness, *Adv. Mater. Res.* 173 (2010) 29-34.
10.4028/www.scientific.net/amr.173.29
- [13] N. Mandal, B. Doloi, B. Mondal, Development of flank wear prediction model of Zirconia Toughened Alumina (ZTA) cutting tool using response surface methodology, *Int. J. Refract. Met. Hard Mater.* 29 (2011) 273-280.
10.1016/j.ijrmhm.2010.12.001
- [14] A Senthil Kumar, a Raja Durai, T. Sornakumar, Machinability of hardened steel using alumina based ceramic cutting tools, *Int. J. Refract. Met. Hard Mater.* 21 (2003) 109-117.
10.1016/s0263-4368(03)00004-0
- [15] E.O. Ezugwu, J. Bonney, R.B. Da Silva, a. R. Machado, Evaluation of the performance of different nano-ceramic tool grades when machining nickel-base, inconel 718, alloy, *J. Brazilian Soc. Mech. Sci. Eng.* 26 (2004) 12-16.
10.1590/s1678-58782004000100002
- [16] A. Kaçal, F. Yıldırım, High Speed Hard Turning of AISI S1 (60WCrV8) Cold Work Tool Steel, 10 (2013) 169-186.
10.12700/aph.10.08.2013.8.11
- [17] R. Arunachalam, M. Mannan, a. . Spowage, Residual stress and surface roughness when facing age hardened Inconel 718 with CBN and ceramic cutting tools, *Int. J. Mach. Tools Manuf.* 44 (2004) 879-887.
10.1016/j.ijmachtools.2004.02.016
- [18] T. Sornakumar, R. Krishnamurthy, C.V. Gokularathnam, Machining performance of phase transformation toughened alumina and partially stabilised zirconia composite cutting tools, *J. Eur. Ceram. Soc.* 12 (1993) 455-460.
10.1016/0955-2219(93)90079-7

Structural and Microstructure Relationship with Fracture Toughness of CeO₂ Addition into Zirconia Toughened Alumina (ZTA) Ceramic Composites

NIK AKMAR REJAB^{1,a}, AHMAD ZAHIRANI AHMAD AZHAR^{1,b},
MANI MARAN RATNAM^{2,c} and ZAINAL ARIFIN AHMAD^{1,d}

¹ School of Materials and Mineral Resources Engineering, Engineering Campus, Universiti Sains Malaysia, 14300 Nibong Tebal, Pulau Pinang, Malaysia

² School of Mechanical Engineering, Engineering Campus, Universiti Sains Malaysia, 14300 Nibong Tebal, Pulau Pinang, Malaysia

^aakmarnik@gmail.com, ^bahmadzahirani@gmail.com, ^cmbaran@eng.usm.my
^dzainal@eng.usm.my,

Keywords: Fracture toughness, tetragonal, crystallite size, grain size.

Abstract. The effect of CeO₂ addition in zirconia toughened alumina (ZTA) was examined. The CeO₂ addition in weight percent (wt %) was varied from 0 wt% to 15 wt%. The fabricated samples were sintered at a temperature of 1600°C. The sintered samples were characterized their properties such as fracture toughness and phase determination. X-ray diffraction patterns confirm the constituent phases present in the samples were alumina and zirconia. Fracture toughness for each sample in the range of 5.87–8.38 MPam^{1/2} respectively. It was observed that the addition of ceria increased the fracture toughness of the zirconia toughened alumina ceramic composites.

Introduction

Zirconia toughened alumina (ZTA) are well established as engineering materials because of their relatively high fracture toughness, resulting from transformation toughening [1-4]. Toughness is crucial to the structural function of ceramics. The presence of stabilised by the addition of oxides such as MgO [5], Y₂O₃[3], Cr₂O₃[6] and CeO₂ [7], undergoes a stress-induced phase transformation to the monoclinic form, resulting in crack resistance (R-curve) behaviour and relatively high fracture toughness [8]. Recently, Maiti and Sal [3] investigated the influence of sintering temperature and soaking time on fracture toughness of undoped and rare earths (Y, La) doped ZTA ceramic composites. Tsukuma and Shimada reported that the presence of CeO₂ in stabilized tetragonal ZrO₂ polycrystals (TZP) obtained high fracture toughness for sintered bodies with 7 to 10 % CeO₂ content with large grain-size [1].

However, there is little work reported in the literature on the effect of CeO₂ on structure and microstructure of ZTA-Ce ceramics on their fracture toughness improvement. For these reason, the effects of ceria in different weight percentage (wt%) on the properties of ZTA were studied. The ZTA and ZTA-CeO₂ samples were characterized by different techniques such as XRD, FESEM and fracture toughness. All these characterization were correlated with ceria addition. Hopefullu, by the addition of ceria, the fracture toughness of ZTA will gets improved.

Materials and Methodology

In this work 80 wt% of alumina and 20 wt% yttrium stabilized zirconia were taken as the initial composition. The ceria was added with different wt% (1 to 20 wt %) into the initial compositions, and the powders were prepared by wet milling method. The mixture were dried to 100°C and crushed to form powders. Cylindrical shapes with dimensions of 12 mm in diameter and 4 mm in height were formed by pressing the crushed powder at 300 MPa. Subsequently, these cylindrical samples were sintered in atmosphere at 1600 °C for 4 hours to yield dense ceramics. The fracture toughness of the sintered samples was determined by Vickers indentation with a 30 kgf load. Samples were then characterized by XRD and FESEM.

Results and Discussion

Structural Analyses. The diffraction peaks at 2θ show the presence of corundum structure of alumina and tetragonal structure for zirconia which is corresponding to (ICDD File No. 00-010-0173) and (ICDD File No. 01-089-9068). In all the samples the corundum phase was retained. The XRD patterns revealed at 2θ of 28° to 32° correspond to (101) peaks belong to tetragonal $Zr_{0.94}Y_{0.06}O_2$ and shifted to (002) as $Ce_2Zr_3O_{10}$ phases, as shown in Fig. 1. These shifted peaks in the zirconia were due to the effect of ceria addition. The presence of $(Zr_{0.94}Y_{0.06})O_2$ phase is referring to the metastable tetragonal form of ZrO_2 which is increased of both toughness and strength [9]. The presence of $Ce_2Zr_3O_{10}$ started to appear from 10 wt% to 15 wt% with reference ICDD 00-026-0359.

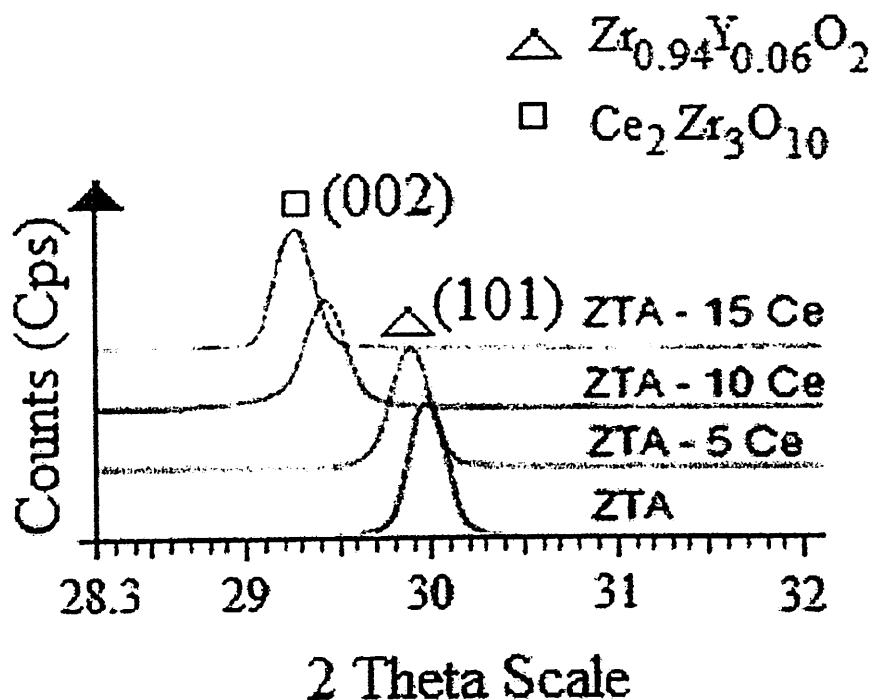


Fig.1: XRD patterns for ZTA-Ce ceramic composites.

Microstructural Observation. FESEM micrographs for the surface samples are shown in Fig. 2 and Fig. 3. Consistent with previous studies [2, 9-13] YSZ and Al_2O_3 grains are well distributed among each other but minor agglomeration was unavoidable. EDX analysis indicates the white areas are representing YSZ grains and the dark areas are representing Al_2O_3 grains. In general, similar microstructural characteristic were observed in these samples i.e. uniformly sized grains with high degree of grain close packing. Almost no abnormal grain growth was observed. However, abnormal growth such as platelet grains occurs among ZrO_2 grains that can be seen substantially in samples up to 10 wt% of CeO addition (Fig. 3). According to Fig. (a), the EDX analysis was targeted on top of lighter grains and results shows that the grains are made of YSZ. However, there is some trace of Al_2O_3 identified by the EDX. Similar observation is also shown in Fig 2(b), where as a small amount of Zr element was detected when targeting to Al_2O_3 grains, indicating that the EDX wave penetrates through the Zr grains. Similar observation was also reported by Maiti and Sil [3], where as their result on the EDX analysis also shows that there are minor value of Zr element detected while examining Al_2O_3 grains as shown in Fig.2.20.

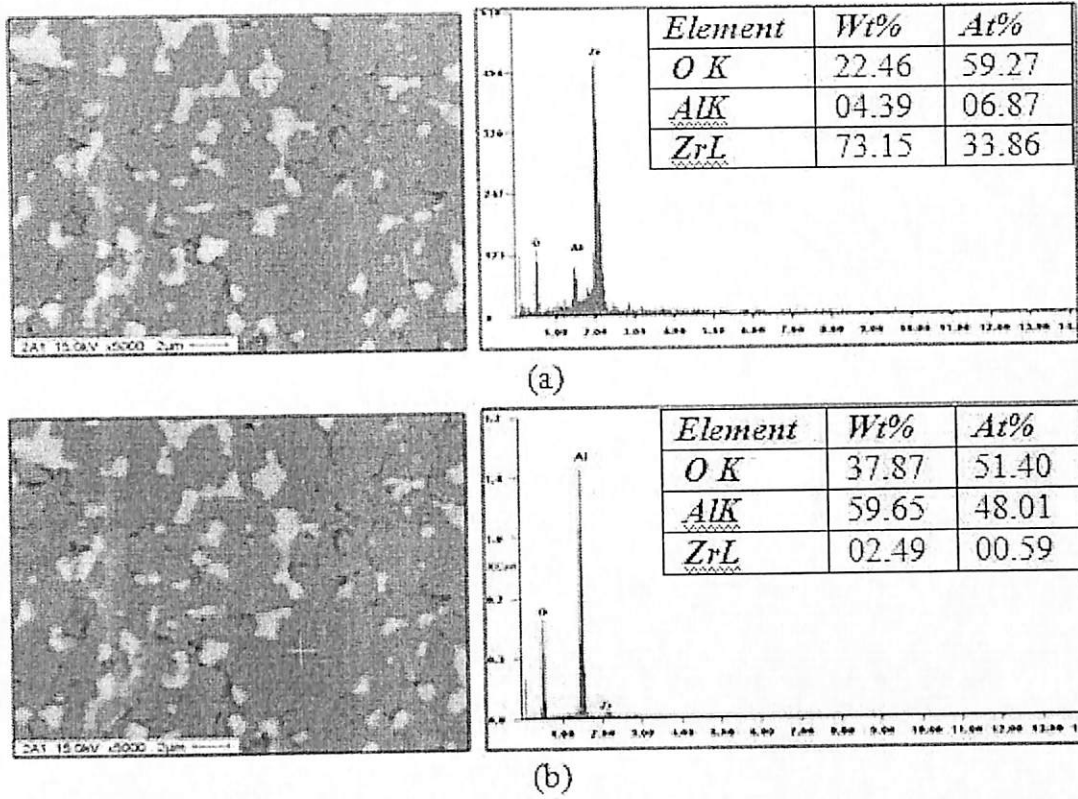


Fig. 2: Quantitative elemental analysis on the sample for (a) YSZ and (b) Al₂O₃.

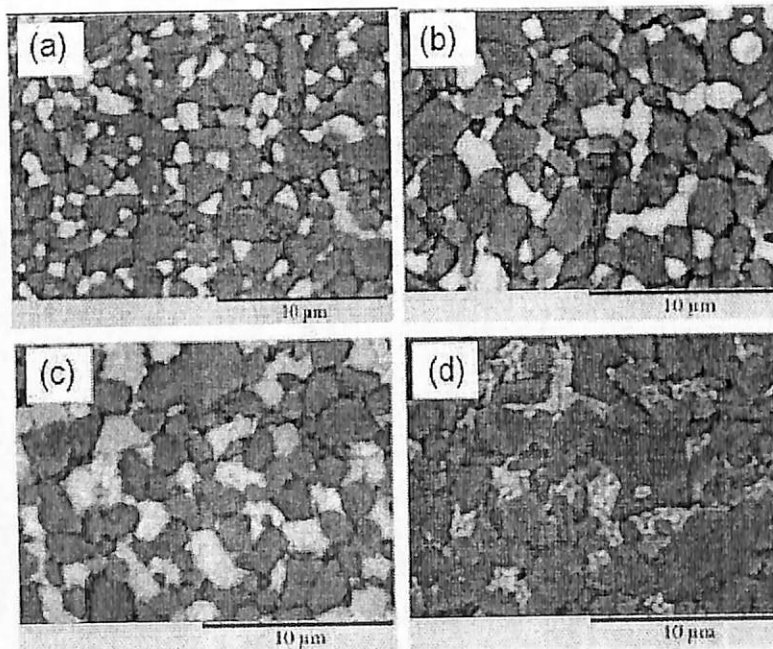


Fig. 3: SEM micrograph of ZTA ceramics with (a) 0 wt% (b) 5 wt% (d) 10 wt% and (e) 15 wt% at 10K magnification.

Fracture Toughness. The additions of ceria increase the fracture toughness values. The effect of ceria on fracture toughness is shown in Fig. 4. The maximum fracture toughness value is obtained with the use of 5wt% CeO₂ as additives i.e. 8.38 MPa·√m. Further addition of up to 15 wt%, fracture toughness decreased to 7.9 MPam^{1/2}.

Advanced X-Ray Characterization Techniques

10.4028/www.scientific.net/AMR.620

Structural and Microstructure Relationship with Fracture Toughness of CeO₂ Addition into Zirconia Toughened Alumina (ZTA) Ceramic Composites

10.4028/www.scientific.net/AMR.620.252

DOI References

- [1] K. Tsukuma and M. Shimada: Journal of Materials Science Vol. 20 (1985), pp.1178-1184.
<http://dx.doi.org/10.1007/BF01026311>
- [2] A.Z.A. Azhar, M.M. Ratnam and Z.A. Ahmad: Journal of Alloys and Compounds Vol. 478 (2009), pp.608-614.
<http://dx.doi.org/10.1016/j.jallcom.2008.11.156>
- [3] K. Maiti and A. Sil: Ceramics International Vol. 37 (2011), pp.2411-2421.
<http://dx.doi.org/10.1016/j.ceramint.2011.05.089>
- [4] S. Lathabai: Scripta Materialia Vol. 43 (2000), pp.465-470.
[http://dx.doi.org/10.1016/S1359-6462\(00\)00415-2](http://dx.doi.org/10.1016/S1359-6462(00)00415-2)
- [5] A.Z.A. Azhar, H. Mohamad, M.M. Ratnam and Z.A. Ahmad: Journal of Alloys and Compounds Vol. 497 (2010), pp.316-320.
<http://dx.doi.org/10.1016/j.jallcom.2010.03.054>
- [6] A.Z.A. Azhar, L.C. Choong, H. Mohamed, M.M. Ratnam and Z.A. Ahmad: Journal of Alloys and Compounds Vol. 513 (2012), pp.91-96.
<http://dx.doi.org/10.1016/j.jallcom.2011.09.092>
- [9] B. Smuk, M. Szutkowska and J. Walter: Journal of Materials Processing Technology Vol. 133 (2003), pp.195-198.
[http://dx.doi.org/10.1016/S0924-0136\(02\)00232-7](http://dx.doi.org/10.1016/S0924-0136(02)00232-7)
- [11] G. Magnani and A. Brillante: Journal of the European Ceramic Society Vol. 25 (2005), pp.3383-3392.
<http://dx.doi.org/10.1016/j.jeurceramsoc.2004.09.025>
- [12] J.K.C. Hao, A. A.Z.A., M.M. Ratnam and Z.A. Ahmad: Materials Science and Technology Vol. 26 (2010), pp.95-103.
<http://dx.doi.org/10.1179/174328408X389733>

The Effects of Cr₂O₃ Addition on Fracture Toughness and Phases of ZTA Ceramic Composite

AHMAD ZAHIRANI AHMAD AZHAR^{1,a}, NIK AKMAR REJAB^{1,b},
HASMALIZA MOHAMED^{1,c}, MANI MARAN RATNAM^{2,d},
and ZAINAL ARIFIN AHMAD^{1,e}

¹School of Materials and Mineral Resources Engineering, Engineering Campus, Universiti Sains Malaysia, 14300 Nibong Tebal, Pulau Pinang, Malaysia.

²School of Mechanical Engineering, Engineering Campus, Universiti Sains Malaysia, 14300 Nibong Tebal, Pulau Pinang, Malaysia.

^aahmad.zahirani@gmail.com, ^bakmarnik@gmail.com, ^cmmaran@ng.usm.my,
^dhasmaliza@eng.usm.my, ^ezainal@eng.usm.my

Keywords: ceramics, Cr₂O₃, composite materials, toughness

Abstract. Fracture toughness and phases of ceramic composites produced from alumina, yttria stabilized zirconia and chromia oxide system was investigated. The Cr₂O₃ weight percent was varied from 0 wt% to 1.0 wt%. Each batch of composition was mixed, uniaxially pressed 13mm diameter and sintered at 1600 °C for 4 h in pressureless conditions. Studies on their mechanical and physical properties such as Vickers hardness and fracture toughness were carried out. Results show that an addition of 0.6 wt% of Cr₂O₃ produces the best mechanical properties. Results of the highest fracture toughness is 4.73 MPa.m^{1/2}.

Introduction

Advanced ceramic materials are a good candidate for cutting insert application due to its high hot hardness [1]. Alumina based materials are one of the potential ceramics used to fabricate cutting inserts as it has high hot hardness, high abrasion resistance and chemical inertness against the environment. Unfortunately, alumina based cutting inserts have disadvantages such as low toughness and causes failures such as chipping and breakage during machining [2]. As a result, reinforcement materials such as yttria stabilized zirconia (YSZ) [3], titanium carbide, silver and ceria are used to improve the mechanical properties of alumina [4, 5]. Among other popular alumina based materials, zirconia-toughened alumina (ZTA) has been another recent addition to the group of high performance ceramics.

The ZTA composite was developed to substitute alumina ceramics in applications where a higher fracture resistance is required. In zirconia containing ceramics, maximum toughness can be achieved by manipulating the advantage of tetragonal-to-monoclinic transformation that can be induced in the stress field of an approaching crack [2, 3, 6-9].

Even though with the reinforcement of YSZ, the properties of fracture toughness of ZTA only improved to ~4.5 MPa.m^{1/2} compared to monolithic Al₂O₃; 3.9 MPa.m^{1/2} [7]. Thus, the performance of a ZTA cutting insert is limited by its fracture toughness. In order to further improve ZTA cutting insert performance, the fracture toughness needs to be improved.

Chromia (Cr₂O₃) is one the many additives potentially able to improve the physical properties of alumina. When chromia is added into an alumina system, isovalent solid solution will form over the full range of compositions due to the fact that both chromia and alumina are sesquioxides and have the same corundum crystal structure (approximately hexagonal close-packed oxide ions with the Al³⁺ and Cr³⁺ ions occupying two thirds of the available octahedral interstitial sites). In reactions at high temperatures (T >1000 °C), complete ranges of substitution solid solutions are obtained [10-12]. Isovalent solid solution happens when an atom or ion replaces an atom or ion of the same charge in the parent structure. It contributes to high refractoriness and chemical stability [11]. The

addition of Cr_2O_3 also increases the hardness, tensile strength and thermal shock resistance of alumina [13]. When a small amount of Cr_2O_3 (~2 mol %) is added, the grains become larger and bimodal in size distribution. At the same time, the fracture toughness and flaw tolerance of alumina are also improved. The hardness as well as elastic modulus is increased. However, fracture strength decreases with the addition of Cr_2O_3 [13].

Even though the study of ZTA and $\text{Al}_2\text{O}_3\text{-Cr}_2\text{O}_3$ has been done extensively for the past 20 years, the studies were carried out individually. The studied on ZTA- Cr_2O_3 as a ceramic composite system for their mechanical properties are rarely reported elsewhere, until now. In this study, the mechanical properties of Cr_2O_3 doped ZTA were investigated.

Materials and Methodology

Monolithic Al_2O_3 (average particle size 0.5 μm , supplier Martinswerck, 95% purity), YSZ (average particle size 1.5 μm , supplier Goodfellow, 95 % purity with Y_2O_3 as stabilizer) and Cr_2O_3 (average particle size 0.5 μm , supplier Sigma-Aldrich, 99.9 % purity) were used as the starting materials. Pellets with 13mm diameter were fabricated via the solid state processing route. Samples with an 80/20 ratio for Al_2O_3 /YSZ respectively were prepared with different Cr_2O_3 wt% ranging from 0 wt% to 1.0 wt%. The powders were then mixed with 0.6 wt % of polyethylene glycol 400 using a ball mill for 8 hours and pressed at 295 MPa using a hydraulic press. The specimens were then sintered in a HTF 1800 Carbolite furnace at 1600 °C for 4 hours with 5°C/min sintering rate.

Fracture toughness was calculated using the formula proposed by Niihara for Palmqvist crack [14]. Value for Young Modulus (E) used in this study is 310 GPa.

$$3K_{Ic} = 0.035 (\text{Ha}^{1/2}) (3E/H)^{0.4} (l/a)^{-0.5} \quad (1)$$

XRD of the sintered samples was carried out to determine the phases present. The XRD patterns of the sintered products were obtained using a Bruker D8 Advanced operated in Bragg-Brentano geometry, with Cu $K\alpha$ radiation, in the $10^\circ \leq 2\theta^\circ \leq 90^\circ$ range. Counting time was fixed at 71.5 s for each $0.03^\circ 2\theta$ step. The X-ray tube was operated at 40 kV and 30 mA. Quantitative phase analysis was measured by Rietveld method using HighScorePlus software. Crystal structure data for each phases present in the samples were taken from ICSD. The refinement was done in stages, with the atomic coordination and thermal parameters held fixed.

Result and Discussion

XRD results for the sintered ZTA- Cr_2O_3 samples are shown in Fig. 1. XRD analysis indicates that Al_2O_3 was present as corundum (ICSD reference 98-001-1621). XRD analysis also showed that YSZ has tetragonal crystal structures together with the presence of yttria (ICSD reference 98-002-0789). There is no monoclinic ZrO_2 phase observed. On the other hand, the XRD result does not detect the presence of Cr_2O_3 phase in the sample. This is due to the low amount of Cr_2O_3 wt % in the sample. According to the XRD analysis no new compound was formed with the addition of Cr_2O_3 . This is due to the behavior of Al_2O_3 and Cr_2O_3 which will form a complete solid solution on all range of composition. Fig 2 shows the comparison of XRD results of ZTA samples with various Cr_2O_3 wt %. It is shown that the addition of Cr_2O_3 would result the monoclinic phase to disappear (shown in the red dotted box), where as the peaks for monoclinic phase are no longer seen for samples of ZTA with the addition of Cr_2O_3 . Table 1 shows the effect of Cr_2O_3 addition to the lattice parameter of Al_2O_3 . It is increased from 4.757754Å to 4.761456Å and from 12.990660Å to 13.003890Å for lattice parameter a and c, respectively. This increment is due to the bigger radii of Cr compare to Al.

Table 1: Unit cell dimensions of Al₂O₃ with different Cr₂O₃ wt %.

Materials	a (Å)	c (Å)
Al ₂ O ₃ pure	4.757754	12.990660
ZTA + 0 Cr ₂ O ₃ wt %	4.758206	12.993020
ZTA + 0.2 Cr ₂ O ₃ wt %	4.759128	12.994950
ZTA + 0.5 Cr ₂ O ₃ wt %	4.759653	12.999820
ZTA + 0.8 Cr ₂ O ₃ wt %	4.760283	13.001680
ZTA + 1.0 Cr ₂ O ₃ wt %	4.761456	13.003890

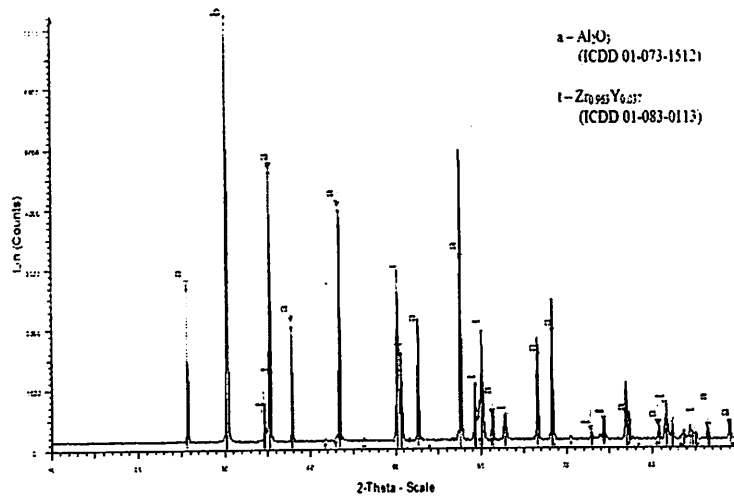


Fig.1 : XRD results of addition of 0.5wt% of Cr₂O₃ into ZTA cutting insert after the sintering process which (a) represent tetragonal alumina corundum (ICSD reference 98-001-1621) and (b) represent the tetragonal yttria stabilized zirconia (ICSD reference 98-002-0789).

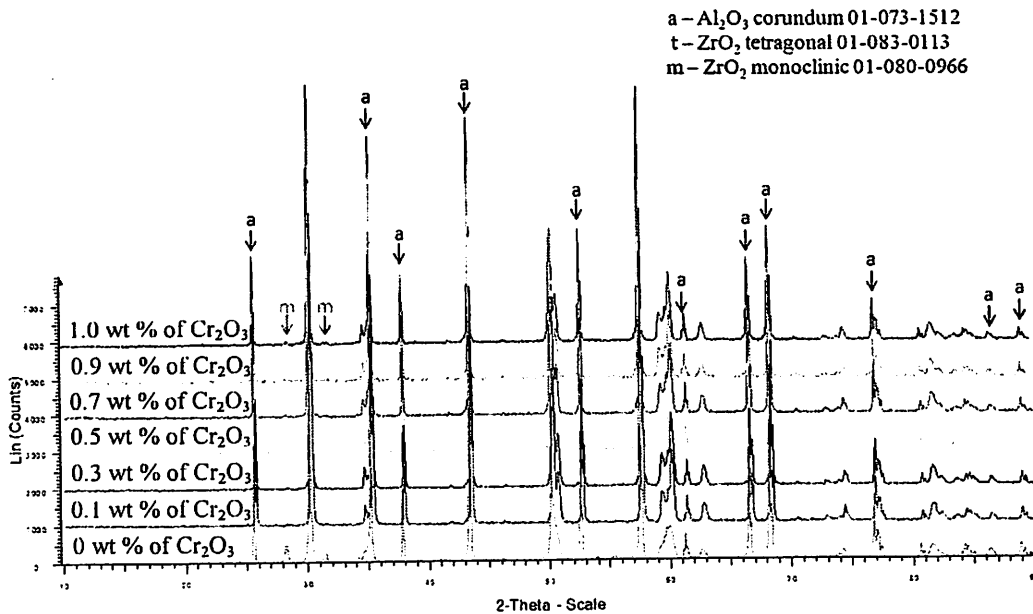


Fig. 2: Comparison of XRD results for ZTA cutting insert with various addition of Cr₂O₃ wt%.

References

- [1] Q. Like, L. Xikun, Q. Guanming, M. Weimin, S. Yanbin and Y. Huadong: *Journal of Rare Earths*, Vol. 25 (2007), p. 309-316.
- [2] A.Z.A. Azhar, M.M. Ratnam and Z.A. Ahmad: *Journal of Alloys and Compounds* Vol. 478 (2009), p. 608-614.
- [3] B. Smuk, M. Szutkowska and J. Walter: *Journal of Materials Processing Technology* Vol. 133 (2003), p. 195-198.
- [4] A. Gatto: *Journal of Materials Processing Technology* Vol. 174 (2006), p. 67-73.
- [5] A.K. Dutta, A.B. Chattopadhyaya and K.K. Ray: *Wear* Vol. 261 (2006), p. 885-895.
- [6] B. Mondal, A.B. Chattopadhyay, A. Virkar and A. Paul: *Wear* Vol. 156 (1992), p. 365-383.
- [7] D. Casellas, M.M. Nagl, L. Llanes and M. Anglada: *Journal of Materials Processing Technology* Vol. 143 (2003), p. 148-115.
- [8] N.P. Bansal and S.R. Choi: *National Aeronautics and Space Administration John H. Glenn Research Center, Ohio*, 2003.
- [9] V. Sergo, V. Lughi, G. Pezzotti, E. Lucchini, S. Meriani, N. Muraki, G. Katagiri, S. Lo Casto and T. Nishida: *Wear* Vol. 214 (1998), p. 264-270.
- [10] G. Magnani and A. Brillante: *Journal of the European Ceramic Society* Vol. 25 (2005), p. 3383-3392.
- [11] F. Bondioli, A.M. Ferrari, C. Leonelli, T. Manfredini, L. Linati and P. Mustarelli: *Journal of the American Ceramic Society* Vol. 83 (2000), p. 2036-2040.
- [12] L. Zhang, M. Kuhn and U. Diebold: *Surface Science* Vol. 375 (1997), p. 1-12.
- [13] D.-H. Riu, Y.-M. Kong and H.-E. Kim: *Journal of the European Ceramic Society* Vol. 20 (2000), p. 1475-1481.
- [14] K. Niihara: *Journal of Materials Science Letters* Vol. 2 (1983), p. 221-223.
- [15] M.T. Hernandez, M. González and A. De Pablos: *Acta Materialia* Vol. 51 (2003), p. 217-228.
- [16] T. Hirata, K. Akiyama and H. Yamamoto: *Journal of the European Ceramic Society* Vol. 20 (2000), p. 195-199.

Experimental Details

A monolithic Al_2O_3 (average particle size, $0.5 \mu\text{m}$) was used as a baseline material. YSZ (GoodFellow Cambridge Limited) particles (yttria content, 5.2%, average particle size, $1.5 \mu\text{m}$) were added to an Al_2O_3 matrix with a ratio of 80 wt. % $\text{Al}_2\text{O}_3/20$ wt. % YSZ. MgO in average particle sizes of 20 nm (Strem Chemicals) was added to the $\text{Al}_2\text{O}_3/\text{YSZ}$. The $\text{Al}_2\text{O}_3/\text{YSZ}$ samples were prepared with 1.1 wt. % MgO. The powders were then mixed using a ball mill for 8 h and pressed at 280 MPa using a hydraulic press. The specimens were then sintered in Intek electric furnace at 1600°C for 4 h with $5^\circ\text{C}/\text{min}$ sintering rate. Properties of fabricated insert were examined and applied in machining of stainless steel 316L with 12 mm diameter. Parameter used during the machining is shown in Table 1. Meanwhile, wear analyses were carried out using the scanning electron microscope (SEM).

Table 1: Machining parameter.

Parameter	Value
Cutting Speed (rpm)	625, 950, 1150, 1400, 1750
Feed rate (mm/rev)	0.1, 0.2, 0.3
Depth of cut (mm)	0.2
Cutting environment	Dry
Cutting length (mm)	20

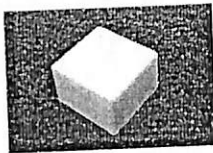


Fig. 1 Fabricated insert

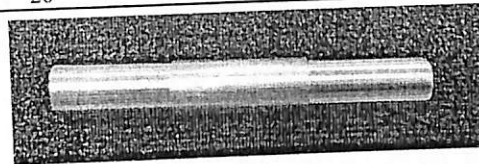


Fig. 2 Stainless Steel 316L used as work piece

Result and Discussion

Result on the properties of the fabricated insert shows in Table 2. This result validates the suitability of the insert to be used in machining process. The density obtained is at optimum value. According to Azhar et., al, [1] $4.31\text{g}/\text{cm}^3$ is the maximum density that can be obtained with addition of MgO and further addition of MgO will show insignificant improvement. The Vickers hardness obtained also in the range of suitable hardness for application in machining as D'Errico et., al. [9] in their study shows that hardness of insert from 1,664 HV and further is suitable for machining process. While the fracture toughness for the fabricated insert is $3.12 \text{MPa}\cdot\text{m}^{1/2}$ which is acceptable for machining process but limited to certain machining condition [8]. Meanwhile, the XRD result of powder after mixing and the sintered body show no sign of change in the raw materials as shown in Fig. 3.

For wear analysis, three types of wears observed in these experiments which are *flank wear*, *notch wear* and *chipping*. Fig. 4 shows the SEM micrograph of the flank wear land of ZTA-MgO ceramic cutting tool. Result of *flank wear* with the various cutting speed is plotted into graph in Fig. 5. The graph exhibit linear increment of flank wear with increment of cutting speed as reported by others [1, 3, 6]. This result is expected as the increment of cutting speed will increase the rubbing rate between the cutting edge and the workpiece [9]. In addition, the graph of flank wear with various feedrate is plotted in Fig.6. Result shows that flank wear decrease when feedrate is increased from 0.1 to 0.2 but increased when feedrate is increased further due to excessive load on the insert [10]. This situation happen due to increment of force on the insert when the feed rate is increased and causing higher friction between the cutting tips and the work piece resulting severe tool wear. From this result also shows that feed rate 0.2 is the most suitable feed rate for machining this set of experiments where the tool wear is at lowest value for all cutting speed change.

Table 2: Properties of ZTA-MgO ceramic insert with 1.1 wt.% MgO

Properties	Value
Density (g/cm ³)	4.31
Vickers Hardness (HV)	1740
Shrinkage (%)	15.82
Fracture Toughness (MPa.m ^{1/2})	3.12

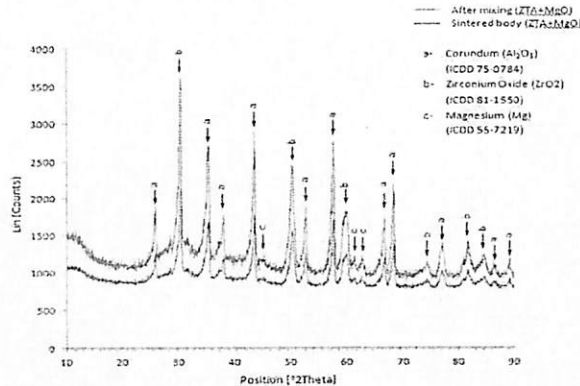


Fig. 3 Result of XRD for after mixing and sintered body of ZTA with 1.1wt% MgO

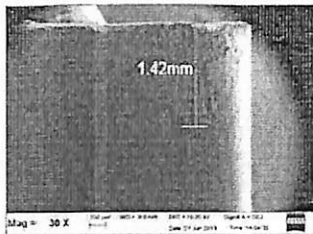


Fig. 4 SEM micrographs of the flank wear of ZTA-MgO insert

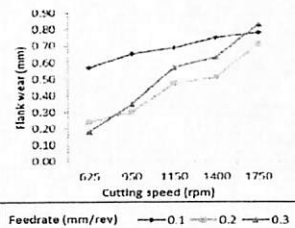


Fig. 5 Flank wear vs. cutting speed

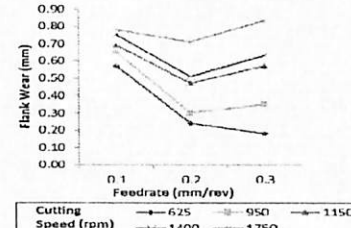


Fig. 6 Flank wear vs feedrate

Another wear observed on ZTA-MgO ceramic cutting insert is *notch wear* as shown in Fig. 7. The graph of notch wear with the change of cutting speed is plotted in Fig. 8 while the change of feedrate in Fig. 9. Based on the graphs plotted, it shows that notch wear start to increase with increment of cutting speed which suits the result with previous work [6]. When cutting speed is increase the cutting edge temperature will become too high ($\sim 700^{\circ}\text{C}$) and cause oxidation at the cutting depth. This is also caused by the continuous segmented chip that form when the cutting speed is increased where this type of chip abrade a notch at the end of the cut zone [8]. However notch wear decrease when feedrate is increased from 0.1 to 0.2 but increased again when feedrate is increased to 0.3. In this case, it happens due to excessive load on the insert when the feedrate is increased further to 0.3 mm/rev.

In this research also, chipping area has been studied through visual based on SEM micrograph as shown in Fig. 10. It shows that chipping or inserts breakage increased as the feedrate increased. However no significant change of chipping area observed as the cutting speed is increased. This result caused by the weak geometry of nose radius where the feedrate used is too high for the insert to withstand. Therefore, higher value of feedrate will increase burden to the insert and causing bigger breakage area [10].

The Cutting Speed Influences on Tool Wear of ZTA Ceramic Cutting Tools and Surface Roughness of Work Material Stainless Steel 316L During High Speed Machining

Afifah MOHD ALI^{1,a}, Norazharuddin Shah ABDULLAH^{1,b},
Manimaran RATNAM^{2,c}, Zainal Arifin AHMAD^{1,d*}

¹ Structural Materials Niche Area, School of Materials and Mineral Resources, Engineering Campus, Universiti Sains Malaysia, 14300 Nibong Tebal, Penang, Malaysia

² School of Mechanical, Engineering Campus, Universiti Sains Malaysia, 14300 Nibong Tebal, Penang, Malaysia

^aafifah.mdali@gmail.com, ^bazhar.abdullah@usm.my, ^cmmaran@usm.my, ^{d*}srzainal@usm.my

Keywords: ZTA, Ceramic tool, Performance, Cutting speed, Turning.

Abstract. The purpose of this research is to find the effects of cutting speed on the performance of the ZTA ceramic cutting tool. Three types of ZTA tools used in this study which are ZTA-MgO (micro), ZTA-MgO (nano) and ZTA-MgO-CeO₂. Each of them were fabricated by wet mixing the materials, and then dried at 100°C before crushed into powder. The powder was pressed into rhombic shape and sintered at 1600°C at 4 hours soaking time to yield dense body. To study the effect of the cutting speed on fabricated tool, machining was performed on the stainless steel 316L at 1500 to 2000 rpm cutting speed. Surface roughness of workpiece was measured and the tool wears were analysed by using optical microscope and Matlab programming where two types of wear measured i.e. nose wear and crater wear. Result shows that by increasing the cutting speed, the nose wear and crater wear increased due to high abrasion. However, surface roughness decreased due to temperature rise causing easier chip formation leaving a good quality surface although the tool wear is increased.

Introduction

High speed machining (HSM) is a modern machining method that is said to increase the efficiency, accuracy and quality [1] of the products and besides reduce the machining time and cost. However, problem with HSM is the extreme tribological conditions at dry condition due to the high friction and temperature [2]. As the contact time of the cutting tips to the cutting surface is shorter, the cutting force will be concentrated adjacent to the cutting tips. Due to this, temperature rises at the cutting tips that make it softer and resulting the deformation and deflection [2]. Therefore, tool wear increase rapidly and the quality of the product deteriorates. As an alternative, ceramic tools has been chosen to improve the problem as they possesses hardness [3-5], chemical inertness [6], fracture strength [3,6,7], toughness [3,8], wear resistance and thermal shock resistance [3].

Though these attributes are good for HSM, the brittleness of the ceramic cutting tool is the main disadvantage that may cause premature breakage of the tool [1,9]. Therefore it is important for the researchers to overcome the brittleness of the ceramic cutting tool by increasing the hardness and fracture toughness. For the ceramic cutting tool use in this research, additives are added to the former ZTA ceramic cutting tool. They are magnesium oxide (MgO), and cerium oxide (CeO₂). MgO is proved as a good additives to improve the microstructure of the fabricated tool [10-11], improve the Vickers hardness [12] and increase the bulk density [10]. On the other hand, Rejab et al. [4] claims that the addition of CeO₂ increased the fracture toughness up to 8.38 MPa.√m and Vickers hardness, 1688 HV of the ZTA ceramic cutting tool.

samples. Smoothly polished specimens were thermally etched at 1400°C for 1 hour in air. Microstructural investigation of the etched specimens was performed using SEM (Hitachi TM3000 Tabletop, Japan). The fracture toughness, which is a critical mechanical property parameter in this work, was determined by the simple indentation technique. The Vickers hardness (HV) was measured on a Shimadzu Vickers hardness tester HSV-20, Japan with different loads of 294 N. The fracture toughness (K_{Ic}) was calculated from the measured radial cracks around the Vickers indentations obtained, according to the formula proposed by Niihara [6]. The toughness was measured on a single specimen from five indentations at each load. Both the diagonal length of the indentation and crack length were measured. K_{Ic} (HV30) was calculated using Eq. (1)

$$3K_{Ic} = 0.035(Ha/2)(3E/H)0.4 (l/a)^{-0.5} \quad (\text{Eq. 1})$$

Where K_{Ic} is the fracture toughness, H is Vickers hardness, a is the half length of Vickers diagonal (μm), E is equal to the Young modulus of the samples, and l is the length of the radial crack size (μm).

Results and Discussion

In this section the observed variation in indentation toughness of the investigated ZTA ceramics is explained in terms of the amount of ceria in sintered microstructures. The physical modifications in the microstructure and their impact on the toughness of ZTA ceramics, established by the mixing route are elucidated. Fig. 1 shows the XRD results of the ZTA ceramics with different CeO_2 additions. The XRD patterns correspond to yttria doped zirconia ($\text{Zr}_{0.935}\text{Y}_{0.065}\text{O}_{1.968}$) peaks (ICDD files No. 01-078-1808) and $\alpha\text{-Al}_2\text{O}_3$ (No. 00-010-0173). The existence of ($\text{Zr}_{0.935}\text{Y}_{0.065}\text{O}_{1.968}$) phase relates to the metastable tetragonal form of ZrO_2 . The magnified diffraction pattern between $2\theta = 28.3^\circ$ to 32° which shows that position of the (101) peak of tetragonal ZrO_2 had slightly shifted for 0 – 5 wt.% CeO_2 additions and further additions of 10 wt.% of CeO_2 additions the $\text{Ce}_2\text{Zr}_3\text{O}_{10}$ phase started to become visible and confirmed by the position of (002, 200 and 100) peaks, with reference to ICDD 00-026-0359.

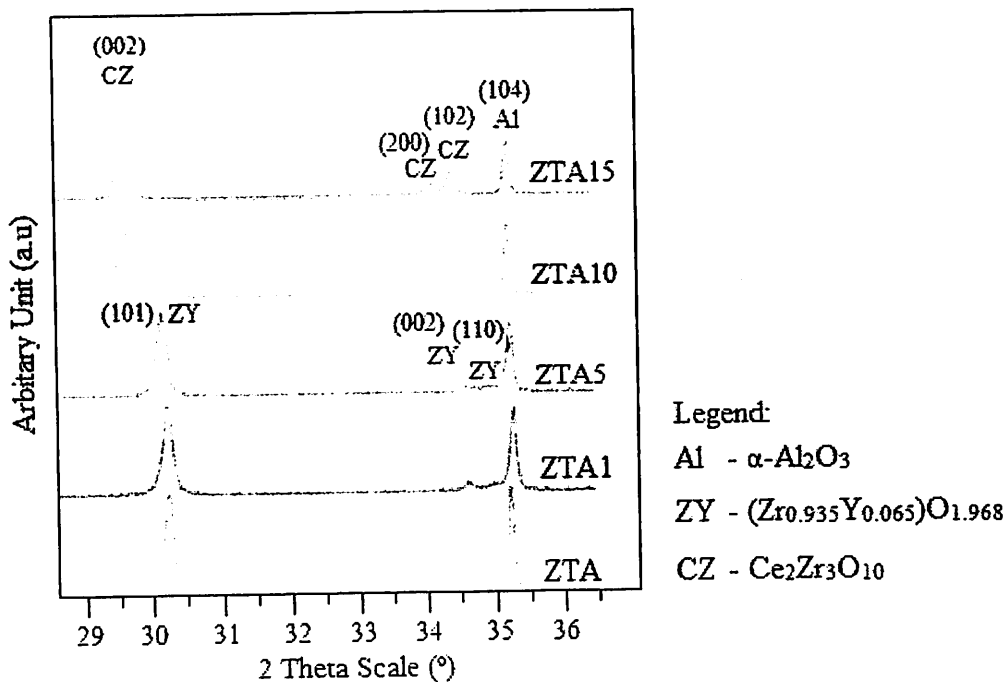


Fig. 1 XRD results of CeO_2 addition in ZTA composites.

The Al_2O_3 and YSZ grains are indicated by dark grains and bright grains in Fig. 2. The YSZ grains and Al_2O_3 grains are impartially distributed among each other. However, abnormal grain growth such as platelet grains appears among YSZ grains which is believe related to $\text{Ce}_2\text{Zr}_3\text{O}_{10}$ phase, it can be recognized in Fig. 2 for samples 10 wt.% of CeO_2 additions. These platelet grain appeared caused by overstabilised addition of CeO_2 which is influence the grain shapes for both YSZ.

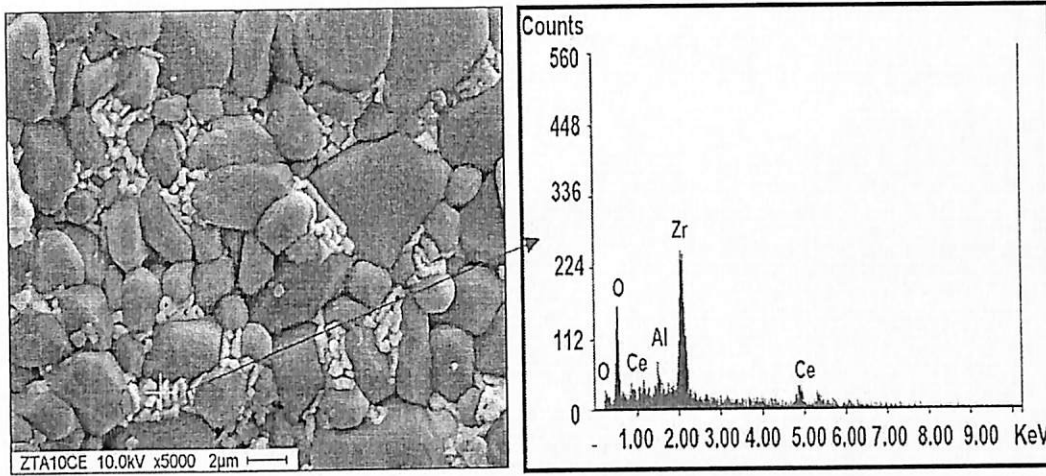


Fig. 2 Microstructure and EDX results for ZTA with 15 wt.% CeO_2 ceramics. Platelet grains in white colour refer to $\text{Ce}_2\text{Zr}_3\text{O}_{10}$ compound.

Fig. 3 gives the results of fracture toughness and Vickers hardness. The fracture toughness values for ZTA (0 wt.%) are $5.87 \text{ MPa}\cdot\sqrt{\text{m}}$, increase to $8.38 \text{ MPa}\cdot\sqrt{\text{m}}$ for 5 wt.% of CeO_2 addition, respectively. By increasing the addition up to 15 wt.% CeO_2 , resulting the decreasing of fracture toughness value to $7.90 \text{ MPa}\cdot\sqrt{\text{m}}$. The increase of fracture toughness values can be ascribed to the existence of CeO_2 in the ZTA.

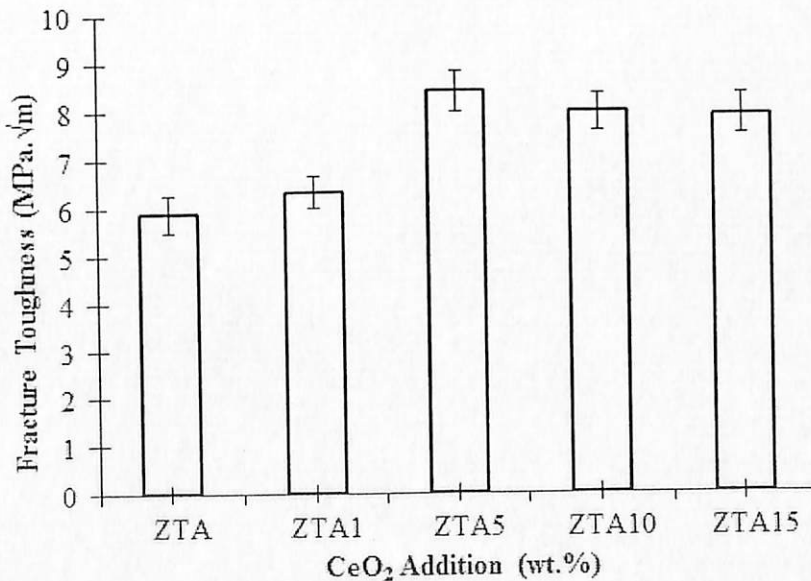


Fig. 3 Results of fracture toughness for varied CeO_2 addition in ZTA composites

Summary

The role of $Ce_2Zr_3O_{10}$ phase on indentation fracture toughness of ZTA ceramics can be tailored from ~ 5 up to ~ 8 $MPa\sqrt{m}$ by the addition of CeO_2 powder in a formulated mixing route. An abnormal grain growth such as platelet grains appears among YSZ grains which is related to the CeO_2 additions. Sintered ZTA with an overall ceria content of 5 wt.% exhibit an excellent indentation toughness ($8.38MPa\sqrt{m}$) in combination with a high Vickers hardness (around 1678 HV).

Acknowledgements

This work was supported by the Universiti Sains Malaysia (USM) under the grant 1001/PBAHAN/811212 and Post-Doctoral Fellowship Scheme.

References

- [1] B. Basu, J. Vleugels, O. Van Der Biest, $ZrO_2-Al_2O_3$ composites with tailored toughness, *J. Alloys Compd.* 372 (2004) 278–284.
- [2] M. Szutkowska, B. Smuk, A. Kalinka, K. Czechowski, M. Boniecki, Selected mechanical properties and microstructure of $Al_2O_3 - ZrO_2$ nano ceramic composites, *J. Achiev. Mater. Manuf. Eng.* 48 (2011) 58–63.
- [3] Y. Ye, J. Li, H. Zhou, J. Chen, Microstructure and mechanical properties of yttria-stabilized ZrO_2/Al_2O_3 nanocomposite ceramics, *Ceram. Int.* 34 (2008) 1797–1803.
- [4] N. Claussen, Strengthening strategies for ZrO_2 -toughened ceramics at high temperatures, *Mater. Sci. Eng.* (1985) 23–38.
- [5] M. Arin, J. Vleugels, K. Vanmeensel, G. Goller, Effect of different stabilizer addition on preparation and hydrothermal stability of ZrO_2-TiN composites with varying TiN content, *Key Eng. Mater.* 363 (2008) 795–798.
- [6] K. Niihara, A fracture mechanics analysis of indentation-induced Palmqvist crack in ceramics, *J. Mater. Sci. Lett.* 2 (1983) 221–223.

Development and Investigation of Materials Using Modern Techniques

10.4028/www.scientific.net/MSF.840

Role of $\text{Ce}_2\text{Zr}_3\text{O}_{10}$ Phase on the Microstructure and Fracture Toughness of ZTA Composites

10.4028/www.scientific.net/MSF.840.57

DOI References

- [1] B. Basu, J. Vleugels, O. Van Der Biest, ZrO₂-Al₂O₃ composites with tailored toughness, *J. Alloys Compd.* 372 (2004) 278-284.
10.1016/j.jallcom.2003.09.157
- [2] M. Szutkowska, B. Smuk, A. Kalinka, K. Czechowski, M. Boniecki, Selected mechanical properties and microstructure of Al₂O₃ - ZrO₂ nano ceramic composites, *J. Achiev. Mater. Manuf. Eng.* 48 (2011) 58-63.
10.4028/www.scientific.net/ast.65.50
- [3] Y. Ye, J. Li, H. Zhou, J. Chen, Microstructure and mechanical properties of yttria-stabilized ZrO₂/Al₂O₃ nanocomposite ceramics, *Ceram. Int.* 34 (2008) 1797-1803.
10.1016/j.ceramint.2007.06.005
- [4] N. Claussen, Strengthening strategies for ZrO₂-toughened ceramics at high temperatures, *Mater. Sci. Eng.* (1985) 23-38.
10.1016/0025-5416(85)90203-4
- [5] M. Arin, J. Vleugels, K. Vanmeensel, G. Goller, Effect of different stabilizer addition on preparation and hydrothermal stability of ZrO₂-TiN composites with varying TiN content, *Key Eng. Mater.* 363 (2008) 795-798.
10.4028/www.scientific.net/kem.361-363.795
- [6] K. Niihara, A fracture mechanics analysis of indentation-induced Palmqvist crack in ceramics, *J. Mater. Sci. Lett.* 2 (1983) 221-223.
10.1007/bf00725625

encourage grain growth of Al_2O_3 and ZTA which leads to a completely dense and strongly finer homogeneous structure. Therefore, the aim of this study is to investigate the effect of TiO_2 addition to ZTA phases and microstructure.

Methodology

The starting raw materials were Al_2O_3 (Martinswerk, 99% purity), YSZ (Goodfellow, 5.4 mole% Y_2O_3 as stabilizer, >96% purity), and TiO_2 (Fluka, $\geq 99\%$ purity). The initial mixture was 80 wt% Al_2O_3 and 20 wt% YSZ. The initial mixture was mixed with different amounts of TiO_2 with the condition that the ratio of Al_2O_3 to YSZ was fixed at 4:1. The details are shown in Table-1-. The mixtures were wet mixing using ABB-Mixer Mill with ZrO_2 balls. Then the slurry was dried for 24 h at 100°C in an oven Memmert-CU 9760 and the dried cake was crushed and sieved to pass $75\ \mu\text{m}$. Powders were hydraulically pressed to form pellets with 13 mm in diameter and 4 mm thickness at 250 MPa for 120 sec. The pellets were sintered in two stages using Udian furnace model KHT-16000X.

Table 1: Code Samples based on TiO_2 contents

Al_2O_3 content (wt %)	YSZ content (wt %)	TiO_2 content (wt %)
80.00	20.00	0
79.20	19.80	1
77.60	19.40	3
76.00	19.00	5
74.40	18.60	7
72.00	18.00	10

Phase compositions of the sintered samples were analyzed by utilizing an XRD (Bruker AXS D2 Advance) with $\text{CuK}\alpha$ radiation operating at 30 kV and 10 mA. The scanning speed was maintained at $0.03^\circ/\text{s}$ in the range of $10^\circ \leq 2\theta \leq 90^\circ$. Counting time was fixed at 38.4 sec. The PANalytical X'PERT Highscore Plus software was used to perform the qualitative and quantitative analyze of XRD profiles. The calibrated standard method (Semi-automatic mode) with fourteen steps of Rietveld refinement was used to obtain a minimum profile error. The Scanning electron microscopy (Hitachi TM3000 Tabletop SEM) was employed to study the microstructure of the samples.

The Vickers indentation technique was employed to measure the Vickers hardness and fracture toughness of the sintered samples. The Hardness Tester Mitutoyo-model HV-114 was used to measure the Vickers hardness by taking average of different five readings for each sample. The polished sintered samples were subjected to HV 30 kgf for 15 sec. Bulk density of the samples were measured based on the Archimedes principle.

Result and Discussion

Figure 1 indicates the results of Vickers hardness for ZTA- TiO_2 ceramic composite with different TiO_2 content. Vickers hardness gradually increases from 1516.13 HV (0 wt% TiO_2) to 1615.8 HV (3 wt% TiO_2), showing improvement of 6.57 %. Result of Vickers hardness is directly related to the result of the bulk density as shown in Fig. 4. The highest value of Vickers hardness 1615.8 HV (3 wt% TiO_2) also has the highest density value ($4.10\ \text{g}/\text{cm}^3$). The increase in hardness with increasing TiO_2 content is related to an increase in densification. Further increment of TiO_2 after 3 wt% cause the Vickers hardness reduced from 1595 HV to 1538.1 HV. This is due to the present of secondary phases which is Al_2TiO_5 in the ZTA- TiO_2 ceramic composite according to the XRD analysis. Addition more than 5 wt% TiO_2 show insignificant effect on the Vickers hardness.

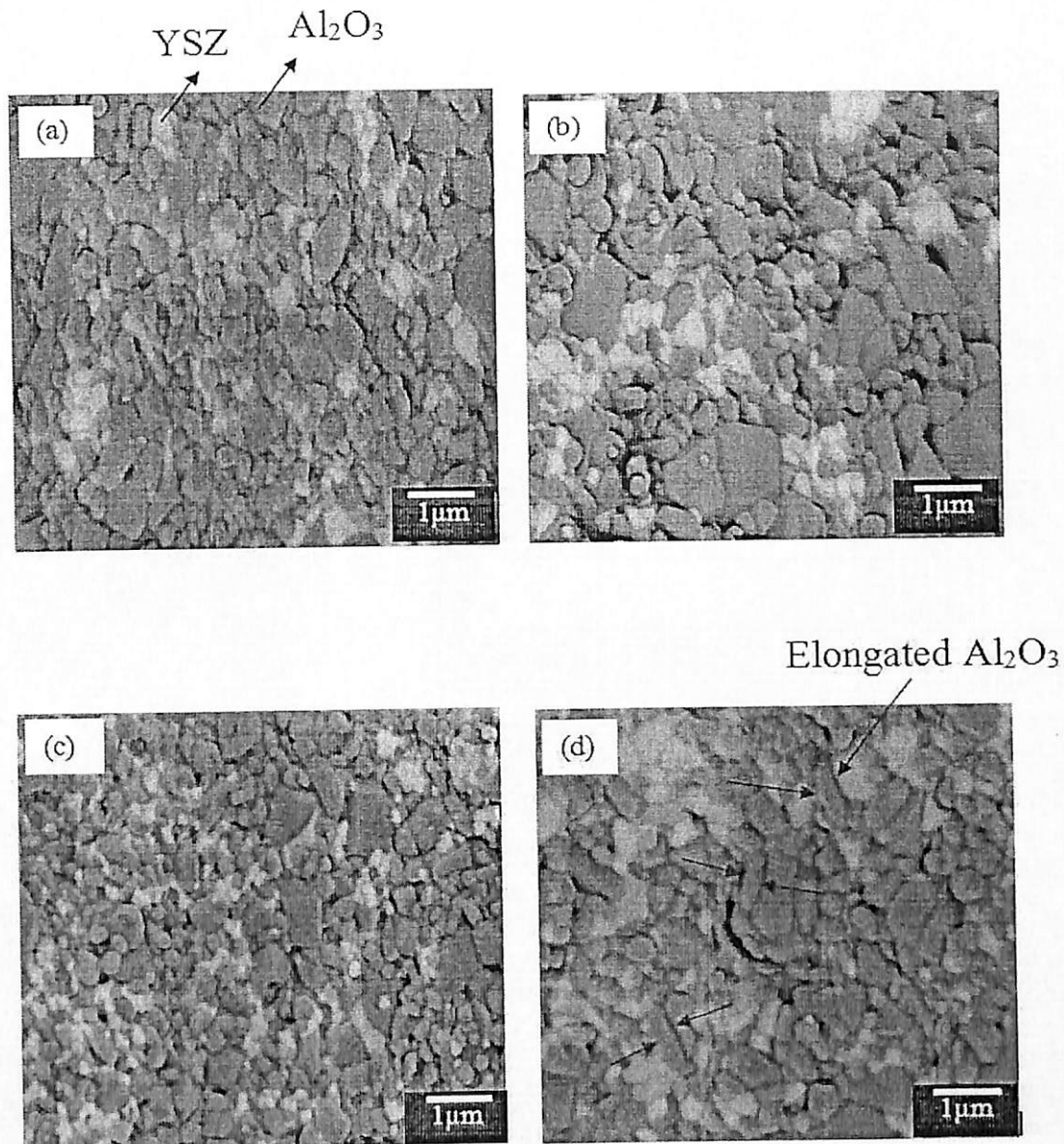


Fig. 3: Microstructures of ZTA-TiO₂ ceramics composites with (a) 0 wt% TiO₂, (b) 1 wt% TiO₂, (c) 3 wt% TiO₂, (d) 5 wt% TiO₂ at magnification 5000x

Figure 4 shows the results of bulk density of the fired samples (0-10 wt% TiO₂) at 1600°C. It is noted that the bulk density of the sintered samples increases with increasing the content of TiO₂ from 3.90 g/cm³ (0 wt% TiO₂) to 4.10 g/cm³ (3 wt% TiO₂), showing a 5.13% increase with the addition of TiO₂. Among them, sample with 3 wt% TiO₂ has the highest bulk density value (4.10 g/cm³). TiO₂ has the ability to inhibit the abnormal grain growth of Al₂O₃, thus at the beginning the higher density obtains when higher TiO₂ wt% is added.

The TiO₂ added after 3 wt% TiO₂ is no longer incorporated into Al₂O₃ but used to form a secondary phases which are Al₂TiO₅ that has been confirmed in XRD analysis shown in Fig. 2, hence the bulk density starts to decrease after 3 wt% TiO₂ from 4.00 g/cm³ (5 wt% TiO₂) to 3.76 g/cm³ (10 wt% TiO₂). The decrease in density for high amount of TiO₂ may be due to the formation of secondary phase which has lower density than Al₂O₃ and TiO₂ [6].

Wear Analysis of ZTA-MgO Ceramic Cutting Inserts On Stainless Steel 316L Machining

AFIFAH Mohd.Ali^{1,a}, AHMAD ZAHIRANI Ahmad Azhar^{2,b},
MANI Maran Ratnam^{3,c}, ZAINAL ARIFIN Ahmad^{1,d*}

¹ School of Materials & Mineral Resources Engineering, Universiti Sains Malaysia, 14300 Nibong Tebal, Penang, Malaysia

² Department of Manufacturing and Materials Engineering, Kulliyah of Engineering, Universiti Islam Antarabangsa Malaysia, 53100 Jalan Gombak, Kuala Lumpur, Malaysia

³ School of Mechanical Engineering, Universiti Sains Malaysia, 14300 Nibong Tebal, Penang, Malaysia

^asakisakura@gmail.com, ^bzahirani@iium.edu.my, ^cmbaran@eng.usm.my, ^dzainal@eng.usm.my

Keywords: ZTA, MgO, ceramic insert, wear, turning

Abstract. The performance of zirconia toughened alumina with addition of MgO additives is investigated. Optimized composition of MgO at 1.1 wt% was used in the composition with alumina/yittria stabilized zirconia (YSZ). The composition was mixed, uniaxially pressed into rhombic 80° cutting inserts with 0.8 mm nose radius and sintered at 1600°C for 4 h in pressureless condition. For machining analysis, commercial stainless steel 316L with 12 mm diameter were used as workpiece. The workpiece was machined at 625 to 1750 rpm. Tool wear and surface roughness of workpiece were measured. Result shows three types of wear behaviour appear which are flank wear, notch wear and chipping. Flank wear and notch wear increased with the cutting speed but decrease by increasing the feed rate before increased after passing the 0.2mm/rev feed rate. While chipping very much related to the feed rate as the chipping area increased when the feed rate increased. Meanwhile, surface roughness increase with increment of cutting speed and feed rate which match the wear pattern.

Introduction

Zirconia toughened alumina (ZTA) has been a popular choice in challenging application due to their excellent mechanical strength and toughness thus making it particularly suited to physically demanding machining condition. To improve the ability of ZTA as a ceramic cutting tool the sintering additives usually utilized. Among the list of additives, magnesium oxide (MgO) shows a promising result on the improvement of hardness [1–3], wear resistance [1,3], density [2–4] and microstructure [1,3] of the cutting insert. Although the element of ZTA-MgO has been comprehensively studied and proved the potential of the composition, previous researches are more focused on the mechanical properties and oversight the detail study on the wear behaviour of this type of ceramic cutting insert [1,3,5,6]. This is proved since study on the wear behaviour of ZTA-MgO ceramic composite system has not been reported elsewhere yet. It is important to understand the wear mechanism and behaviour as it is an essential factor for proper utilization of tool material [7]. The wear mechanisms usually observed in ceramic cutting tools are abrasive, adhesive, tribochemical wear, wear by plastic deformation and fracture [8]. These mechanisms leads to several formation of tool wear such as flank wear, notch wear, crater wear, chipping and etc. [7].

In this study, the wear performances and behaviour of ZTA-MgO ceramic cutting insert were investigated and the influence of these wears to surface roughness of work piece is studied at various parameter. It is important to use variation of parameter i.e. cutting speed and feed rate to see the behaviour of wear while the value of the parameter being increased. Types of wear that appeared on the insert has been observed and measured respectively by using SEM and optical stereotypes microscope. Apart from that, average surface roughness of the machined surface were measured and reported.

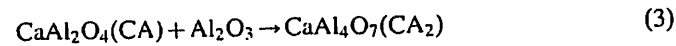
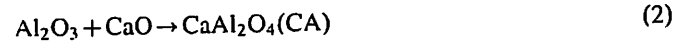
hexaaluminates ($\text{LaAl}_{11}\text{O}_{18}$, $\text{LaMgAl}_{11}\text{O}_{19}$, $\text{SrAl}_{12}\text{O}_{19}$ and $\text{Mg}_2\text{NaAl}_{15}\text{O}_{25}$) and established the positive influences on Al_2O_3 -based ceramics.

One of the hexaaluminates which is considered a “new” material for the Al_2O_3 toughening route is calcium hexaaluminate ($\text{CaAl}_{12}\text{O}_{19}$) or CA_6 [24]. In their research, Asmi et al. [20], the precursor powder of $\text{CaAl}_{12}\text{O}_{19}$ was firstly synthesized from a reaction between CaCO_3 and Al_2O_3 powders. Then, the $\text{CaAl}_{12}\text{O}_{19}$ precursor powder was mixed with Al_2O_3 powder to produce $\text{Al}_2\text{O}_3/\text{CaAl}_{12}\text{O}_{19}$ samples. They found that this new composition led to improved toughness but it decreased hardness, reduced density, and increased porosity. In addition, Nagaoka et al. [25] used CaO precursor powder and found that in-situ formation of $\text{CaAl}_{12}\text{O}_{19}$ in Al_2O_3 matrix led to improved toughness and better flexural strength but it decreased hardness, Young's modulus, and density, and increased porosity. Many researchers have produced elongated $\text{CaAl}_{12}\text{O}_{19}$ using the in-situ method [20,25,26] or through the direct addition of $\text{CaAl}_{12}\text{O}_{19}$ into Al_2O_3 matrix to improve toughness [3,23]. Elongated $\text{CaAl}_{12}\text{O}_{19}$ also has advantages of reducing processing time and cost [22]. The formation of $\text{CaAl}_{12}\text{O}_{19}$ in the Al_2O_3 - CaO system during the sintering process are shown by Eqs. (1)–(9) [10,20].

First CaCO_3 decomposes into CaO and CO_2 at 763 °C, as shown in the following equation:

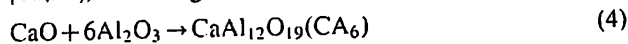


Further heating between 1100 and 1400 °C produces various intermediate phases [16,20,27], as shown in the following equations:

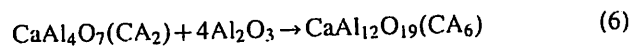
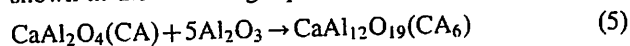


The ultimate in-situ reaction in the Al_2O_3 - CaO system is $\text{CaAl}_{12}\text{O}_{19}$ which can be formed by various possible ways as shown in Eqs. (4)–(9):

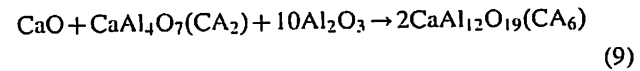
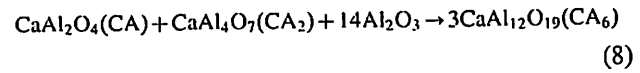
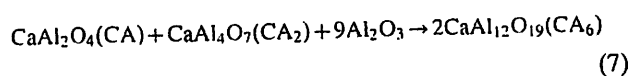
- i. Direct formation of $\text{CaAl}_{12}\text{O}_{19}$ starts around 1350 °C [18,28], according to the following equation [10]:



- ii. the earlier two phases, (CA) and (CA₂) fully transform to $\text{CaAl}_{12}\text{O}_{19}$ (CA₆) at 1600 °C through further reactions, as shown in the following equations [10,20,26,29]:



- iii. The reaction between CaO , CA, CA₂ and Al_2O_3 , according to the following equations [10]:



The performance of pure Al_2O_3 can be further enhanced by incorporating ZrO_2 to form zirconia-toughened-alumina (ZTA) as it has higher fracture toughness [2,4–6,30–35]. Similarly, ZTA properties can be further improved by in-situ formation of a second phase such as hexaaluminates. For example, Guio et al. [12] introduced La_2O_3 into ZTA to produce $\text{LaAl}_{11}\text{O}_{18}$ which increased the toughness to more than 27% at optimum sintering temperature. It also improved bending strength but reduced hardness and Young's modulus. Oungkulsolmongkol et al. [1] introduced SrCO_3 into ZTA to produce $\text{SrAl}_{12}\text{O}_{19}$ which improved toughness but reduced hardness. To date, no studies have been conducted on the effects of in-situ formation of $\text{CaAl}_{12}\text{O}_{19}$ on the microstructure and mechanical properties of ZTA. This is attributed to the very porous microstructure due to the decomposition of CaCO_3 and volume expansion accompanied by in-situ formation of $\text{CaAl}_{12}\text{O}_{19}$ [23]. According to An et al. [36] the $\text{CaAl}_{12}\text{O}_{19}$ produced using CaCO_3 as the starting powder had elongated grains, while that produced using CaO as the starting powder had equiaxed grains. Therefore, the aim of this study is to investigate the effect of in-situ formation of $\text{CaAl}_{12}\text{O}_{19}$ elongated grains on the microstructure and mechanical properties of ZTA.

2. Experimental procedure

The starting raw materials used were Al_2O_3 (Martinswerk, 99% purity), YSZ (Goodfellow, 5.4 mol% Y_2O_3 as stabilizer, $\geq 96\%$ purity), and CaCO_3 (Fluka, $\geq 99\%$ purity). The initial mixture was composed of 80 wt% Al_2O_3 and 20 wt% YSZ. It was then mixed with different amounts of CaCO_3 under the condition that the ratio of Al_2O_3 to YSZ was fixed at 4:1. The details are shown in Table 1. The mixtures were wet-mixed using ABB-Mixer with ZrO_2 balls. The slurries were dried for 24 h at 100 °C in an oven (Mettler-CU 9760) and the dried cakes were crushed and sieved to pass 40 μm . Then, the powders were hydraulically pressed to form pellets 13 mm in diameter and 4 mm thickness at 330 MPa for 120 s. The pellets were sintered in two stages under normal atmosphere (Udian furnace model KHT-16000X). During stage 1, the pellets were sintered from room temperature to 800 °C at 5 °C/min heating

Table 1
Sample codes based on CaCO_3 contents.

Sample code	Al_2O_3 content (wt%)	YSZ content (wt%)	CaCO_3 content (wt%)
ZTA-0.0	80	20	0
ZTA-0.5	79.60	19.90	0.5
ZTA-2.0	78.43	19.60	1.97
ZTA-5.0	76.19	19.04	4.77
ZTA-13.0	69.56	17.39	13.05

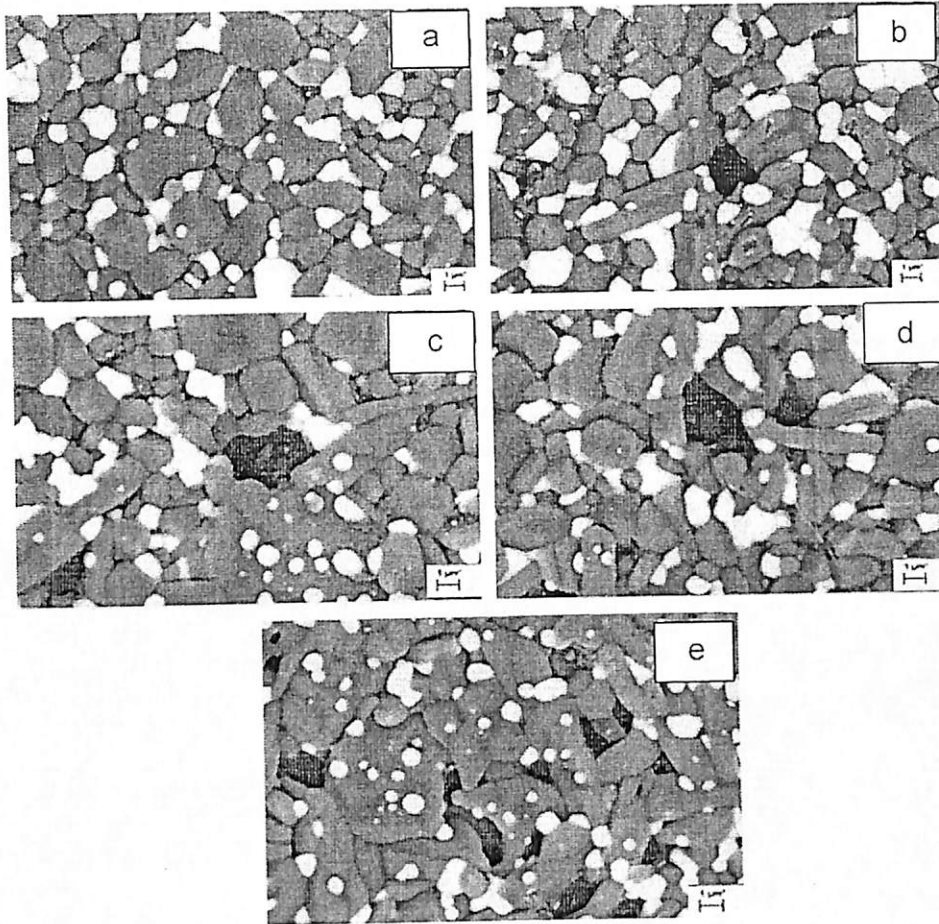


Fig. 2. FESEM micrographs of surfaces of (a) ZTA-0.0, (b) ZTA-0.5, (c) ZTA-2.0, (d) ZTA-5.0 and (e) ZTA-13.0.

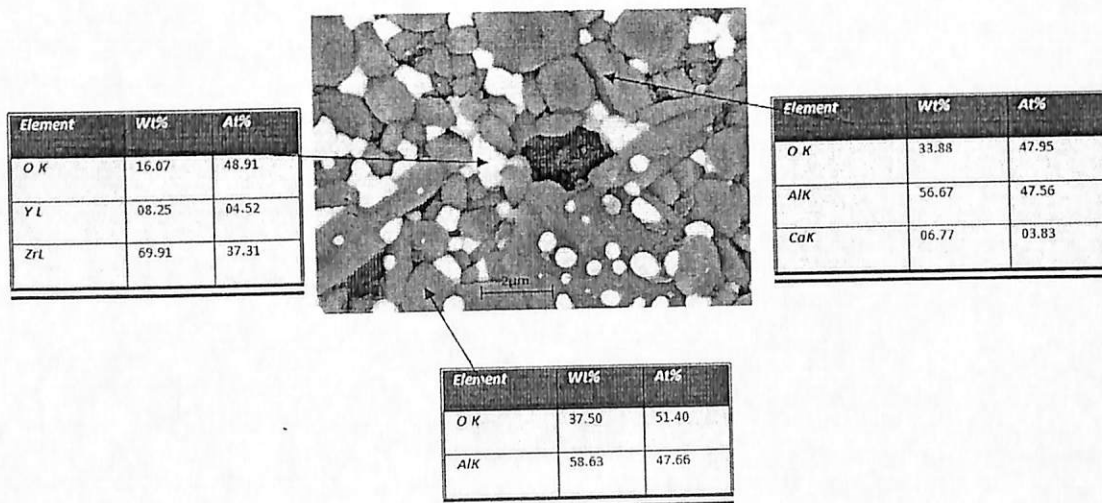


Fig. 3. EDX analysis for ZTA-2.0 (a) ZrO_2 , (b) Al_2O_3 and (c) $CaAl_2O_9$.

$CaCO_3$ decomposition, as indicated by Eq. (1). Furthermore, Dominguez et al. [26] have proven that the elongated grains are found only in porous samples as they are a result of

agglomeration during processing. For this reason, the properties of ZTA are heavily dependent on the amount of in-situ $CaAl_2O_9$ formation. The porosity increased from 0.77% to

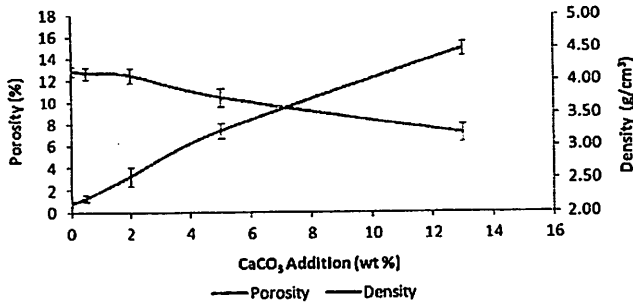


Fig. 4. Bulk density and percentage of porosity for ZTA samples as a function of CaCO₃ wt%.

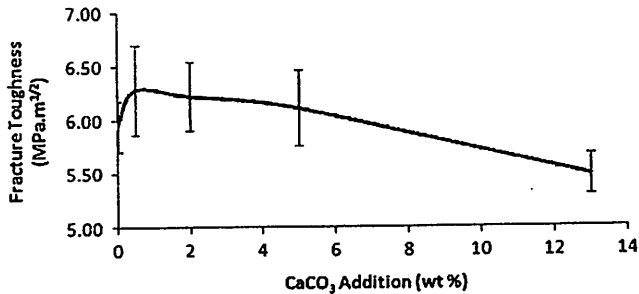


Fig. 5. Fracture toughness of ZTA–CaCO₃ samples as a function of CaCO₃ wt%.

14.91% (Fig. 4). The bulk density also decreased from 4.14 g/cm³ to 3.20 g/cm³ (Fig. 4).

Fig. 4 shows the bulk density and porosity percentage as a function of CaCO₃ wt% addition. The density decreased and porosity increased with CaCO₃ addition. The decrease in bulk density is attributed to the in-situ formation of CaAl₁₂O₁₉ during sintering for three reasons. The first reason is the low relative density of CaAl₁₂O₁₉ compared to Al₂O₃ i.e. 3.79 g/cm³ [26]. The second reason is that during the formation of CaAl₁₂O₁₉ grains, the grains were interlocked due to their elongated shape which caused pores to be trapped between them. The same observation was also reported by Vishista et al. [10] and Nagaoka et al. [25]. With higher CaCO₃ concentrations, more CaAl₁₂O₁₉ grains were produced, thereby leading to higher porosity (Fig. 2). Higher CaCO₃ percentages lead to higher emission of CO₂, consequently triggering the production of more pores in the structure. The third reason is the formation of different Ca–Al₂O₃ compounds during sintering that are usually accompanied by volume expansion which retards the densification process, as stated by Asmi et al. [20] and Herencia et al. [23].

Fig. 5 shows the effect of CaCO₃ addition on fracture toughness. The value was higher with the addition of a small amount of CaCO₃. The maximum fracture toughness was 6.3 MPa m^{1/2}, taken from ZTA-0.5. At first, the fracture toughness increased with CaCO₃ addition but gradually decreased as the added amount increased. A similar trend was also obtained by other researchers [1,11,12,20,25,38,39]. The FESEM images show the mixture of intergranular and

transgranular fracture modes of toughness. These images indicate that the transgranular fracture is more frequent with samples containing CaAl₁₂O₁₉. Fig. 6 clearly shows both fracture modes in ZTA samples. A transgranular fracture mode has higher fracture toughness compared to an intergranular fracture mode due to higher energy consumption by the former.

The increase of toughness with the increase of CaCO₃ wt% can be attributed to the crack deflection mechanism due to the presence of CaAl₁₂O₁₉. The higher the percentage of CaAl₁₂O₁₉, the more crack deflection mechanism was observed. This trend was also found by other researchers [1,6,12,14,24]. According to this mechanism, anisotropy grains of CaAl₁₂O₁₉ causes the crack propagation direction to be deflected along grain boundaries. However, at higher amounts of CaCO₃ wt%, the toughness gradually decreased from 6.3 MPa m^{1/2} for ZTA-2.0 to 5.5 MPa m^{1/2} for ZTA-13.0. This phenomenon is due to the formation of more pores as a result of decomposition of CaCO₃ to CaO and CO₂. Therefore, with in-situ formation of elongated CaAl₁₂O₁₉, a lower amount of K_{IC} was obtained as compared to that reported for SiC-whisker [11,19,40]. Besides that, volume expansion simultaneously occurred during the formation of CaAl₁₂O₁₉ [1,23]. Therefore, to obtain the optimum fracture toughness, a balance between the amount of CaAl₁₂O₁₉ platelets, number of pores, and control of volume expansion must be achieved.

As shown in Fig. 7, the Vickers hardness decreased from 1603.4 HV to 654 HV with the increase in CaCO₃ addition in ZTA. This trend is very much related to the formation of CaAl₁₂O₁₉ (Fig. 2). There are two reasons for how CaAl₁₂O₁₉ presence can reduce the Vickers hardness of the samples. First, its hardness is lower than Al₂O₃ [20] and second, the increase of porosity following the in-situ CaAl₁₂O₁₉ formation. This reduces the resistance of these samples against applied loads. Similar trends have been investigated by various researchers. For instance, Oungkulsolmongkol et al. [1] reported a tremendous decrease in hardness with increased SrAl₁₂O₁₉ formation, while Chen et al. [11] found a decrease in hardness with the formation of LaAl₁₁O₁₈. Asmi et al. [20] found a major reduction in Vickers hardness of Al₂O₃ composites with increased formation of CaAl₁₂O₁₉.

4. Conclusion

The properties of ZTA are greatly influenced by the formation of elongated hibonite (CaAl₁₂O₁₉) grains. The more CaCO₃ added into ZTA, the more CaAl₁₂O₁₉ grains were formed in the microstructure. At the same time, more pores were found due to volume expansion, accompanied by the decomposition of CaCO₃ and the formation of CaAl₁₂O₁₉ that resulted in the decrease in bulk density. Similarly, the fracture toughness and hardness were also affected with the presence of pores and CaAl₁₂O₁₉. The fracture toughness increased due to a fracture deflection mechanism for a short range. Beyond this range, more addition of CaCO₃ led to an increase in porosity following in-situ formation of CaAl₁₂O₁₉, hence leading to the reduction in fracture toughness. The Vickers hardness decreased with in-situ formation of CaAl₁₂O₁₉, not only

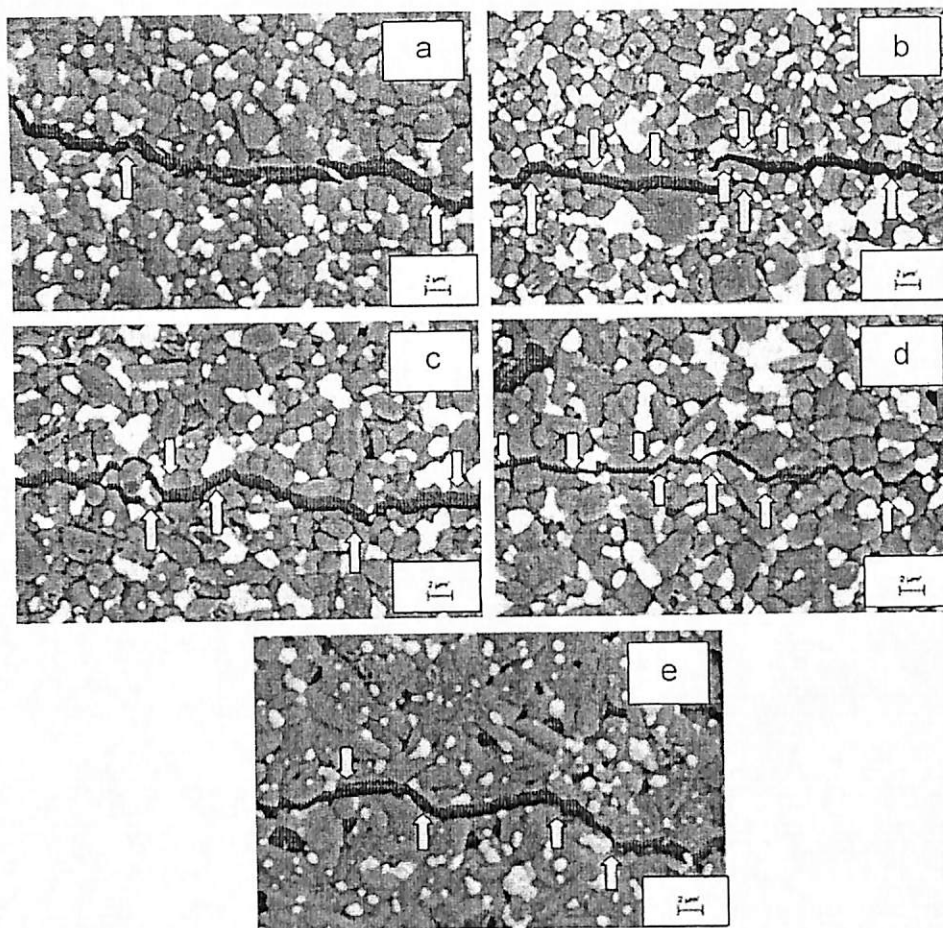


Fig. 6. Micrograph of crack propagation after indentation for (a) ZTA-0.0, (b) ZTA-0.5, (c) ZTA-2.0, (d) ZTA-5.0 and (e) ZTA-13.0 represents crack deflection and represents transgranular fracture mode.

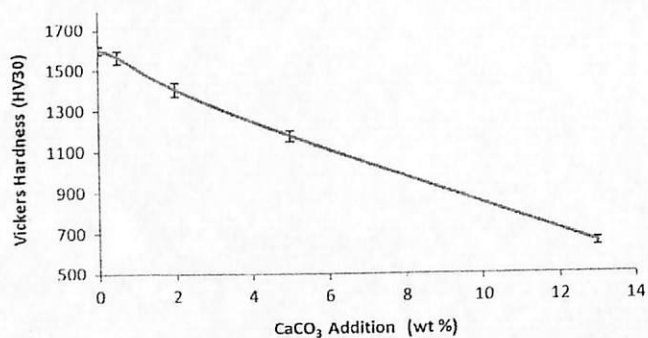


Fig. 7. Vickers hardness of ZTA–CaCO₃ samples as a function of CaCO₃ wt%.

due to the increase in porosity but also due to lower hardness value of CaAl₁₂O₁₉ compared to Al₂O₃.

Acknowledgment

Universiti Sains Malaysia (USM) funded this work under the Grant 1001/PBAHAN/811212. The authors are grateful to all colleagues at the School of Materials and Mineral Resource

Engineering (USM) Laboratory and to the technicians for their technical support.

References

- [1] T. Oungkulsomkol, P. Salec-art, Hardness and fracture toughness of alumina-based particulate composites with zirconia and strontia additives, *J. Met., Mater. Miner.* 20 (2) (2010) 71–78.
- [2] M. Hu, M. Fang, S. Cheng, T. Yang, Z. Huang, Y. Liu, Effects of Calcium hexaluminate addition on the mechanical properties of zirconia-toughened-alumina, *Key Eng. Mater.* 544 (2013) 286–290.
- [3] D. Asmi, I.M. Low, Self-reinforced Ca-hexaluminate/alumina composites with graded microstructures, *Ceram. Int.* 34 (2008) 311–316.
- [4] F. Sommer, R. Landfried, F. Kern, R. Gadow, Mechanical properties of zirconia toughened alumina with 10–24 vol%. 1Y-TZP reinforcement, *J. Eur. Ceram. Soc.* 32 (2012) 4177–4184.
- [5] A.Z.A. Azhar, L.C. Choong, H. Mohamed, M.M. Ratnam, Z.A. Ahmad, Effects of Cr₂O₃ addition on the mechanical properties, microstructure and wear performance of zirconia-toughened-alumina (ZTA) cutting inserts, *J. Alloys Compd.* 513 (2012) 91–96.
- [6] B. Mondal, A.B. Chattopadhyay, A. Virkar, A. Paul, Development and performance alumina ceramic tools of zirconia-toughened, *Wear* 156 (1992) 365–383.
- [7] Y.A.O. Yijun, L.I. Chuncheng, W. Ling, J. Xiaolong, Q.I.U. Tai, Mechanical behaviors of alumina ceramics doped with rare-earth oxides, *Rare Met.* 29 (2010) 456–459.

- [8] M. Dehestani, E. Adelfsson, Phase stability and mechanical properties of zirconia and zirconia composites, *Int. J. Appl. Ceram. Technol.* 141 (2013) 129–141.
- [9] O.L. Ighodaro, O.I. Okoli, Fracture toughness enhancement for alumina systems: a review, *Int. J. Appl. Ceram. Technol.* 5 (2008) 313–323.
- [10] K. Vishista, Sol-gel synthesis and characterization of alumina-calcium hexaaluminate composites, *J. Am. Ceram. Soc.* 88 (5) (2005) 1175–1179.
- [11] P.-L. Chen, L.-W. Chen, In-situ alumina/aluminate platelet composites, *J. Am. Ceram. Soc.* 75 (1992) 2610–2612.
- [12] R. Guo, D. Guo, Y. Chen, Z. Yang, Q. Yuan, In situ formation of $\text{LaAl}_{11}\text{O}_{19}$ rodlike particles in ZTA ceramics and effect on the mechanical properties, *Ceram. Int.* 28 (2002) 699–704.
- [13] K. Vishista, F.D. Gnanam, Microstructural development of SrAl_2O_7 in alumina-strontia composites, *J. Eur. Ceram. Soc.* 29 (2009) 77–83.
- [14] Y. Wu, Y. Zhang, X. Huang, J. Guo, In-situ growth of needlelike LaAl_3O_8 for reinforcement of alumina composites, *Ceram. Int.* 27 (2001) 903–906.
- [15] Y. Wu, Y. Zhang, X. Huang, J. Guo, Microstructural development and mechanical properties of self-reinforced alumina with CAS addition, *J. Eur. Ceram. Soc.* 21 (2001) 581–587.
- [16] L. An, H.M. Chan, R-Curve behavior of in-situ-toughened $\text{Al}_2\text{O}_3/\text{CaAl}_2\text{O}_7$ ceramic composites, *J. Am. Ceram. Soc.* 79 (12) (1996) 3142–3148.
- [17] H. Gong, Y. Yin, R. Fan, J. Zhang, Mechanical properties of in-situ toughened $\text{Al}_2\text{O}_3/\text{Fe}_3\text{Al}$, *Mater. Res. Bull.* 38 (2003) 1509–1517.
- [18] L. Xu, Z. Xie, L. Gao, X. Wang, F. Lian, T. Liu, et al., Synthesis, evaluation and characterization of alumina ceramics with elongated grains, *Ceram. Int.* 31 (2005) 953–958.
- [19] Xie Zhipeng, Gao Lichun, Xu Lihua, W. Xidong, U.L.I.W.Y. High toughness alumina ceramics with elongated grains, *Sci. China (Series E)* 46 (5) (2003) 527–536.
- [20] D. Asmi, I.M. Low, Physical and mechanical characteristics of in-situ alumina/calcium hexaluminate composites, *J. Mater. Sci. Lett.* 17 (1998) 1735–1738.
- [21] K. Vishista, F.D. Gnanam, Effect of strontia on the densification and mechanical properties of sol-gel alumina, *Ceram. Int.* 32 (2006) 917–922.
- [22] O. Sbaizero, S. Maschio, G. Pezzotti, I.J. Davie, Microprobe fluorescence spectroscopy evaluation of stress fields developed along a propagating crack in an $\text{Al}_2\text{O}_3/\text{CaO} \cdot 6\text{Al}_2\text{O}_3$ ceramic composite, *J. Mater. Res.* 16 (10) (2001) 2798–2804.
- [23] A.J. Sanchez, R. Moreno, C. Baudóñan, Fracture behaviour of alumina-calcium hexaluminate composites obtained by colloidal processing, *J. Eur. Ceram. Soc.* 20 (2000) 2575–2583.
- [24] C. Domínguez, Á. Chevalier, R. Torrecillas, L. Grenillard, G. Fantozzi, Thermomechanical properties and fracture mechanisms of calcium hexaluminate, *J. Eur. Ceram. Soc.* 21 (2001) 907–917.
- [25] T. Nagaoka, M. Yasuoka, K. Hirao, S. Kanzaki, Effects of CaO addition on sintering and mechanical properties of Al_2O_3 , *J. Mater. Sci. Lett.* 15 (1996) 1815–1817.
- [26] Á. Chevalier, R. Torrecillas, G. Fantozzi, C. Domínguez, Microstructure development in calcium hexaluminate, *J. Eur. Ceram. Soc.* 21 (2001) 381–387.
- [27] Y. Tian, Y. Qiu, Y. Chai, P. Bai, C. Gong, The effect of sintering temperature on the structure and properties of calcium hexaluminate/anorthite ceramics, *Sci. Sintering* 45 (2013) 141–147.
- [28] M.H.F. Xue, Y. Liu, Y.G. Liu, D.X. Yang, D.Y. Ye, Z.H. Huang, Fabrication and properties of $\text{CaAl}_2\text{O}_7\text{-Al}_2\text{O}_3$ composite ceramics, *Key Eng. Mater.* 512–515 (2012) 539–542.
- [29] P.G. De La Iglesia, O. García-Morceno, R. Torrecillas, J.I. Menéndez, Influence of different parameters on calcium hexaluminate reaction sintering by Spark plasma, *Ceram. Int.* 38 (2012) 5325–5332.
- [30] G. Magnani, A. Brillante, Effect of the composition and sintering process on mechanical properties and residual stresses in zirconia-alumina composites, *J. Eur. Ceram. Soc.* 25 (2005) 3383–3392.
- [31] K. Maui, A. Sil, Microstructural relationship with fracture toughness of undoped and rare earths (Y, La) doped $\text{Al}_2\text{O}_3\text{-ZrO}_2$ ceramic composites, *Ceram. Int.* 37 (2011) 2411–2421.
- [32] J.F. Ma, S.Q. Wang, R.X. Du, X.D. Li, Pressureless sintering of gelcast $\text{ZrO}_2\text{-MgO-TiO}_2$ systems as potential dental ceramics, *Adv. Appl. Ceram.* 110 (5) (2011) 275–279.
- [33] F. Kern, R. Gadow, Alumina toughened zirconia from yttria coated powders, *J. Eur. Ceram. Soc.* 32 (2012) 3911–3918.
- [34] S. Nath, N. Sinha, B. Basu, Microstructure, mechanical and tribological properties of microwave sintered calcia-doped zirconia for biomedical applications, *Ceram. Int.* 34 (2008) 1509–1520.
- [35] F. Cesari, L. Esposito, F. Furgiele, C. Maletta, A. Tucci, Fracture toughness of alumina-zirconia composites, *Ceram. Int.* 32 (2006) 249–255.
- [36] L. An, H.M. Chan, K.K. Soni, Control of calcium hexaluminate grain morphology in in-situ toughened ceramic composites, *J. Mater. Sci.* 31 (1996) 3223–3229.
- [37] K. Niihara, A fracture mechanics analysis of indentation-induced Palmqvist crack in ceramics, *J. Mater. Sci. Lett.* 2 (1983) 221–223.
- [38] X.Q. Liu, X.M. Chen, Effects of $\text{Sr}_2\text{Nb}_2\text{O}_7$ additive on microstructure and mechanical properties of $3\text{Y-TZP}/\text{Al}_2\text{O}_3$ ceramics, *Ceram. Int.* 28 (2002) 209–215.
- [39] D. Asmi, I.M. Low, B.H.O. Connor, Physical, thermal, and mechanical properties of $\text{Al}_2\text{O}_3/\text{CaAl}_2\text{O}_7$ composites processed by in-situ reaction sintering, *Jurnal Sains Teknol.* 12 (2006) 1–8.
- [40] C. K-Sik, C. H-Jin, L. J-Gunn, K. Y-Wook, Effects of additive amount on microstructure and fracture toughness of SiC-TiB_2 composites, *Ceram. Int.* 24 (1998) 299–305.

The increase of $\text{CaAl}_{12}\text{O}_{19}$ could be further confirmed by the backscattered FESEM micrographs of the samples as shown in Fig. 2. The white grains are ZrO_2 , while the grey grains are Al_2O_3 and $\text{CaAl}_{12}\text{O}_{19}$. However, the $\text{CaAl}_{12}\text{O}_{19}$ grains are somehow brighter because of higher atomic weight of Ca compared to Al. Although the colour difference is insufficient enough to distinguish between them, but the elongated shape of $\text{CaAl}_{12}\text{O}_{19}$ grains compared to Al_2O_3 grains can be a good indication to recognise $\text{CaAl}_{12}\text{O}_{19}$ grains. The sizes of $\text{CaAl}_{12}\text{O}_{19}$ grains decreased with more addition of CaO, however, they can still be distinguishable from Al_2O_3 grains. As shown in Fig. 2(a) (0.0 wt% CaO), the shape of $\text{CaAl}_{12}\text{O}_{19}$ grain is more elongated compare to Fig. 2(e) (0.5 wt% CaO). Therefore, it is proven that addition of CaCO_3 created better $\text{CaAl}_{12}\text{O}_{19}$ elongated grains compared to CaO. This phenomenon has been

explained by Chen et al. [33] in the report of their investigation on the difference mechanisms of reactivity between CaO and CaCO_3 . Another observation from the FESEM micrographs (Fig. 2) is the relationship between larger amount of equiaxed $\text{CaAl}_{12}\text{O}_{19}$ grains formation with reduction of porosity when CaO replacing CaCO_3 as the additive in ZTA samples. Samples which have lower porosity created more equiaxed $\text{CaAl}_{12}\text{O}_{19}$ grains because their rapid growth that bounded by other grains before being able to develop high aspect ratios as explained by Dominguez et al [35]. These results are confirmed by Table 3 which shows a continuous decrease of aspect ratio for $\text{CaAl}_{12}\text{O}_{19}$ grains from 6.12 (ZTA-0.0C) to 4.17 (ZTA-0.5C). However, the $\text{CaAl}_{12}\text{O}_{19}$ grains remained as more elongated compared to Al_2O_3 grains.

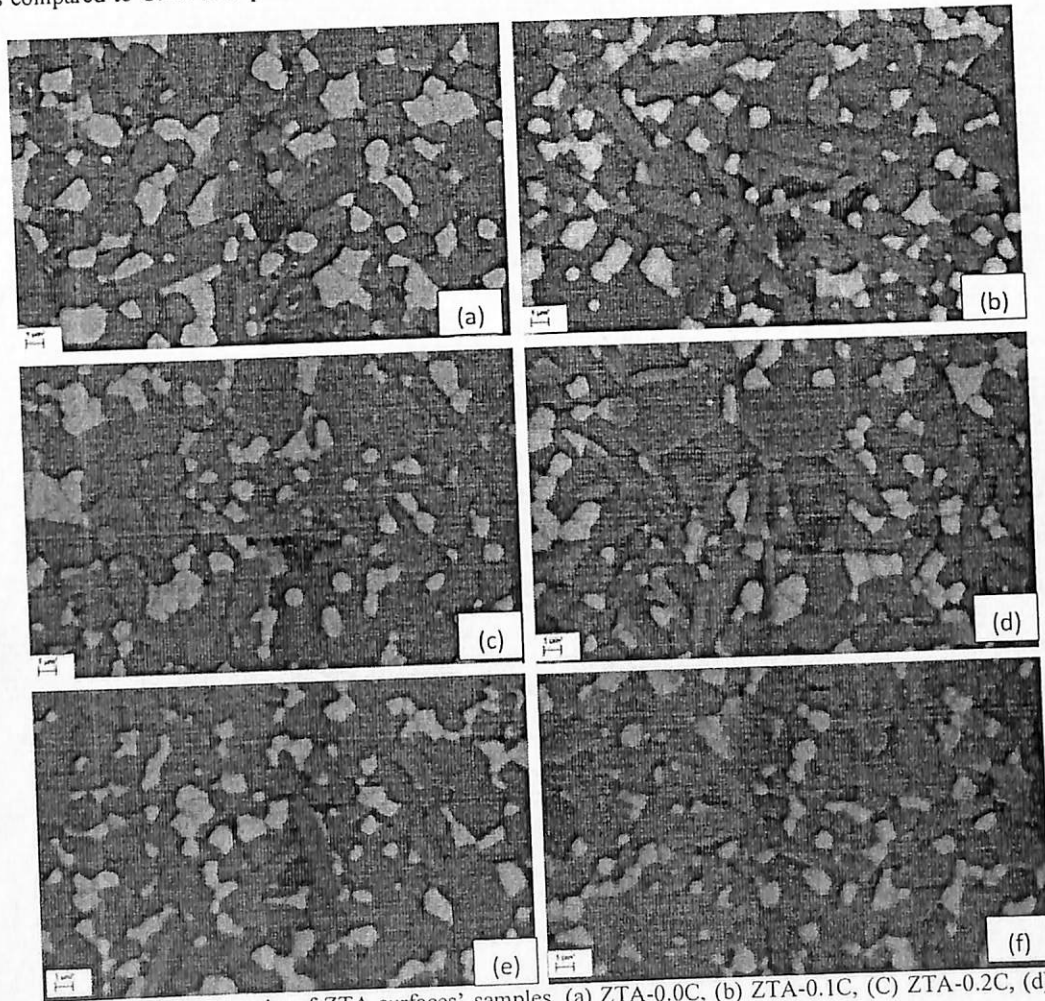


Figure 2. FESEM micrographs of ZTA surfaces' samples. (a) ZTA-0.0C, (b) ZTA-0.1C, (c) ZTA-0.2C, (d) ZTA-0.3C, (e) ZTA-0.4C and (f) ZTA-0.5C

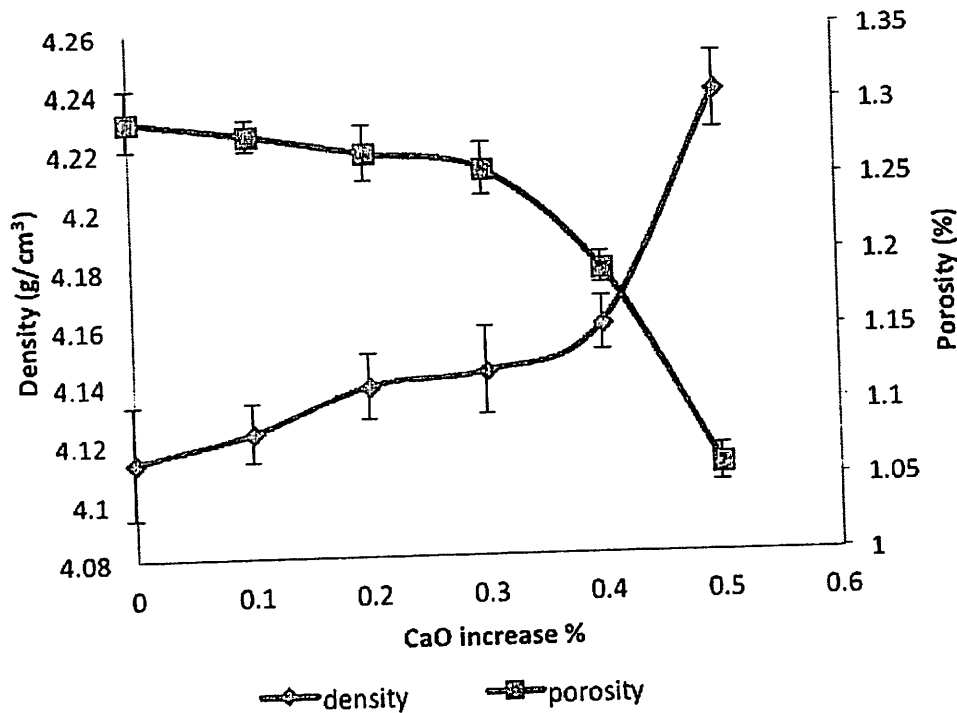


Figure 4. Bulk density and porosity percentage of the ZTA samples as a function of CaO and CaCO₃ addition.

Fig. 5 shows the beneficial impact of the combination addition between CaO and CaCO₃ to improve the Vickers hardness (HV) and at the same time maintaining the fracture toughness of ZTA samples. It is seen that by systematically replacing CaCO₃ with CaO additions, the HV increases. The hardness of the samples is dependent on their ability to resist against indentation loads which is also influenced by the number of pores, pore sizes in the sample's microstructure, shape of CaAl₁₂O₁₉ grains and samples' density. Therefore, the increase of this HV is parallel with the reducing porosity of the samples as shown in FESEM micrographs (Fig. 2), decreasing aspect ratio of CaAl₁₂O₁₉ grains (Table 3) and increasing of bulk density (Fig.4). This similar observation was observed by Oungkulsolmongkol et al. (2010) when they studied ZTA added with SrCO₃ and SrO, study done by Chen et al. (1992) when they studied the effect of different hexaaluminates (LaAl₁₁O₁₈, LaMgAl₁₁O₁₉, SrAl₁₂O₁₉ and Mg₂NaAl₁₁O₁₉) on the hardness of Al₂O₃ and the research done by Asmi et al. (1998) when they studied Al₂O₃ added with CaCO₃.

Fig. 5 also indicates that the HV curve can be divided into two different regions. The first region (ZTA-0.0C to ZTA-0.3C) shows a steady increase of HV which is attributed to the balancing effects from four different

factors i.e. increase of CaAl₁₂O₁₉ amount (Table 2), decreasing of porosity, increase of bulk density (Fig. 4) and aspect ratio reduction of CaAl₁₂O₁₉ (Table 3). The amount of CaAl₁₂O₁₉ has increased from 4 wt% to 5.9 wt% and this has reduced the hardness of the composite since CaAl₁₂O₁₉ has lower hardness (Mohs hardness 7.5-8) [41] compared to Al₂O₃ (Mohs hardness 9) [24,37]. On the other hand, the porosity decreased from 1.29% to 1.25%, bulk density increased from 4.11 (gm/cm³) to 4.14 (gm/cm³) and the aspect ratio of CaAl₁₂O₁₉ decreased from 6.12 to 5.27 to form a more rounded equiaxed shape. The formation of more equiaxed grains in ZTA microstructure accompanying the decreasing porosity and increasing densities of these samples which can also enhance the HV [11]. Therefore, the HV improvement is resulted from lower porosity which can compensate the negative impact of more CaAl₁₂O₁₉ formation. Consequently, the HV curve is clearly reflected by balancing effects of these opposite parameters which shows a slight increase from 1568HV to 1578HV. The second region (ZTA-0.4C and ZTA-0.5C) shows that HV is rapidly increased due to the impact of small increased of CaAl₁₂O₁₉ phase (Table 2), much lower porous and denser samples (Fig. 4) and further reduction of CaAl₁₂O₁₉ grains' aspect ratio (Table 3). The quantity of CaAl₁₂O₁₉ increased only from 19wt% to 19.7wt%

and this can only contribute a minor effect to the ZTA hardness. On the hand, the biggest contributors to the increase of hardness come from decreasing porosity (from 1.25% to 1.05% as shown in Fig. 4), much denser samples (4.14 gm/cm^3 to 4.23 gm/cm^3) and also reducing of the aspect ratio of CaAl_2O_9 grains (from 5.27 to 4.17). From the above observation, it is obvious that the hardness of ZTA samples is under the influence of the four main contributing factors i.e. the amount of CaAl_2O_9 , shape of CaAl_2O_9 grains, bulk density and porosity. The lower HV value should be observed with more CaAl_2O_9 formation through larger amount of CaO addition. However, formation of more equiaxed CaAl_2O_9 grains is parallel with the porosity reduction and densification of these samples which contributed to better hardness. Therefore, ZTA-0.5C has the highest hardness of 1627HV even though has the highest amount of CaAl_2O_9 , since it has the lowest porosity (1.05%), highest density (4.23 gm/cm^3) and the most equiaxed CaAl_2O_9 grains with the lowest aspect ratio (4.17).

The fracture toughness of the samples is almost stable as shown in Fig. 5 and is governed by the amount and aspect ratio of CaAl_2O_9 grains. As shown in Table 2, the amount of CaAl_2O_9 has increased from 10 wt% to 19.7 wt%. According to other researchers [23,24,26,27,29,42], the elongated CaAl_2O_9 grains can improve the fracture toughness either by crack deflection or crack bridging mechanism or combination of both. However, FESEM micrographs

(Fig. 2) shows the CaAl_2O_9 grains tend to be more equiaxed as indicated in Table 3 (from 6.12 to 4.17 following the increasing amount of CaO addition). This reduction of aspect ratio is reflected by the presence of more rounded-like or shorter elongated CaAl_2O_9 grains which have minor contribution to toughness improvement either by deflecting the cracks or avoiding their path by bridging effect as shown in Fig. 6. In this figure it is clearly seen the presence of both crack deflection and crack bridging mechanisms in ZTA samples. The path of cracks is more tortuous in the ZTA samples which contain larger amount of CaAl_2O_9 grains. The reason is related to the fact that although CaAl_2O_9 grains tend to be more equiaxed with more CaO addition, yet their aspect ratio is always bigger than Al_2O_3 grains as shown in FESEM micrographs (Fig. 2 and Table 3). Therefore, when there are large numbers of CaAl_2O_9 grains, more tortuous paths of cracks are observed. However, when the ZTA is without CaCO_3 addition (ZTA-0.5C), the CaAl_2O_9 grains are approaching rounded shape with the lowest aspect ratio (4.17), consequently fewer cracks are deflected by these equiaxed CaAl_2O_9 grains (Fig. 6). Therefore, the sample (ZTA-0.4C) that contains both CaCO_3 and CaO has the highest fracture toughness ($6.51 \text{ MPa.m}^{1/2}$). From the above observations it is clear that in order to optimize the hardness and fracture toughness of ZTA, the right combination between CaO and CaCO_3 as the additive can serve as a suitable approach.

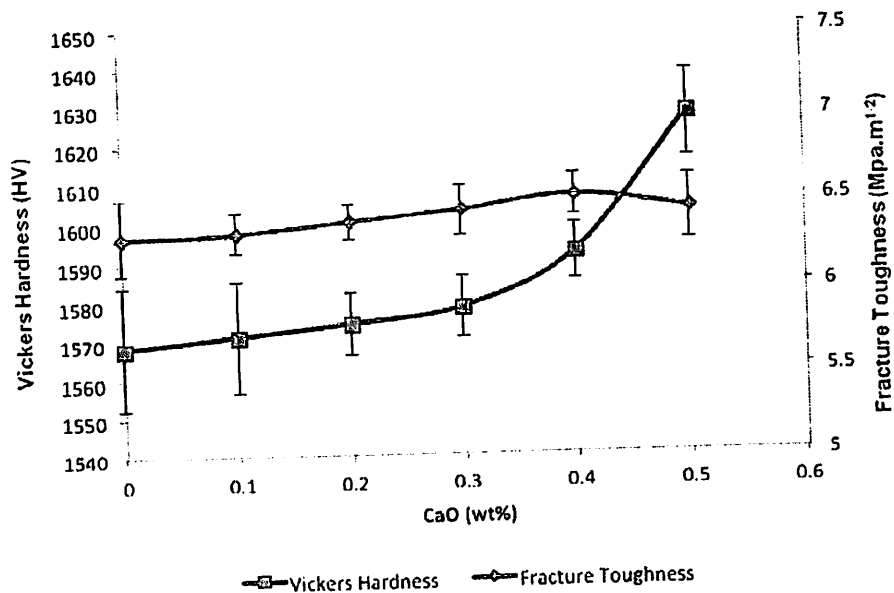


Fig. 5: The Vickers hardness and fracture toughness of the ZTA samples as a function of CaO and CaCO_3 addition.

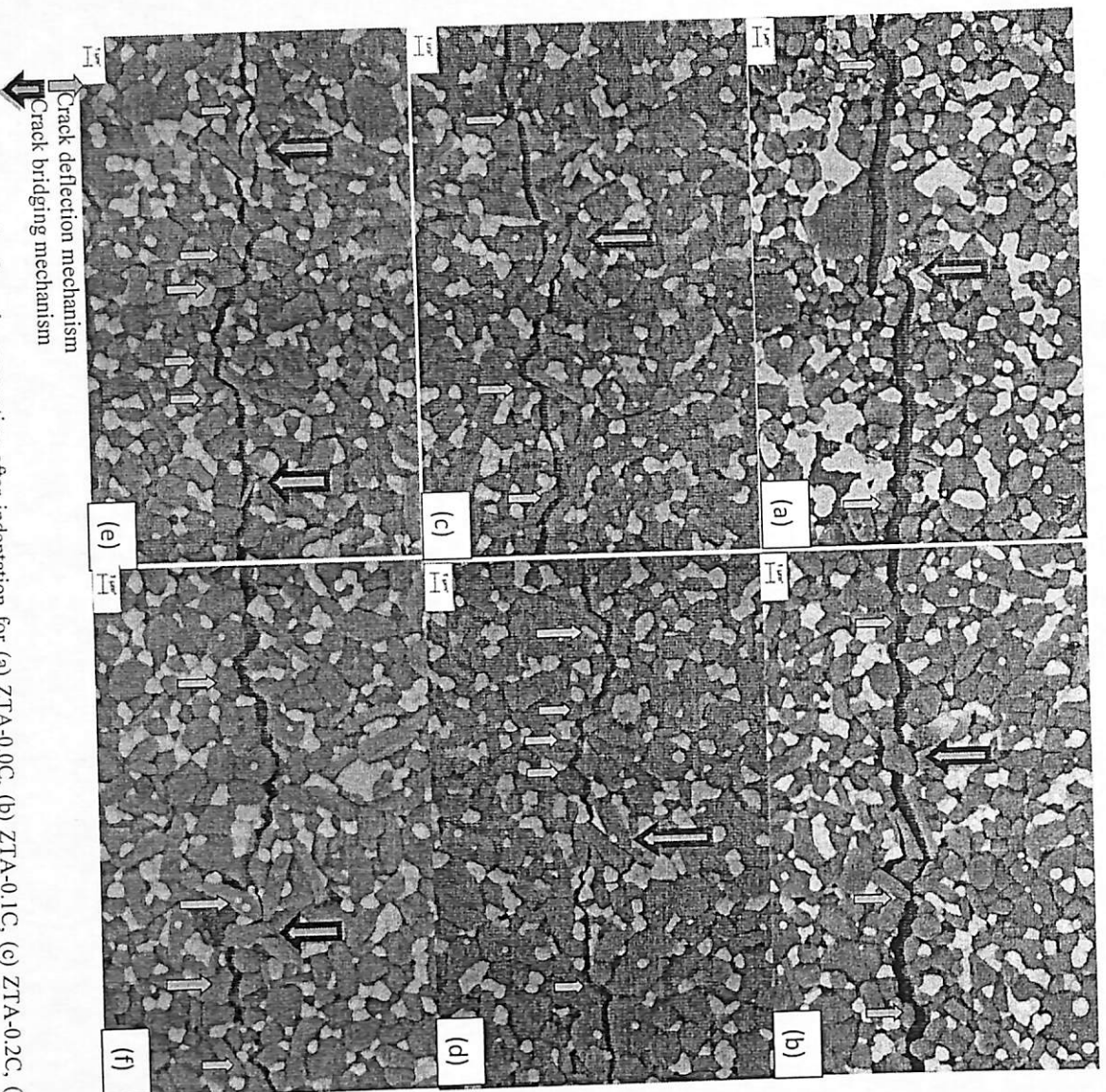


Figure 6. Micrograph of crack propagation after indentation for (a) ZTA-0.0C, (b) ZTA-0.1C, (c) ZTA-0.2C, (d) ZTA-0.3C, (e) ZTA-0.4C and (f) ZTA-0.5C

4. CONCLUSIONS

The combined effects of CaO and CaCO₃ additions on the ZTA mechanical properties and microstructure have been optimised. Addition of CaCO₃ alone into ZTA samples produced elongated CaAl₁₂O₁₉ grains, which improves the fracture toughness. However, hardness is reduced due to the formation of pores accompanying the decomposition of CaCO₃ during sintering process. To overcome this challenge, CaO was added together with CaCO₃ to make denser and lower pores microstructures of ZTA samples. Therefore, the Vickers hardness considerably

increased. Even though, the quantity of CaAl₁₂O₁₉ increased when CaO replaced CaCO₃ addition, but on other hand the produced CaAl₁₂O₁₉ grains has lower aspect ratios and tend to be more equiaxed instead being elongated. Hence, the fracture toughness values of ZTA samples almost remain stable. Crack bridging and crack deflection mechanisms are found in crack paths. Therefore, by carefully choosing combination of CaO and CaCO₃ additions, the best hardness and fracture toughness can be achieved through optimizing the combination of these substances for possible cutting tool insert applications.

Role of $\text{Ce}_2\text{Zr}_3\text{O}_{10}$ phase on the Microstructure and Fracture Toughness of ZTA Composites

Nik Akmar REJAB^{a*}, Zhwan Dilshad Ibrahim SKTANI^b, Afifah MOHD ALI^c,
Zainal Arifin AHMAD^d

Structural Materials Niche Area, School of Materials and Mineral Resources, Engineering Campus,
Universiti Sains Malaysia, 14300 Nibong Tebal, Penang, Malaysia

^{a*}akmarnik@gmail.com, ^bjhwan82@gmail.com, ^csakisakura@gmail.com, ^dsrzainal@usm.my

Keywords: Sintering; Grain size; Toughness and toughening; ZrO_2 ; Y_2O_3

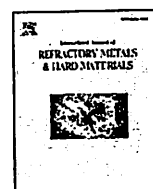
Abstract. Despite the impressive development in understanding transformation toughening, tailoring the toughness of zirconia toughened alumina (ZTA) ceramics remained a major challenge. In our research, a simple route based on the powders mixing process of ZTA powders with varying CeO_2 additions (0 - 10 wt.%) is developed to investigate this issue. The experimental results clearly reveal that the fracture toughness of ZTA ceramics can be tailored by mixing of ZTA starting powders.

Introduction

In the world of ceramic materials, zirconia toughened alumina (ZTA) ceramics are regarded as a strong candidate for structural applications due to their excellent strength and toughness in combination with high wear resistance and chemical inertness [1]. The excellent mechanical properties combined with biocompatibility, wear resistance, high chemical, and corrosion resistance, make this material one of the best candidates for industrial applications [2]. Toughness control and optimization is considered as one of the key criteria in the development of ZTA materials with structural reliability and functional applications. Most of the published literature concerning the transformation toughening is based on the results obtained with yttria stabilized ZrO_2 reinforced in $\alpha\text{-Al}_2\text{O}_3$ starting powders [3]. The achievement of high toughness in ZTA ceramics is only possible by growing the $t\text{-ZrO}_2$ grains via optimization of the sintering parameters or by post-sintering annealing for long times at high temperature [4]. In recent years, more attention is given to the new materials were developed by adding more than one stabilizer to zirconia. The mechanical properties of ZTA ceramics obtained from Y_2O_3 stabilized zirconia starting powders are reported to have low temperature degradation, while retaining a relative high fracture toughness [5]. In this paper, the microstructure and mechanical properties, especially toughness, of ZTA ceramics by means of mixing ZTA powders with 0 to 10 wt.% CeO_2 is described. It is shown how the toughness of ZTA can be considerably improved by tuning the composition of the starting powders.

Materials and Methods

Starting powders of highly pure, thermally reactive type Al_2O_3 (Alcoa, A16SG, 99.0 %), yttrium stabilized zirconia (Goodfellow, 94.6%), 20 nm MgO (Strem Chemicals, 99.9%), and CeO_2 (Sigma Aldrich, 99.0 %) were used. In this work, 80 wt.% of Al_2O_3 and 20 wt.% yttrium stabilized zirconia were taken as the baseline composition. The amount of ceria was added in different wt.% (0 to 10 wt.%) into the initial compositions. The mixtures were prepared by the wet milling method. Subsequently, the mixtures were dried to 100°C and crushed to form powders. Cylindrical shapes with dimensions of 13 mm in diameter and 4 mm in height were formed by pressing the crushed powder at 300 MPa. Afterwards, these cylindrical samples were sintered in atmosphere at 1600°C for 4 hours to yield dense ceramics. The analysis of crystal structure was carried out by X-ray diffraction (XRD) using the Bruker D8 Advance with $\text{CuK}\alpha$ radiation (40 kV, 30 mA) diffracted beam monochromator, using a step scan mode with a step size of 0.1° in the range of 20°–80° of $2\theta^\circ$. Scanning electron microscopy (SEM) was employed to study the microstructure of the polished



Short communication

Effects of yttria stabilized zirconia (3Y-TZP) percentages on the ZTA dynamic mechanical properties

Ali Arab^{a,b}, Zainal Arifin Ahmad^{b,*}, Roslan Ahmad^a^a School of Mechanical Engineering, Universiti Sains Malaysia, Engineering Campus, 14300 Nibong Tebal, Penang, Malaysia^b Structural Materials Niche Area, School of Materials and Mineral Resources Engineering, Universiti Sains Malaysia, Engineering Campus, 14300 Nibong Tebal, Penang, Malaysia

ARTICLE INFO

Article history:

Received 30 October 2014

Received in revised form 22 December 2014

Accepted 9 January 2015

Available online 12 January 2015

Keywords:

ZTA

SHPB

Dynamic mechanical properties

Fracture toughness

Hardness

ABSTRACT

Ceramics materials are extensively used in armor applications. Various parameters were considered for selecting the most suitable ceramic materials such as hardness, fracture toughness, and dynamic properties. However, better understanding of the dynamic properties i.e., hardness and toughness required deep insight so as to predict mechanical behavior of ceramic subjected to dynamic loadings. In this paper, these properties were investigated by using different amounts of 3Y-TZP (10–40 wt.%) in zirconia toughened alumina (ZTA) for the purpose of evaluating the relationship between the strength, hardness and fracture toughness of dynamically loaded ceramics. The highest dynamic strength of 4.9 GPa was obtained with the combination of ZTA with 20 wt.% of 3Y-TZP. In addition, the composition also had better hardness and fracture toughness responses in comparison with others.

© 2015 Elsevier Ltd. All rights reserved.

1. Introduction

After the World War II, ceramics comprehensively used in military applications and ceramic armor were developed for personal and mobile devices such as tank, aircraft and helicopter. Ceramic materials have lower density, higher hardness and a good compressive strength compared to metals. On the other hand, ceramic material is brittle, and this reduces their ability when used as an armor to withstand multiple impacts. This brittleness also facilitates propagation and coalescence of microcracks and may lead to the damage and comminution of ceramic due to impact and penetration.

For the design of advanced ceramic armor, the knowledge on the mechanical properties of ceramics is very essential. Fracture toughness and hardness are two major parameters that armor designer focus on [1,2]. Fracture toughness shows the ability of ceramic to withstand the multiple impacts and crack propagations, while hardness affects erosion and plastic deformation of the impact projectile. However, in armor design the dynamic properties of ceramic are more important. This is due to the difference in the behavior of materials in high strain rate compared to its behavior under a static load. Dynamic properties of materials are tested by many different methods like drop weight testing [3], split Hopkinson pressure bar (SHPB) and flying impact plate. SHPB is a very common test for measuring the dynamic properties of materials and its application on ceramic has been reviewed by Subhash and Ravichandran [4].

Testing a ceramic material by using SHPB is normally accompanied with a typical indentation problem that causes stress concentration due to the metallic nature of the indenter, which is softer than ceramic. For this reason, Nemat-Nasser [5] modified the SHPB for SiC sample testing by using two tungsten carbide platens on two faces of sample to prevent damage of the bars. Wide range of tests in dynamic load have been done on SiC [5–8], B₄C [9–12], alumina [13–15] and AlN [16,17]. During the ballistic impact, the ceramics damage when the localized stress exceeds the ceramic strength. Further, shattering ceramic under the impact load affects the resistance of ceramic under multi impacts. Woodward and Baxter [18] observed that the toughness of ceramic tiles in an armor system could significantly affect the fragmentation process. With higher material toughness, the volume of fragments decreased in all the size range of the fragments. Many approaches have been tried with the aim at improving the toughness of ceramics. One of them is the adding of zirconia into the alumina (ZTA) to give better properties compared to pure alumina. However, few studies are available on the dynamic properties of ZTA [19].

Since there is no sufficient information available on the dynamic properties of ZTA, the precise evaluation of materials to be used as ceramic armor is not yet defined [20]. Therefore, investigation on the dynamic properties of ZTA with various amounts of yttria stabilized zirconia (3Y-TZP) will contribute to the better understanding of the dynamic properties of ZTA. The measurement of stress and strain rate is very essential to ensure the suitability of ZTA for ceramic armor. Therefore, the dynamic property was measured by a modified SHPB apparatus with a view to investigating the relationship between the fracture toughness and hardness to the dynamic compressive strength.

* Corresponding author.

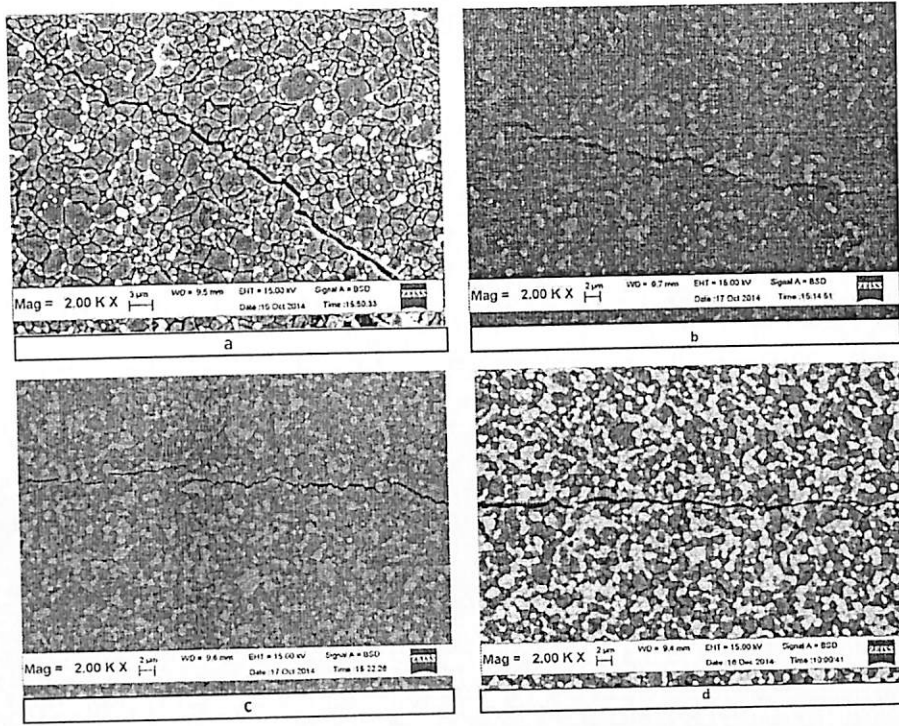


Fig. 6. Crack propagation for a) 10 wt.% 3Y-TZP, b) 20 wt.% 3Y-TZP, c) 30 wt.% 3Y-TZP and d) 40 wt.% 3Y-TZP.

Table 1
Dynamic properties of different compositions of ZTA.

Name of composition	Maximum stress (MPa)	Maximum strain	Damage
ZTA (10 wt.% 3Y-TZP)	2688	0.3	Completely damaged
ZTA (20 wt.% 3Y-TZP)	4609	0.28	Completely damaged
ZTA (30 wt.% 3Y-TZP)	2112	0.8	Completely damaged
ZTA (40 wt.% 3Y-TZP)	1920	0.1	Completely damaged

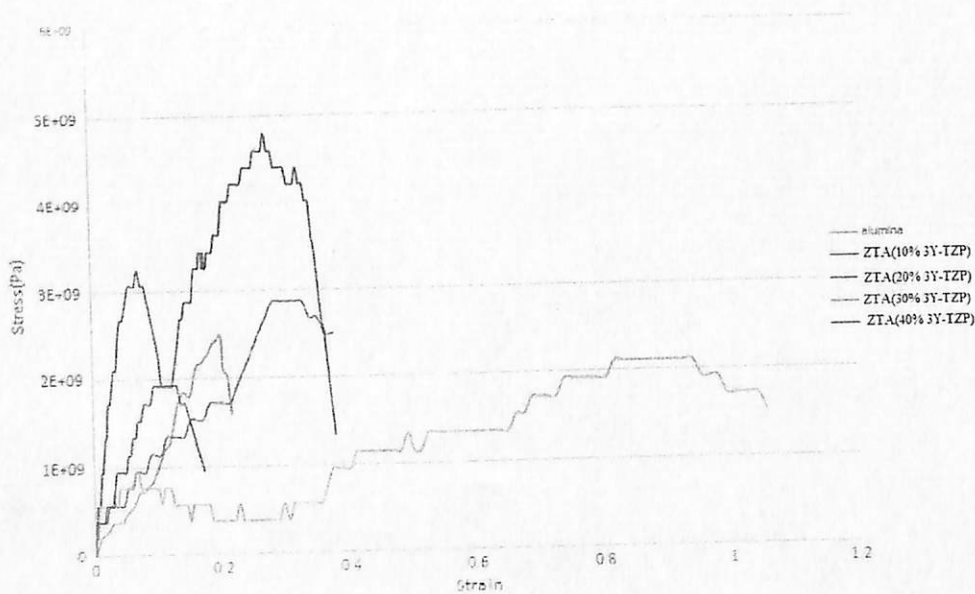


Fig. 7. Stress and strain of ZTA with different 3Y-TZP percentages.



The influence of in-situ formation of hibonite on the properties of zirconia toughened alumina (ZTA) composites

Zhwan Dilshad Ibrahim Sktani^a, Ahmad Zahirani Ahmad Azhar^b, Mani Maran Ratnam^c,
Zainal Arifin Ahmad^{a,*}

^aStructural Materials Niche Area, School of Materials and Mineral Resources Engineering, Engineering Campus, Universiti Sains Malaysia,
14300 Nibong Tebal, Penang, Malaysia

^bDepartment of Manufacturing and Materials Engineering, Faculty of Engineering, International Islamic University Malaysia, 50728 Gombak, Selangor, Malaysia

^cSchool of Mechanical Engineering, Engineering Campus, Universiti Sains Malaysia, 14300 Nibong Tebal, Penang, Malaysia

Received 27 September 2013; received in revised form 16 November 2013; accepted 16 November 2013
Available online 3 December 2013

Abstract

This paper reports an investigation on the impact of in-situ formation of $\text{CaAl}_{12}\text{O}_{19}$ (hibonite) on the microstructure and mechanical properties of zirconia-toughened-alumina (ZTA). Various amounts of CaCO_3 (0–13 wt%) were added to ZTA to form $\text{CaAl}_{12}\text{O}_{19}$. Samples were sintered at 800 °C for 4 h to obtain CaO from decomposition of CaCO_3 , and then at 1600 °C for 4 h to produce elongated $\text{CaAl}_{12}\text{O}_{19}$ grains. Analyses of samples were done using XRD and FESEM. The higher the amount of CaCO_3 added, the higher the amounts of $\text{CaAl}_{12}\text{O}_{19}$ and pores observed. The toughness value increased with the increase of $\text{CaAl}_{12}\text{O}_{19}$ for a critical range, and subsequently decreased; the reverse trend was observed for the hardness and density results. The sample with 0.5 wt% CaCO_3 addition produced the highest toughness ($6.3 \text{ MPa m}^{1/2}$), reasonable hardness (1568.6 HV), density (4.11 g/cm^3), and porosity (1.29%) values.
© 2013 Elsevier Ltd and Techna Group S.r.l. All rights reserved.

Keywords: ZTA; Hibonite ($\text{CaAl}_{12}\text{O}_{19}$); In-situ formation; Fracture toughness

1. Introduction

Alumina (Al_2O_3) based ceramics are good candidates for cutting tool applications owing to their excellent properties such as high hot hardness, good corrosion resistance, high insulation, process flexibility, and high chemical resistance. However, their application as cutting tools is restricted due to their brittleness [1–9]. Therefore, it is necessary to improve this property so as to increase their fracture resistance and toughness.

Since the 1980s, there has been great interest in the toughening of Al_2O_3 -based ceramics via in-situ formation of a second phase during the sintering process. These in-situ products contribute to a highly anisotropic growth habit and toughen the ceramic composites. The in-situ method has many advantages compared to the method of adding second phases into Al_2O_3 -based matrices.

The advantages include lower cost and ease of processing to avoid the use of complicated methods like hot pressing, isostatic pressing, and colloidal processing. Besides that, it also reduces hazards and promotes a more practical way of achieving elongated grains [10–16]. In-situ formation of elongated grains toughening has been successfully applied for Al_2O_3 -based ceramics in previous works [10–19]; the results show that it is an effective way to achieve better toughness and mechanical properties. The formation of elongated grains or secondary phases in the microstructure improves fracture toughness of Al_2O_3 -based ceramics due to crack bridging mechanism [11,16,20–22] and crack deflection mechanism [1,6,14,23] or both [12,15,17,18,24].

Hexaaluminates are best examples of in-situ toughened materials. They are obtained from reactions between oxides (or after calcinations from carbonates, nitrates, etc.) and Al_2O_3 [1,16,20,23–25]. Oungkulsolmongkol et al. [11] produced elongated grains of strontium hexaaluminate ($\text{SrAl}_{12}\text{O}_{19}$) with good mechanical properties from the reaction between SrO and Al_2O_3 . Chen et al. [11] discussed in-situ formation of many

*Corresponding author. Tel.: +60 45996127; fax: +60 45941011.
E-mail address: zainal@eng.usm.my (Z.A. Ahmad).

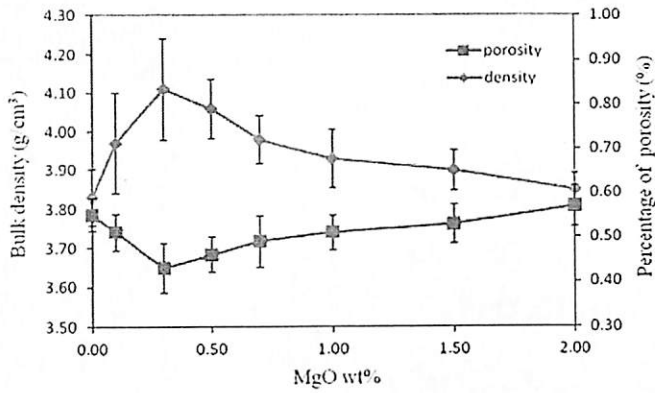


Fig. 5. Bulk density and percentage of porosity for various MgO wt%.

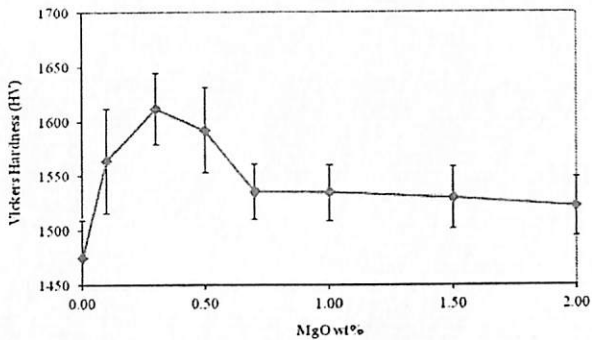


Fig. 6. Results of Vickers hardness for ZTA-CeO₂ as a function of MgO wt%.

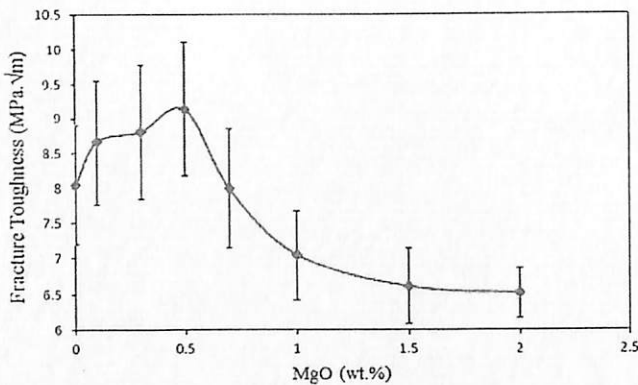


Fig. 7. Results of fracture toughness as a function of MgO wt%.

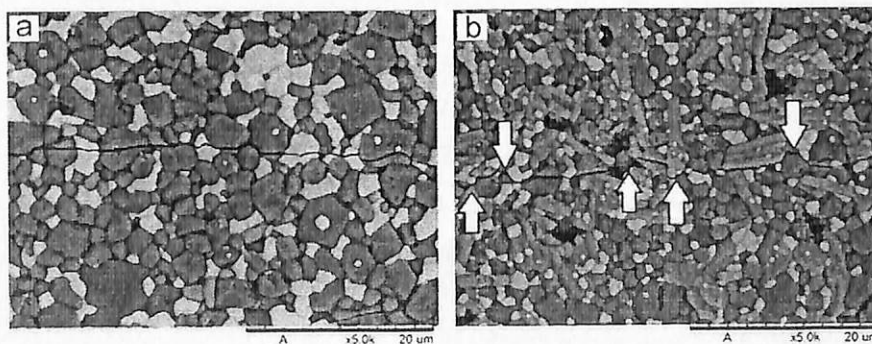


Fig. 8. Crack path in the (a) ZTA-CeO₂ without MgO and (b) ZTA-CeO₂-0.5 wt% MgO, induced by Vickers indentation. Arrows indicate that major toughening mechanisms are crack deflection.

addition on grain size was also observed in previous works [9,30,31]. Further addition of MgO (0.5 wt% MgO) led to the formation of elongated secondary phase MgAl₁₁CeO₁₉ (indicated by the yellow circle); therefore, the grain size started to increase because the pinning effect was diminished.

Previous research show similar trends with the current study in terms of microstructure features, where the grain size of Al₂O₃ was reduced with the addition of MgO [9,14,17,20,30,32]. Based on Fig. 2, the elongated phase lessened as the MgO wt% was increased; this is similar to the XRD results that were discussed earlier. In order to confirm the trend of elongated phases decreasing as MgO wt% increased, phase identification analysis was carried out using IMT iSolution DT software to identify the area percentage of different phases in the micrographs. The results are shown in Fig. 4.

Fig. 4 shows that as the MgO percentage increases, the percentage of MgAl₁₁CeO₁₉ phase will reduce. At 0.5 wt% MgO, the area of elongated secondary phase detected was 23.66%. The percentage of area was reduced from 23.66% (0.5 wt% MgO) to 6.97% (2.0 wt% MgO) as the MgO wt% increased.

When the percentage of MgAl₁₁CeO₁₉ decreases, another phase MgAl₂O₄ should occur. Unfortunately, the MgAl₂O₄ cannot be detected because its contrast is similar to that of the Al₂O₃ phase. The decrease of MgAl₁₁CeO₁₉ phase and occurrence of MgAl₂O₄ caused a decrease in fracture toughness. This will be discussed further in the section of Vickers hardness and fracture toughness.

Phase quantification for each phase is shown in Table 2. With the further addition of MgO, the amount of MgAl₂O₄ increased up to 13.9% with 2.0 MgO wt%. On the other hand, the amount of MgAl₁₁CeO₁₉ phase continuously decreased with the addition of MgO. Results from Table 2 suggest that the addition of MgO results in a tendency for the formation of MgAl₂O₄. This may be due to the fixed amount of CeO₂ which cannot accommodate the presence of additional MgO to form MgAl₁₁CeO₁₉. The results in Table 2 are in agreement with the visual analysis shown in Fig. 4.

Fig. 5 indicates the bulk density and percentage of porosity for ZTA-CeO₂ ceramic composites with different MgO contents. At the beginning, the density of ZTA-CeO₂ samples increased from 3.83 g/cm³ (0 wt% MgO) to 4.11 g/cm³ (0.3 wt% MgO), showing a 7.31% increase with the addition of MgO. Among them, the sample with 0.3 wt% MgO had the highest bulk density value (4.11 g/cm³). MgO has the ability to inhibit the abnormal grain growth of Al₂O₃ due to a microstructure pinning effect, thus resulting in higher density with higher beginning amounts of MgO.

Additions of more than 0.3 wt% MgO were not used to pin the grain growth of alumina but was used to form secondary phases, i.e. MgAl₁₁CeO₁₉ and MgAl₂O₄ instead. Since the pinning effect was diminished, the bulk density started to decrease with the addition of MgO of more than 0.3 wt%, from 4.06 g/cm³ (0.5 wt% MgO) to 3.85 g/cm³ (2.0 wt% MgO). Among them, the sample with 2.0 wt%

Role of MgO nanoparticles on zirconia-toughened alumina-5 wt-% CeO₂ ceramics mechanical properties

N. A. Rejab¹, A. Z. Ahmad Azhar², M. M. Ratnam³ and Z. A. Ahmad*¹

The poor hardness of zirconia-toughened alumina (ZTA) with 5 wt-% CeO₂ (ZTA5CeO₂) ceramic has limited its applications as a cutting insert. Therefore, in this work, the possibility of MgO nanoparticles (20 nm) as reinforcement to ZTA5CeO₂ ceramics was investigated. MgO nanoparticles with different weight percentages (0-2 wt-%) were added to ZTA5CeO₂ ceramics. ZTA5CeO₂ with 0.5 wt-%MgO showed the highest fracture toughness of 9.14 MPa.√m. The addition of 0.5 wt-%MgO nanoparticles showed the excellent role of MgAl₁₁CeO₁₉ grains as a crack deflector, which consequently produced a reasonable hardness value of 1591 HV and lowered the wear areas to 0.0528 mm².

Keywords: Cutting inserts, Fracture toughness, MgO nanoparticles, Nose wear area, ZTA

Introduction

The benefit of 'transformation toughening' has been utilized for the fabrication of zirconia toughened alumina (ZTA) with the characteristics of non-oxide materials as cutting insert. A number of attempts have been made to enhance the mechanical properties of ZTA composites by controlling their microstructure via composition control^{2,3,10,14}. Hao *et al.*¹⁰ reported that microstructural coarsening within ZTA was found to increase fracture toughness from 3.95 to 6.37 MPa.√m. Li *et al.*¹⁴ reported a novel way of enhancing the hardness of a zirconia-toughened alumina (ZTA) composite using zirconia content of 20 vol.-% by surface treatments and blended with boehmite sol. All findings referred to the significant increase in the hardness of the ZTA composite, which is attributed mainly to an increase in the volume fraction of alumina phase with greater hardness.

However, in the cutting insert applications, the high hardness and wear resistance have been compromised by the deficient fracture toughness that results in premature and chipping or catastrophic tool failure¹⁵. A similar finding by Ezugwu and Wallbank⁸ reported the premature and chipping or catastrophic failure of ceramic tools. Therefore, considerable efforts have been made to improve the fracture toughness of ZTA, for example, by adding ceramic whiskers, platelets or particles as reinforcements to the alumina matrix. Other approach is

the incorporation of any phase that undergoes a phase transition and volume expansion. These changes are associated with phase transformation that is initiated by stress field of a propagating crack. Zeng found that, an increment in ZrO₂ content increases the relative density of the samples, which is beneficial to both strength and toughness²⁷.

Recently, several researchers reported the effects of other reinforcing agents and particle sizes to overcome the low-fracture-toughness problem in ZTA. The other reinforcing agents such as Y₂O₃, MgO¹, Cr₂O₃², CaCO₃³, CeO₂¹ and TiO₂¹⁶ have been introduced in ZTA ceramics through solid-state mixing.

Besides retaining the tetragonal ZrO₂ phase at room temperature⁶, these reinforcing agents also acted to control their microstructure and fabrication process⁵. The tetragonal ZrO₂ phase in ZTA ceramics is metastable, which could lead to the transformation of tetragonal phase into monoclinic phase^{11,25} during heating. This could also relate to volume expansion and prevention of crack growth, thereby consequently improving the fracture toughness¹³. Another solution to increase the ZTA fracture toughness is by using the finer particle size of the raw materials to ensure a better superplastic deformation²⁶. The deformation rate is proportional to the inverse square of the grain diameter, but depending on the kind of deformation mechanism in control⁷. Decreasing the grain size to nanoscale level can also drastically increase both deformation rate and total strain during sintering operation. Azhar *et al.*⁴ reported that nanoparticles of MgO with (80 nm) acted as grain growth inhibitor, thereby contributing to the highest Vickers hardness (1704 HV).

Although the potential of MgO additives has been investigated thoroughly by the authors, the use of nanoadditives in ZTA-CeO₂ cutting insert is yet to be investigated. Nanoscale materials usually have high surface

¹Structural Materials Niche Area, School of Materials and Mineral Resources Engineering, Engineering Campus, Universiti Sains Malaysia, 14300 Nibong Tebal, Penang, Malaysia

²Department of Manufacturing and Materials Engineering, Faculty of Engineering, International Islamic University Malaysia, 50728 Gombak, Selangor, Malaysia

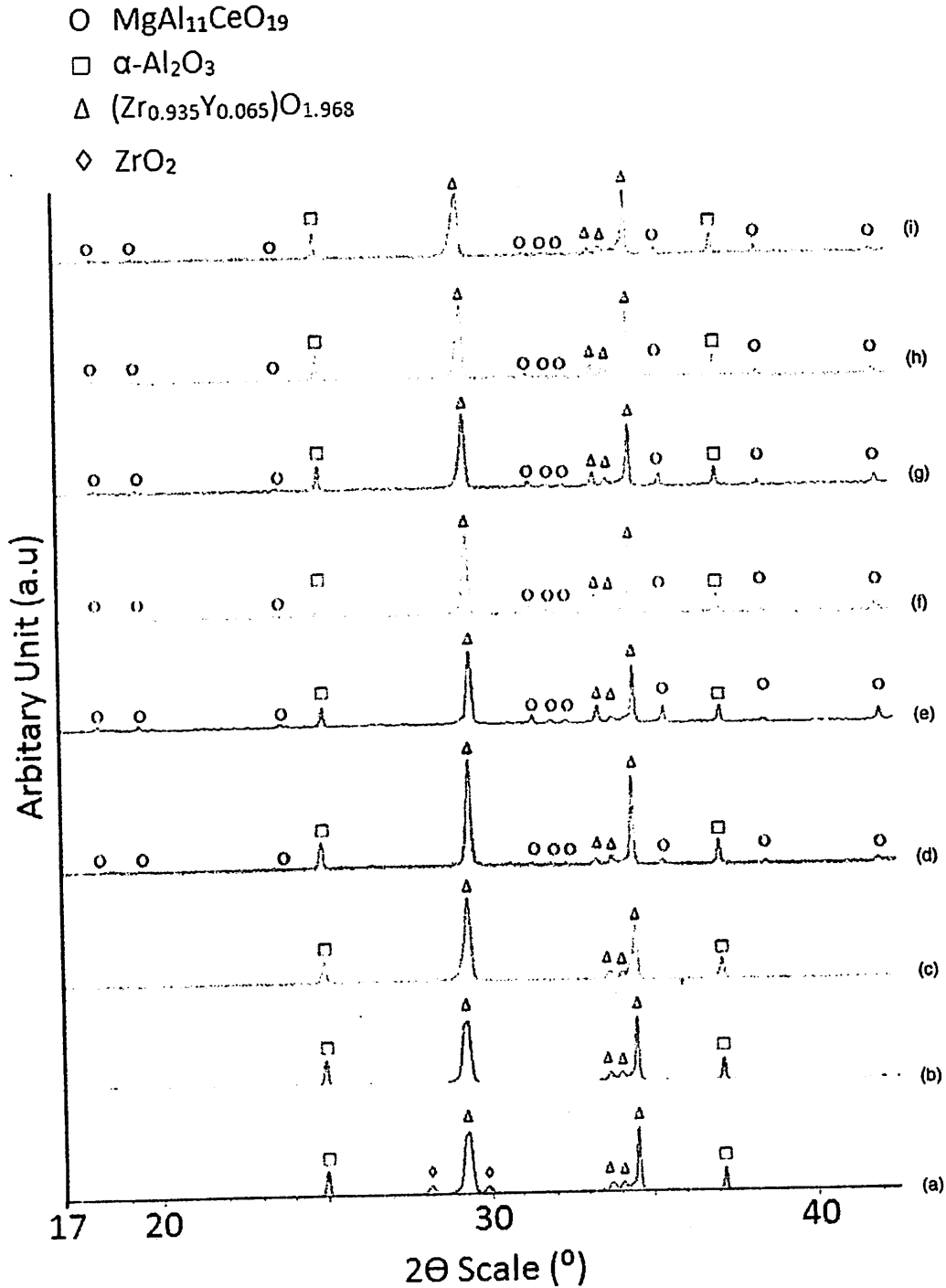
³School of Mechanical Engineering, Engineering Campus, Universiti Sains Malaysia, 14300 Nibong Tebal, Penang, Malaysia

*Corresponding author, email srzainal@usm.my

calculate the area differences between the two images (Fig. 3a and b), and this area is indicated by the black colour. Based on nose wear area (Fig. 3c), a larger black area indicates that the inserts have experienced a greater degree of wear, that is, more material loss occurred due to machining.

Results and discussion

Fig. 4 shows the phase analysis due to addition of MgO nanoparticles into ZTA5CeO₂. A quantitative evaluation of phase analysis was performed using the EVA software at 2θ° = 17°-42.5° and recorded in Table 3. In this work, the presence of MgAl₁₁CeO₁₉ phases plays significant



4 X-ray diffraction analysis of ZTA5CeO₂ with MgO nanoparticles ceramics, a 0 wt-%, b 0.1 wt-%, c 0.3 wt-%, d 0.5 wt-%, e 0.7 wt-%, f 1 wt-%, g 1.5 wt-% and h 2 wt-%

Therefore, the influence of sintering additives, such as MgO and CeO₂ with different volume fractions on the microstructural characteristics, fracture toughness, and crack behavior of ZTA compositions was investigated. The fracture toughness and hardness of each sample were determined at room temperature. In addition, bulk density, Vickers hardness, and phase identification of the sintered samples which are also dependent on sintering additives were determined.

2. Materials and methodology

Starting powders of highly pure, thermally reactive type Al₂O₃ (Alcoa, A16SG, 99.0%), yttrium stabilized zirconia (Goodfellow, 94.6%), 20 nm MgO (Strem Chemicals, Inc., 99.9%), and CeO₂ (Sigma-Aldrich Corporation, 99.0%) were used. The particle size analysis of starting materials was carried out with Sympatec Nanophox (NX0064). In this work, 80 wt.% of Al₂O₃ and 20 wt.% yttrium stabilized zirconia were taken as the baseline composition. The amount of MgO was fixed at 0.7 wt.% due to its excellent hardness values [9]. The ceria were added in different wt.% (0.5 to 7 wt.%) into the initial compositions. Table 1 shows the addition in weight percentage (wt.%) for each powder composition used. The mixtures were prepared by the wet milling method. Subsequently, the mixtures were dried to 100 °C and crushed to form powders. Cylindrical shapes with dimensions of 13.0 mm in diameter and 4.0 mm in height were formed by pressing the crushed powder at 300 MPa. Afterwards, these cylindrical samples were sintered in atmosphere at 1600 °C for 4 h to yield dense ceramics.

The density and porosity values were obtained according to the ASTM C 830-00 test procedure. The analysis of crystal structure was carried out by X-ray diffraction (XRD) using the Bruker D8 Advance with CuK α radiation (40 kV, 30 mA) diffracted beam monochromator, using a step scan mode with a step size of 0.1° in the range of 20°–80° of 2 θ . Scanning electron microscopy (SEM) was employed to study the microstructure of the polished samples. The IMT iSolution DT software was used to discriminate and measure the percentage of each phase from the SEM microstructure. The fracture toughness, which is a critical mechanical property parameter in this work, was determined by the indentation technique. The samples were carefully diamond-polished to produce an optical finish. In the indentation test (Shimadzu Vickers hardness tester HSV-20, Japan), a 294 N load was applied by pressing the indenter onto the sample surface. Both the diagonal length of the indentation and crack length were measured. 10 indent points were made for each sample and the average was taken. K_{IC} (HV30) was calculated using Eq. (1) [15]:

$$3K_{IC} = 0.035 \left(Ha^{1/2} \right) (3E/H)^{0.4} (l/a)^{-0.5} \quad (1)$$

where K_{IC} is the fracture toughness, H is Vickers hardness, a is the half length of Vickers diagonal (μm), E is the Young modulus of the samples, and l is the length of the radial crack size (μm). Young modulus for all the samples was determined using rules of mixtures and calculated with respect to the composition of each sample.

Table 1
Addition of CeO₂ in weight percentage (wt.%) for each composition.

Sample	ZTA	MgO (wt.%)	CeO ₂ (wt.%)
ZTA*	100	0.0	0.0
ZTA-MgO	99.3	0.7	0.0
ZTA-MgO-0.5CeO ₂	98.8	0.7	0.5
ZTA-MgO-0.7CeO ₂	98.6	0.7	0.7
ZTA-MgO-1.0CeO ₂	98.3	0.7	1.0
ZTA-MgO-5.0CeO ₂	94.3	0.7	5.0
ZTA-MgO-7.0CeO ₂	92.3	0.7	7.0

* Composition of all ZTA was fixed to 80 wt.% Al₂O₃ and 20 wt.% YSZ.

3. Results and discussion

Fig. 1 shows the average particle size, particle size distribution, and morphology for all of the raw powders used. The average particle sizes for Al₂O₃ and YSZ were 1.05 μm and 0.71 μm , while the MgO nano particle and CeO₂ powder were 18.35 nm and 138.69 nm, respectively. Table 2 summarizes the overall results for grain size, Vickers hardness, fracture toughness, theoretical density, bulk density, and porosity. The comparison of crack propagation between pure Al₂O₃ and ZTA is shown in Fig. 2. The scanning electron microscope (SEM) micrographs of the indentation show cracks emanating from the corners of the Vickers indentation. The crack mode for both samples resulted in some crack deflections, as indicated by the white arrows at the Al₂O₃ and YSZ grains. However, the propagated crack experienced less deflection in pure Al₂O₃ compared to ZTA; the crack directly propagated through these grains, showing transgranular tendency. ZTA samples show more crack deflection due to the presence of $t \rightarrow m$ phase transformation during the crack propagation. A similar observation was reported by previous authors [16,17]. The behavior of crack propagation for Al₂O₃ would suggest that Al₂O₃ fracture toughness is lower compared to ZTA. The values of fracture toughness for Al₂O₃ and ZTA are $2.85 \pm 0.40 \text{ MPa} \cdot \sqrt{\text{m}}$ and $4.42 \pm 0.35 \text{ MPa} \cdot \sqrt{\text{m}}$, respectively. Although sintered Al₂O₃ shows a larger grain size ($4.30 \pm 3.00 \mu\text{m}$) compared to ZTA, their fracture toughness was reported to be lower [11].

Fig. 3 shows the indentation profile for the sample ZTA-MgO with 0 wt.% CeO₂. An enlarged view of one crack path is shown in an inset in Fig. 3. The crack path, as can be seen in the inset, indicates the crack propagation with associated crack deflection behavior on the surface. Fig. 4 (a)–(b) shows the surface morphology of cracks for samples ZTA-MgO and ZTA-MgO-0.7 wt.% CeO₂, respectively. The crack deflection can be observed under indentation load of 294 N. The fracture toughness value for ZTA-MgO-0 wt.% CeO₂ (baseline sample) and ZTA-MgO-1.0 wt.% CeO₂ were $5.75 \pm 0.33 \text{ MPa} \cdot \sqrt{\text{m}}$ and $6.59 \pm 0.23 \text{ MPa} \cdot \sqrt{\text{m}}$, respectively. ZTA-MgO-1.0 wt.% CeO₂ has higher fracture toughness due to a higher number of crack deflections found on the crack propagation compared to a sample of ZTA-MgO-0 wt.% CeO₂, as shown in Fig. 4. With the presence of CeO₂, ZTA-CeO₂ samples show more crack deflection due to Al₂O₃ strengthening by CeO₂ [14].

Besides the modes of crack propagation in ZTA, the presence of YSZ in the Al₂O₃ clearly contributed to the increase of fracture toughness. XRD spectra of the ZTA-MgO-CeO₂ compositions sintered at 1600 °C for 4 h are shown in Fig. 5. From the XRD patterns, it is observed that the major diffraction peaks can be indexed as yttria doped zirconia ($\text{Zr}_{0.935}\text{Y}_{0.065}\text{O}_{1.968}$ (designated as \circ , ICDD files No. 01-078-1808), and α -Al₂O₃ (designated as \square , ICDD files No. 00-010-0173). Three minor phases were also identified, i.e., m -ZrO₂ (designated as \ast , ICDD files No. 01-078-1807), MgAl₂O₄ (designated as \diamond , ICDD files No. 01-073-1959), and CeAl₁₁O₁₈ (designated as Δ , ICDD files No. 00-048-0055). Various literatures [1,8,18,19] suggest that the transformation toughening inside ZTA is an efficient mechanism that improves the toughness of ceramic composites containing YSZ. Furthermore, addition of CeO₂ also acts as a stabilizing agent. XRD results in Fig. 5 show that the peak for the monoclinic phase decreases with increased addition of CeO₂. The reduction of the monoclinic phase resulted in the increase of the tetragonal phase, thus promoting more transformation toughening $t \rightarrow m$ in ZTA ceramic composites. The addition of CeO₂ also decreases the monoclinic phase, as shown at 28° and 32° Bragg angles. Previous work done by Huang et al., who studied the reduction of CeO₂ in ZrO₂ ceramics, also shows a reduction of the monoclinic phase with the addition of CeO₂ [20]. The reduction of the monoclinic phase in ZTA-MgO-CeO₂ system increases the overall toughness of the ceramic composite. This is due to the presence of more tetragonal ZrO₂, which promotes the transformation toughening mechanism. A similar observation was also reported by Azhar et al. and Rejab et al. on the ZTA-Cr₂O₃ system where the presence of Cr₂O₃ can be used to lower the presence of the monoclinic phase. The presence of monoclinic zirconia phase was an unavoidable

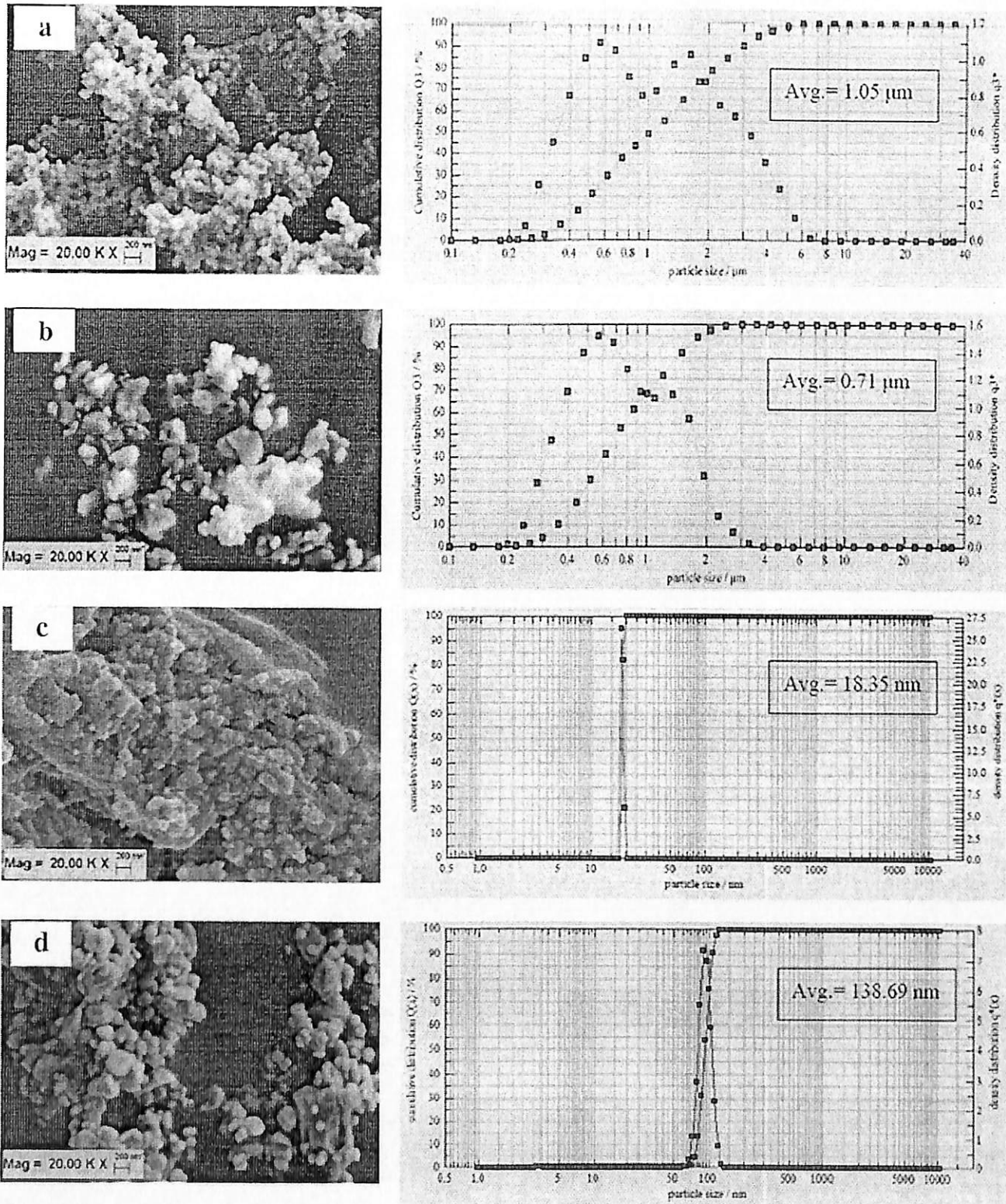


Fig. 1. The average particle size, particle size distribution and morphology for all of the raw powders used (a) Al_2O_3 , (b) YSZ, (c) MgO-nano, and (d) CeO_2 .

phenomenon and the small amount of monoclinic ZrO_2 would not affect the mixture as a whole. Sergio et al. reported that at least 15% of monoclinic phase will always be present, even in zirconia toughened alumina (ZTA) commercial cutting tools [21]. The presence of MgAl_2O_4 phase

was first detected for ZTA–MgO without CeO_2 addition (Fig. 5b). The MgAl_2O_4 peaks were more apparent at the Bragg angle of 37.02° , as shown in Fig. 5. An image analyzer proved that the percentage area of MgAl_2O_4 phase at 0.5 to 1.0 wt.% CeO_2 addition was diminished from

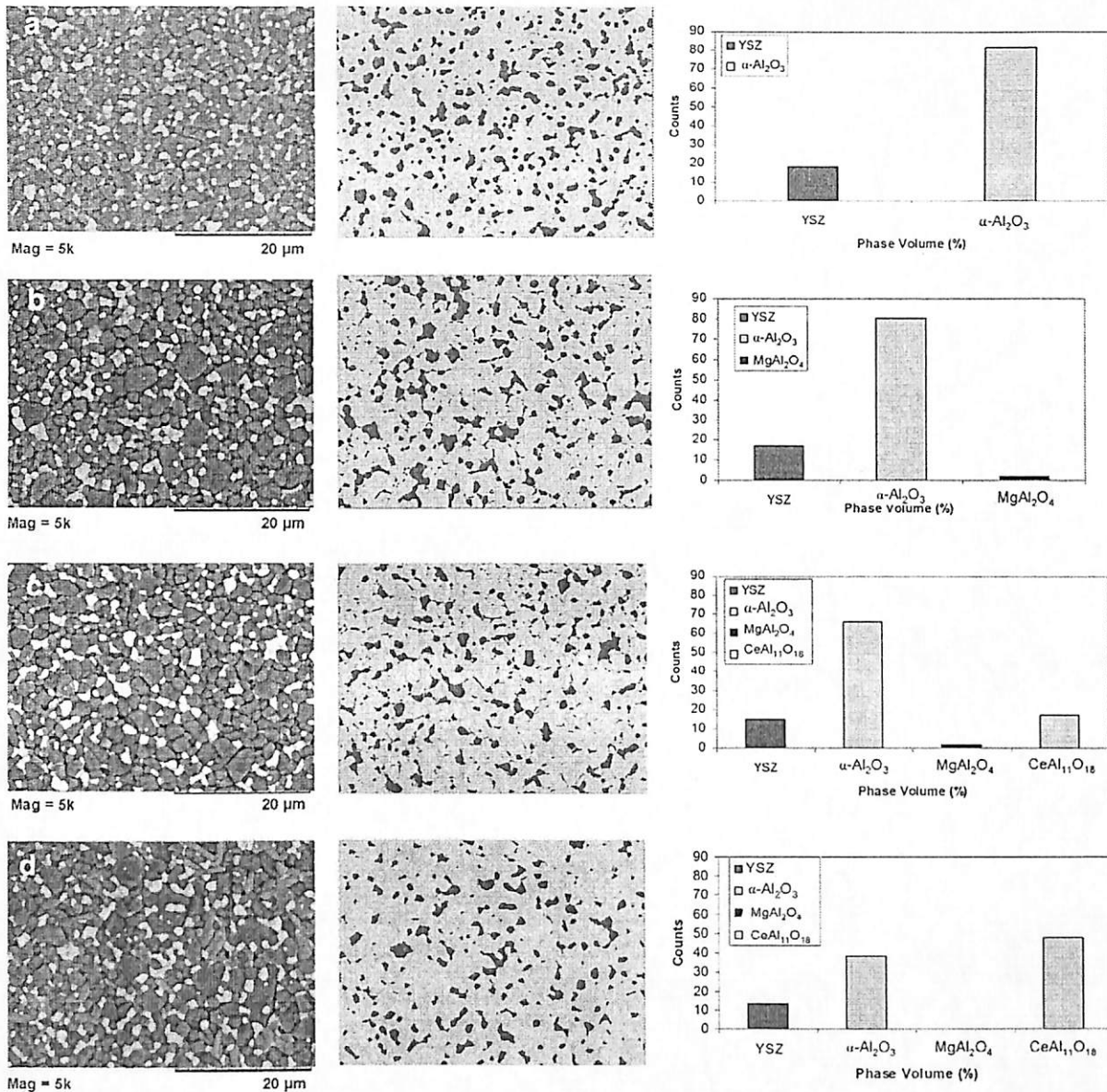


Fig. 6. Quantitative phase analysis of (a) ZTA, (b) ZTA-MgO, (c) ZTA-MgO-1.0 wt.% CeO₂, and (d) ZTA-MgO-7.0 wt.% CeO₂ based on their respective micrograph.

average grain size for Al₂O₃ obtained was the one corresponding to the sample with 5.0 wt.% ($2.98 \pm 0.56 \mu\text{m}$); the smallest average grain size was obtained for the sample ZTA-MgO without CeO₂ addition ($2.14 \pm 0.82 \mu\text{m}$). Furthermore, in the case of YSZ grains, the average grain size was ($1.70 \pm 0.41 \mu\text{m}$) with increased CeO₂ additions. The

Table 3
Phase area percentage for each composition in ZTA-MgO-CeO₂ composites.

Composition	Phase area (%)			
	Al ₂ O ₃	YSZ	MgAl ₂ O ₄	CeAl ₁₁ O ₁₈
ZTA	81.72	18.23	0.00	0.00
ZTA-MgO	78.87	17.12	3.31	0.00
ZTA-MgO-0.5CeO ₂	76.15	18.39	4.43	0.00
ZTA-MgO-0.7CeO ₂	80.56	16.65	2.09	0.00
ZTA-MgO-1.0CeO ₂	66.07	14.80	1.73	17.28
ZTA-MgO-5.0CeO ₂	52.02	12.83	0.00	30.88
ZTA-MgO-7.0CeO ₂	38.54	13.08	0.00	47.66

formation of elongated grains of CeAl₁₁O₁₈ in the matrix of fine-grained Al₂O₃ was observed in the composites containing 5.0 and 7.0 wt.% CeO₂. Furthermore, the average length of CeAl₁₁O₁₈ grains was found to increase with the addition of CeO₂. The formation of CeAl₁₁O₁₈ promotes bonding between Al₂O₃ and CeO₂, which also has a contributing effect on the mechanical properties of the composite. Moreover, CeO₂ exhibits sensitivity to the sintering atmosphere and can form nonstoichiometric oxides such as Ce₂O₃ when sintering at low oxygen pressure atmosphere [22]. As shown in Fig. 9, the addition of CeO₂ above 5 wt.% clearly shows the formation of CeAl₁₁O₁₈ elongated grains. These elongated grains of CeAl₁₁O₁₈ tend to have larger grain sizes. The average size of elongated CeAl₁₁O₁₈ grains is 4–6 μm in length and 0.7–1 μm in width. The average length of elongated grains increased with increasing CeO₂ content from 5 wt.% ($1.89 \pm 0.41 \mu\text{m}$) to 7 wt.% ($1.91 \pm 0.45 \mu\text{m}$).

Previous work done by Akin et al. also observed the formation of CeAl₁₁O₁₈ during spark plasma sintering (SPS) of Al₂O₃-YSZ-CeO₂ system. According to Akin et al., the presence of elongated CeAl₁₁O₁₈ grains

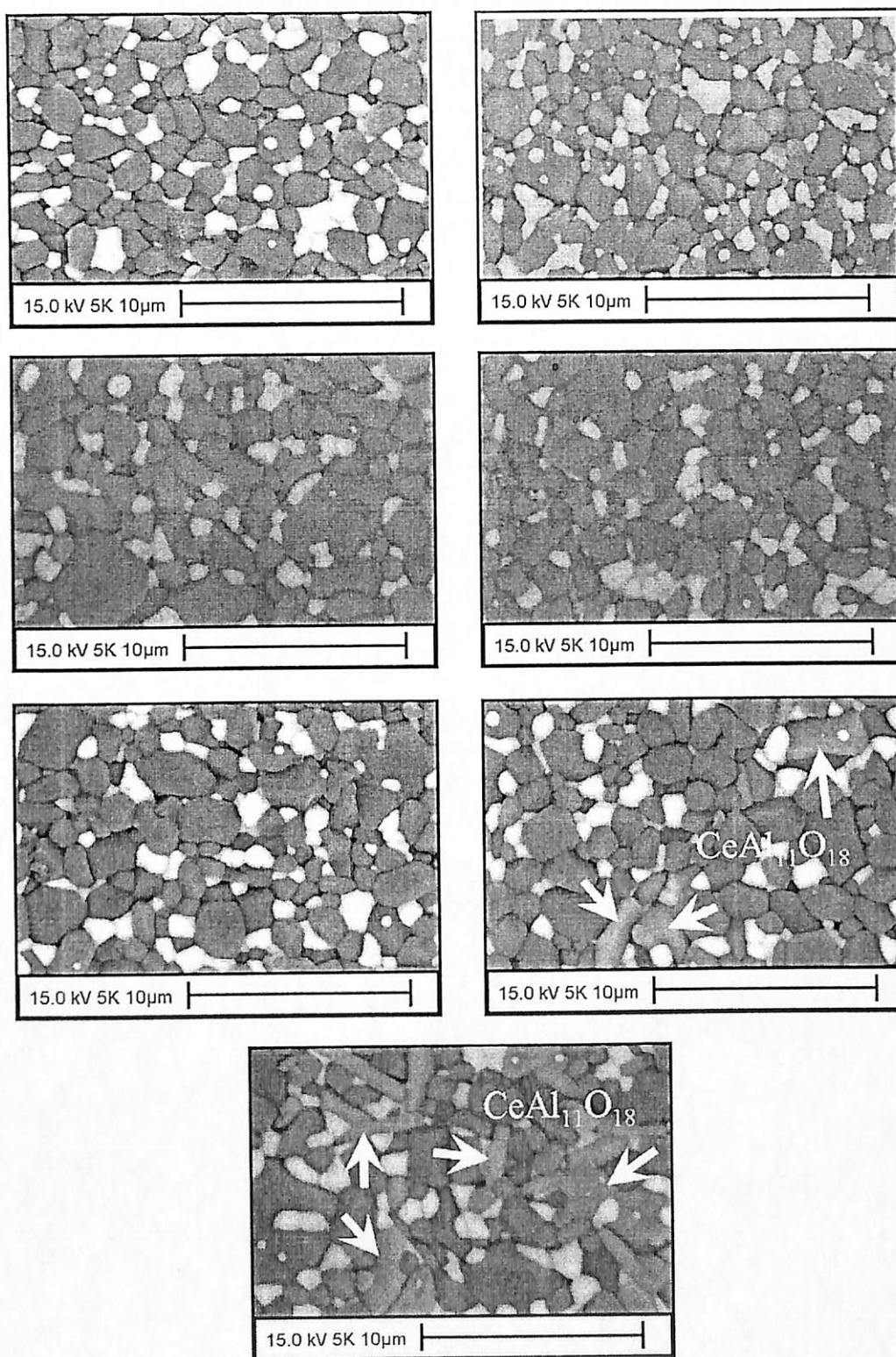


Fig. 9. SEM micrograph of the microstructure of ZTA and ZTA-MgO with CeO₂ addition (a) ZTA, (b) ZTA-MgO, (c) ZTA-MgO-0.5 wt.% CeO₂, (d) ZTA-MgO-0.7 wt.% CeO₂, (e) ZTA-MgO-1.0 wt.% CeO₂, (f) ZTA-MgO-5.0 wt.% CeO₂, and (g) ZTA-MgO-7.0 wt.% CeO₂.

6.59 ± 0.23 MPa · √m. The addition of CeO₂ was found to significantly enhance both hardness and fracture toughness of ZTA-MgO composites. The Vickers hardness increased from 14.51 GPa to 14.99 GPa with the addition of 1.0 wt.% CeO₂, while the fracture toughness increased to

6.59 ± 0.23 MPa · √m with 1.0 wt.% CeO₂ addition. However, the presence of CeAl₁₁O₁₈ reduced the Vickers hardness and fracture toughness of the overall ceramics, which is in agreement with observations made by Akin et al. [22].

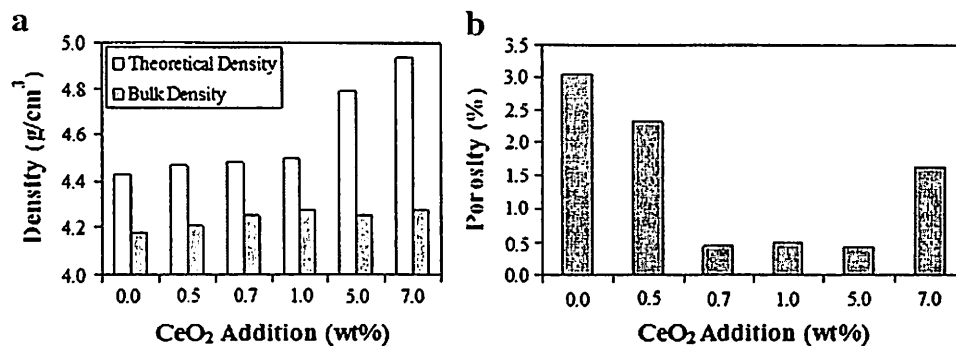


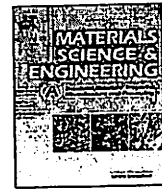
Fig. 10. Comparison of density of theoretical and bulk density for ZTA-MgO-CeO₂ compositions.

Acknowledgment

This work was funded by Universiti Sains Malaysia (USM) under grant 1001/PBAHAN/811212 and MyBrain15. The authors are grateful to Dr. Anasyida Abu Seman, Mr. Mokhtar Mohamad, Mr. Sharul Ami, Mr. Wan Fahmin, Mr. Khairi, and Mr. Abdul Rashid for their technical support.

References

- Cesari F, Esposito L, Furgiuele FM, Maletta C, Tucci A. Fracture toughness of alumina-zirconia composites. *Ceram Int* 2006;32:249–55.
- Maiti K, Sil A. Microstructural relationship with fracture toughness of undoped and rare earths (Y, La) doped Al₂O₃-ZrO₂ ceramic composites. *Ceram Int* 2011;37:2411–21.
- Kosinac T, Swain M, Claussen N. The role of tetragonal and monoclinic ZrO₂ particles in the fracture toughness of Al₂O₃-ZrO₂ composites. *Mater Sci Eng* 1985;71:57–64.
- Shukla S, Seal S, Vij R. Effect of nanocrystallite morphology on the metastable tetragonal phase stabilization in zirconia. *Nano Lett* 2002;2:989–93.
- Do an CP, Hawk JA. Role of zirconia toughening in the abrasive wear of intermetallic and ceramic composites. *Wear* 1997;212:110–8.
- Smuk B, Szutkowska M. Alumina ceramics with partially stabilized zirconia for cutting tools. *J Mater Proc* 2003;133:195–8.
- Szutkowska M. Fracture resistance behavior of alumina-zirconia composites. *J Mater Process Technol* 2004;153–154:868–74.
- Basu B, Vleugels J, Biest OVD. ZrO₂-Al₂O₃ composites with tailored toughness. *J Alloys Compd* 2004;372:278–84.
- Azhar AZA, Ratnam MM, Ahmad ZA. Effect of Al₂O₃/YSZ microstructures on wear and mechanical properties of cutting inserts. *J Alloys Compd* 2009;478:608–14.
- Azhar AZA, Mohamad H, Ratnam MM, Ahmad ZA. The effects of MgO addition on microstructure, mechanical properties and wear performance of zirconia-toughened alumina cutting inserts. *J Alloys Compd* 2010;497:316–20.
- Hao JKC, Azhar AZA, Ratnam MM, Ahmad ZA. Wear performance and mechanical properties of 80 wt.% Al₂O₃/20 wt.% YSZ cutting inserts at different sintering rates and soaking times. *Mater Sci Technol* 2010;26:95–103.
- Azhar AZA, Mohamad H, Ratnam MM, Ahmad ZA. Effect of MgO particle size on the microstructure, mechanical properties and wear performance of ZTA-MgO ceramic cutting inserts. *Int J Refract Metals Hard Mater* 2011;29:456–61.
- Azhar AZA, Choong LC, Mohamed H, Ratnam MM, Ahmad ZA. Effects of Cr₂O₃ addition on the mechanical properties, microstructure and wear performance of zirconia-toughened-alumina (ZTA) cutting inserts. *J Alloys Compd* 2012;513: 91–6.
- Rejub NA, Azhar AZA, Ratnam MM, Ahmad ZA. The effects of CeO₂ addition on the physical, microstructural and mechanical properties of yttria stabilized zirconia toughened alumina (ZTA). *Int J Refract Metals Hard Mater* 2013;36:162–6.
- Niihara K. A fracture mechanics analysis of indentation-induced Palmqvist crack in ceramics. *J Mater Sci Lett* 1983;2:221–3.
- Wang J, Stevens R. Review: zirconia-toughened alumina (ZTA) ceramics. *J Mater Sci* 1989;24:3421–40.
- Mondal B, Chattopadhyay A, Virkar A, Paul A. Development and performance of zirconia-toughened alumina ceramic tools. *Wear* 1992;156:365–83.
- Basu B, Vleugels J, Biest OVD. Toughness tailoring of yttria-doped zirconia ceramics. *Mater Sci Eng A* 2004;380:215–21.
- Magnani G, Brillante A. Effect of the composition and sintering process on mechanical properties and residual stresses in zirconia-alumina composites. *J Eur Ceram Soc* 2005;25:3383–92.
- Huang SG, Vanmeensel K, Biest OVD, Vleugels J. Influence of CeO₂ reduction on the microstructure and mechanical properties of pulsed electric current sintered Y₂O₃-CeO₂ co-stabilized ZrO₂ ceramics. *J Am Ceram Soc* 2007;90:1420–6.
- Sergo V, Vanni L, Giuseppe P, Elio L, Sergio M, Nanki M, et al. The effect of wear on the tetragonal-to-monoclinic transformation and the residual stress distribution in zirconia-toughened alumina cutting tools. *J Wear* 1998;214:264–70.
- Akin I, Yilmaz E, Sahin F, Yuce O, Goller G. Effect of CeO₂ addition on densification and microstructure of Al₂O₃-YSZ composites. *Ceram Int* 2011;37:3273–80.
- Senthil Kumar A, Raja Durai A, Sornakumar T. Development of yttria and ceria toughened alumina composite for cutting tool application. *Int J Refract Metals Hard Mater* 2007;25:214–9.
- Oh UC, Chung YS, Kim DY, Yoon DN. Effect of grain growth on pore coalescence during the liquid-phase sintering of MgO-CaMgSiO₄ systems. *J Am Ceram Soc* 1988;71: 854–7.
- German R, editor. Critical reviews in solid state and materials sciences, vol. 35 4. California: Taylor & Francis; 2010.



Effects of MgO addition on the phase, mechanical properties, and microstructure of zirconia-toughened alumina added with CeO₂ (ZTA–CeO₂) ceramic composite

Nik Akmar Rejab^a, Ahmad Zahirani Ahmad Azhar^b, Khoo Seng Kian^a,
Mani Maran Ratnam^c, Zainal Arifin Ahmad^{a,*}

^a Structural Materials Niche Area, School of Materials and Mineral Resources, Engineering Campus, Universiti Sains Malaysia, 14300 Nibong Tebal, Penang, Malaysia

^b Department of Manufacturing and Materials Engineering, Faculty of Engineering, International Islamic University Malaysia, 50728 Kuala Lumpur, Malaysia

^c School of Mechanical, Engineering Campus, Universiti Sains Malaysia, 14300 Nibong Tebal, Penang, Malaysia

ARTICLE INFO

Article history:

Received 6 September 2013

Received in revised form

13 November 2013

Accepted 27 November 2013

Available online 4 December 2013

Keywords:

Microstructure

Vickers hardness

Fracture toughness

MgO

ABSTRACT

The effects of MgO addition on properties such as density, firing shrinkage, microstructure, Vickers hardness, and fracture toughness of ZTA–CeO₂ ceramics composites were investigated. The amount of CeO₂ used in the experiment was fixed at 5.0 wt% while the MgO addition was varied from 0 wt% to 2.0 wt%. Each composition was weighed, mixed, and pressed using hydraulic press under 300 MPa into 13 mm pellets. The pellets were sintered at 1600 °C for 4 h under pressureless condition. Vickers hardness and fracture toughness of the sintered samples were measured using the Vickers indentation method. Based on the SEM microstructures, elongated secondary phase, i.e. MgAl₁₁CeO₁₉, started to occur at 0.5 wt% MgO. This elongated phase was responsible for the increase in fracture toughness of the ceramic composites. Similarly, the addition of more than 0.5 wt% MgO produced another secondary phase (MgAl₂O₄), as detected by XRD. This phase was shown to have low intrinsic fracture toughness. Therefore, the sample with 0.5 wt% MgO showed the optimum properties with the highest fracture toughness (9.14 MPa \sqrt{m}) and Vickers hardness (1591 HV) values.

© 2013 Elsevier B.V. All rights reserved.

1. Introduction

Alumina(Al₂O₃)-based ceramics have excellent properties such as high hot hardness, high abrasion resistance, and chemical inertness against extreme environments. With these properties, Al₂O₃ is often used as cutting inserts compared to high-speed steels and carbides as it is inert when applied at elevated temperatures. Al₂O₃-based cutting inserts are also used in abrasive wear environments such as ball mills, grinders, mixers, and coal chutes [1–8]. However, Al₂O₃-based cutting tools lack toughness which leads to failures such as chipping during machining [9,10]. Zirconia-toughened-alumina (ZTA) ceramic composites are intended to replace various applications of Al₂O₃ ceramics due to their higher value of fracture toughness and chemical stability of up to 1650 °C [11]. These characteristics make it possible for ZTA ceramic tools to be used in high-speed machining of various types of steel, cast iron, non-ferrous metals, and refractory nickel-based alloys [12].

Research carried out by Coble [13], Wang et al. [14], and Rittidech et al. [15] indicated that the presence of MgO in the Al₂O₃ matrix will significantly affect the mechanical properties of bulk Al₂O₃. The addition of small amounts of MgO (< 0.25 wt%) enable the Al₂O₃ to sinter to near-theoretical density [13,16,17]. Wang et al. [14] showed that MgO addition can efficiently improve the sinterability of Al₂O₃. The Al₂O₃–MgO ceramic system has higher Vickers hardness values compared to the conventional Al₂O₃ system due to MgO's pinning effect which forms smaller Al₂O₃ grains. Furthermore, Azhar et al. [9] concluded that the introduction of fine MgO particles into ZTA will increase its Vickers hardness and wear-resistance properties. Besides hardness, fracture toughness is also important so that a cutting insert will be able to perform without experiencing premature failure [18]. Tsukuma and Shimada [19] found that fracture toughness and hardness were very dependent on the amount of CeO₂ added into tetragonal zirconia polycrystals (TZP). Previous work done by Azhar et al. [20] showed that the addition of MgO increased the Vickers hardness up to 1740 HV. However, the fracture toughness of the ZTA composite decreased with further addition of MgO due to a finer Al₂O₃ grain size. The decrease of fracture toughness would cause the ZTA insert to become vulnerable to chipping and catastrophic failure during the machining process.

* Corresponding author. Tel.: +604 5996128; fax: +604 5941011.
E-mail address: zainal@eng.usm.my (Z.A. Ahmad).

grains are well distributed among each other. The secondary phase of $MgAl_2O_4$ was not detectable because it did not contrast enough due to MgO 's atomic mass which is very close to that of Al_2O_3 grains [9,20]. In general, similar microstructural characteristic

were observed in these samples and no abnormal grain growth was observed. The grain size is uniform with a high degree of grain close-packing [27–29].

Fig. 3 shows the result of average grains intercept value (N_L) which is the number of Al_2O_3 grain intercepts per unit length (μm) with different MgO wt%. Smaller grain sizes will show higher N_L value. From Fig. 2 and Fig. 3, it is proven that the Al_2O_3 grains are greatly affected by the MgO wt%. The addition of MgO at the beginning (0–0.3 wt% MgO) serves as a pinning agent to inhibit the grain growth of Al_2O_3 but not YSZ grains. The effects of MgO

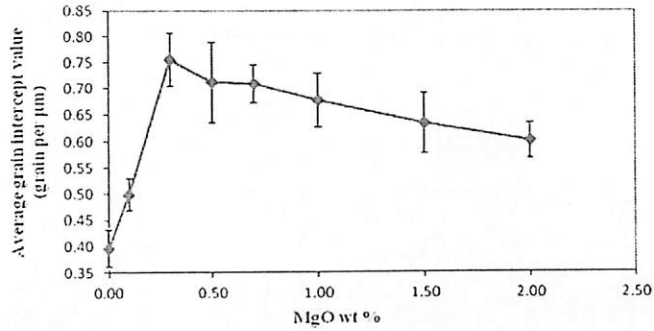


Fig. 3. Average grains intercept value for ZTA– CeO_2 ceramics composite with various MgO wt%.

Table 2
Estimation of phase contents for sintered samples.

MgO, wt%	Al_2O_3	YSZ	$MgAl_{11}CeO_{19}$	$MgAl_2O_4$
0	78.13	21.87	–	–
0.3	70.10	20.33	3.07	6.15
0.7	70.40	15.28	2.72	11.58
2.0	72.80	11.56	1.58	13.90

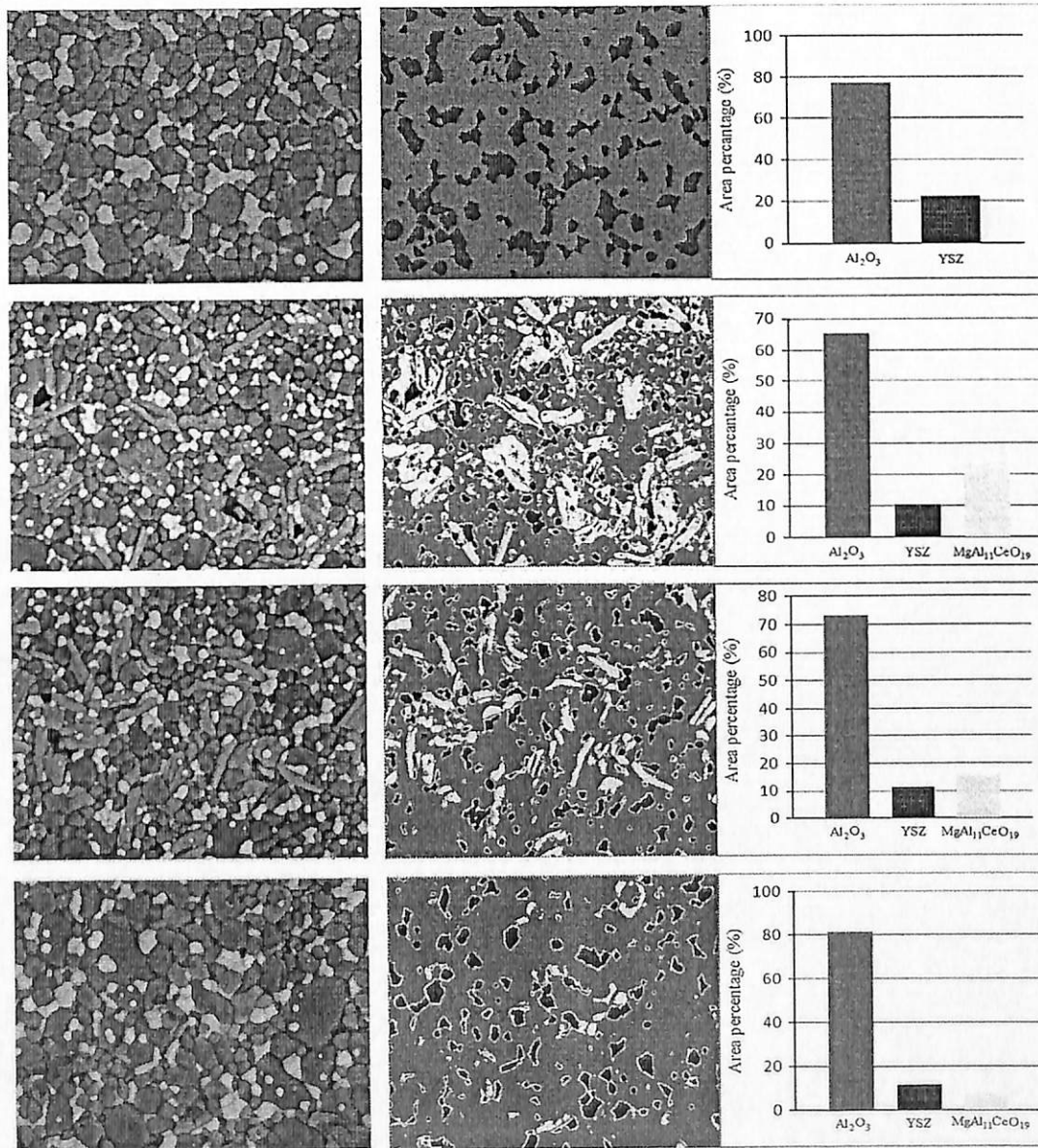
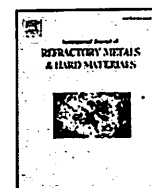


Fig. 4. Results of percentage of area for various phases in the micrograph of different MgO wt%. (a) 0 wt% MgO , (b) 0.5 wt% MgO , (c) 0.7 wt% MgO and (d) 2.0 wt% MgO .

A COPY OF THE
PUBLICATIONS/PROCEEDINGS
LISTED IN
SECTION D(II) (RESEARCH
OUTPUT)



The effects of CeO₂ addition on the physical, microstructural and mechanical properties of yttria stabilized zirconia toughened alumina (ZTA)

Nik Akmar Rejab^a, Ahmad Zahirani Ahmad Azhar^a, Mani Maran Ratnam^b, Zainal Arifin Ahmad^{a,*}

^a School of Materials and Mineral Resources Engineering, Engineering Campus, Universiti Sains Malaysia, 14300 Nibong Tebal, Penang, Malaysia

^b School of Mechanical Engineering, Engineering Campus, Universiti Sains Malaysia, 14300, Nibong Tebal, Penang, Malaysia

ARTICLE INFO

Article history:

Received 31 May 2012

Accepted 17 August 2012

Keywords:

Fracture toughness

CeO₂

Grain sizes

Phase transition

Substitutions

ABSTRACT

The effects of CeO₂ addition on the structure, microstructure and fracture toughness of yttria stabilized zirconia toughened alumina (ZTA) ceramics were investigated. The CeO₂ addition to the powder mixtures was varied from 0 wt.% to 15 wt.%. The powders of each composition were pressed into pellets and sintered at 1600 °C for 4 h under pressureless conditions. The fracture toughness of the sintered samples was determined by the Vickers indentation technique with a 30 kgf load. Based on the XRD analysis, only corundum and yttria doped zirconia phases were present. Shift in position of the zirconia peaks were observed due to the CeO₂ addition. Microstructure investigations showed that the grain sizes of both corundum and yttria doped zirconia increased with increasing CeO₂ addition. Fracture toughness and hardness values were dependent on the CeO₂ addition. The highest fracture toughness (8.38 MPa·√m) and hardness (1688 HV) was obtained with the sample with 5 wt.% CeO₂ additions. ZTA prepared with CeO₂ additives showed an increase of 30% in fracture toughness compared to ZTA without additives.

© 2012 Elsevier Ltd. All rights reserved.

1. Introduction

A great deal of attention has been given to zirconia toughened alumina (ZTA) as it is a promising structural material due to its excellent mechanical properties such as strength, fracture toughness, and hardness [1,2]. These properties are enhanced by a mechanism known as stress induced transformation toughening. In the ZTA system, the stress induced transformation toughening mechanism occurs when the crystal structure of the zirconia particles in the region near the tip of the crack changes from the metastable tetragonal phase to the stable monoclinic phase. The change enlarges the volume of the particles and produces compressive stresses in the alumina matrix. These stresses effectively close the crack and block further crack growth, which can improve the strength, fracture toughness, and hardness of the ZTA [3–5]. Many compositional developments have been made to improve the mechanical properties and controlled microstructure of ZTA. The utilization of sintering additives such as Cr₂O₃, NiO, TiO₂ and MgO was selected by researchers because these additives enable the achievement of fine grain size and high density at low sintering temperatures [6]. Tsukuma et al. [7] found that, with the addition of CeO₂ into tetragonal zirconia polycrystals (TZP), the fracture toughness and hardness were very dependent on the CeO₂ content and grain size of the sintered body. Cerium oxide (CeO₂) is used to stabilize zirconia completely in its tetragonal phase (t-phase), called

tetragonal zirconia polycrystals, and increase the fracture toughness of the composite [8,9].

Previous work done by Mangalaraja et al. [10] in 2003 indicated that the presence of CeO₂ in the Al₂O₃ matrix reduces the mechanical properties of ZTA due to the higher apparent porosity, which possibly resulted from the addition of CeO₂. Smuk et al. [4] reported that with the introduction of a stabilizer of tetragonal ZrO₂ such as MgO, Y₂O₃, CaO and CeO₂, zirconia toughened alumina with greater fracture toughness than pure Al₂O₃ can be obtained. They confirmed that, the mechanical properties of ZTA, such as its fracture toughness, can be improved with an accurate and efficient dosage of partially stabilized tetragonal ZrO₂ addition with definitely sized particles.

However, there are only scarce reports about the effects of CeO₂ additions on the phases, microstructure and mechanical properties of ZTA. Therefore, in this study, we examine the effects of CeO₂ addition (1–15 wt.%) on the phases, microstructure, and mechanical properties of ZTA systems. The phases and microstructure of the sample were measured using XRD and SEM. The mechanical properties, such as fracture toughness and Vickers hardness, were measured to determine the potential of the ZTA–CeO₂ compositions.

2. Experimental procedure

In the present study, the powders of highly pure, thermally reactive type alumina (Martinswerk), yttria stabilized zirconia (5.4 mol%, Goodfellow) and cerium (IV) oxide (Sigma Aldrich) were used. Powder mixtures of 80 wt.% alumina and 20 wt.% yttria stabilized zirconia were taken as the initial composition.

* Corresponding author. Tel.: +60 4 5996128; fax: +60 4 5941011.
E-mail address: zainal@eng.usm.my (Z.A. Ahmad).

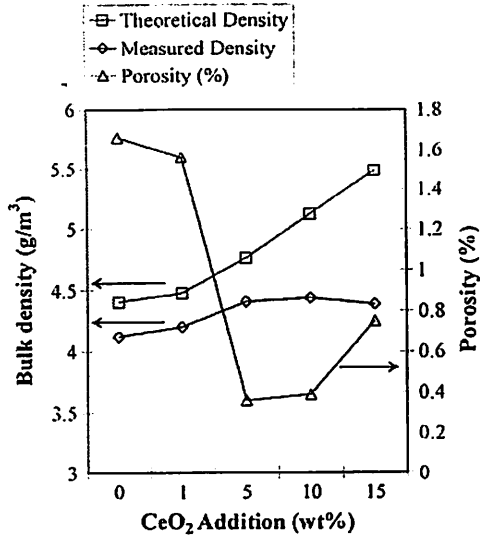


Fig. 7. Results of density and porosity for ZTA-CeO₂ ceramics with different CeO₂ additions.

4. Conclusion

The effects of excess CeO₂ addition on the physical, microstructural and mechanical properties of yttria stabilized ZTA were studied. The overall results are shown in Table 1. The presence of the Ce₂Zr₃O₁₀ phase proved the exceeding limit of CeO₂ addition in ZTA composites. Additionally, abnormal growth such as platelet grains occur among ZrO₂ grains for samples with 10 wt.% and 15 wt.% CeO₂ additions. The composites showed increased mechanical properties such as hardness and fracture toughness with increasing wt.% addition of CeO₂. The highest values were recorded for the sample with 5 wt.% addition, which produced 8.38 MPa·√m and 1688 HV, respectively. The increased mechanical properties were found to be due to the lower apparent porosity, which possibly resulted due to the addition of CeO₂. This shows that CeO₂ is useful for improving fracture toughness without deteriorating the properties of the ZTA.

Acknowledgments

This work was funded by the Universiti Sains Malaysia (USM) under the grant 1001/PBAHAN/811074, 1001/PBAHAN/8043043, 1001/PBAHAN/811212 and MyBrain15. The authors are grateful to

Table 1
Physical and mechanical properties of ZTA with various amounts of CeO₂ addition.

Ce addition (wt.%)	Tetragonality factor (c/a) (Å)	Average grain size (μm)		Fracture toughness (MPa·√m)	Vickers hardness (MPa)	Bulk density (g/m ³)	Porosity (%)
		YSZ	Al ₂ O ₃				
0	1.44	1.21	2.67	5.87	15602	4.13	1.66
1	1.43	1.30	3.15	6.31	15944	4.21	1.56
5	1.43	1.55	3.48	8.38	16559	4.41	0.36
10	1.43	1.96	3.71	7.95	16540	4.44	0.39
15	1.44	2.32	3.71	7.90	16131	4.40	0.75

Mr. Sharul Ami, Mr. Wan Fahmin, Mr. Khairi and Mr. Abdul Rashid for their technical support.

References

- [1] Azhar AZA, Mohamad H, Ratnam MM, Ahmad ZA. Effect of MgO particle size on the microstructure, mechanical properties and wear performance of ZTA-MgO ceramic cutting inserts. *Int J Refract Metals Hard Mater* 2011;29:456-61.
- [2] Wang J, Stevens R. Review: Zirconia-toughened alumina (ZTA) ceramics. *J Mater Sci* 1989;24:3421-40.
- [3] Tuan W, Chen R, Wang T, Cheng C, Kuo P. Mechanical properties of Al₂O₃/ZrO₂ composites. *J Eur Ceram Soc* 2002;22:2827-33.
- [4] Smuk B, Szutkowska M, Walter J. Alumina ceramics with partially stabilized zirconia for cutting tools. *J Mater Process Technol* 2003;133:195-8.
- [5] Azhar AZA, Mohamad H, Ratnam MM, Ahmad ZA. The effects of MgO addition on microstructure, mechanical properties and wear performance of zirconia-toughened alumina cutting inserts. *J Alloys Compd* 2010;497:316-20.
- [6] Like Q, Xikun L, Guanming Q, Weimin M. Study on toughness mechanism of ceramic cutting tools. *J Rare Earths* 2007;25:309-16.
- [7] Tsukuma K, Shimada M. Strength, fracture toughness and Vickers hardness of CeO₂-stabilized tetragonal ZrO₂ polycrystals (Ce-TZP). *J Mater Sci* 1985;20:1178-84.
- [8] Annamalai V, Gokularathnam CV, Krishnamurthy R. On the sintering behaviour of 12 mol% ceria-stabilized zirconia. *J Mater Sci Lett* 1992;11:642-4.
- [9] Senthil Kumar A, Raja Durai A, Sornakumar T. Development of yttria and ceria toughened alumina composite for cutting tool application. *Int J Refract Metals Hard Mater* 2007;25:214-9.
- [10] Mangalaraja R, Chandrasekhar B, Manohar P. Effect of ceria on the physical, mechanical and thermal properties of yttria stabilized zirconia toughened alumina. *Mater Sci Eng A* 2003;343:71-5.
- [11] Niihara K. A fracture mechanics analysis of indentation-induced Palmqvist crack in ceramics. *J Mater Sci Lett* 1983;2:221-3.
- [12] Duran P, Gonzalez M, Moure C, Jurado J, Pascual C. A new tentative phase equilibrium diagram for the ZrO₂-CeO₂ system in air. *J Mater Sci* 1990;25:5001-6.
- [13] Yang S. Sintering behavior of Y-doped ZrO₂ ceramics: the effect of Al₂O₃ and Nb₂O₅ addition. *Solid State Ionics* 2004;172:413-6.
- [14] Azhar AZA, Choong LC, Mohamed H, Ratnam MM, Ahmad ZA. Effects of Cr₂O₃ addition on the mechanical properties, microstructure and wear performance of zirconia toughened-alumina (ZTA) cutting inserts. *J Alloys Compd* 2012;513:91-6.